# Mapping flood extent and understanding mechanisms of surface inundation in areas of impermeable soils using the ANUGA hydrodynamic model: A study from Fredonia, Kansas

by

Tyler L. Vaughn

B.S., Kansas State University, 2016

A THESIS

submitted in partial fulfillment of the requirements for the degree

MASTER OF SCIENCE

Department of Geology
College of Arts and Sciences

KANSAS STATE UNIVERSITY
Manhattan, Kansas

2019

Approved by:

Major Professor
Saugata Datta

# Copyright

# Abstract

The present study is one of the first attempts to document the mechanisms and model the flooding within Salt Creek watershed. Available historical data have been analyzed to deduce changes to the physical landscape and the climate within the watershed. An analysis of soil physical properties was done to assess permeability. Real-time measurements of precipitation and water level were collected from the Salt Creek over a course of four months. An ANUGA hydrodynamic model based on variation in precipitation intensity and depth simulated flood extent of three precipitation intensities: 1.12cm/hour, 2.54 cm/hour, and 3.73cm/hour. Historical data shows that Salt Creek watershed has experienced a 7.9% decrease in natural grasslands from 1990 to 2005 and a 15cm increase in average annual precipitation from 1902 to 2016. The precipitation and water level data taken in the field show that there is a 5-7 hour lag time between peak precipitation intensity and peak water level. Particle size analyses (PSA) show that, out of twenty-four soil samples, sixteen (67%) are a silty loam, three (13%) are silty clay loam, two (8%) are very fine sandy loam, with one (4%) each of silt, coarse sand, and coarse sandy loam. Falling-head permeability tests determined an average saturated hydraulic conductivity ($K_s$) of 0.29µm/s. Associated ponding times for dry soils are ~66% longer than those of wet soils, and ponding times decrease rapidly at precipitation rates in excess of a 2.54cm/hour precipitation intensity. The ANUGA models produced are unable to accurately simulate the flood events, as simulated flood extents are much lower than those from actual flood events. It is hypothesized that the nearby Fall River influences water levels within Salt Creek during large-scale, high-volume precipitation events by pushing excess floodwater into the Salt Creek's channel. This is likely the result of a constricted floodplain in the Fall River drainage, due to the presence of a limestone formation downstream from the confluence of Salt Creek with the Fall River.

# Table of Contents

# List of Figures

# List of Tables

# Acknowledgements

I would like to graciously thank those that have supported this project with their time and/or finances. First and foremost, I thank my family and friends for their support and encouragement during all of my studies. I would like to thank my committee members Dr. Saugata Datta, Dr. Abby Langston, Dr. Claudia Adam, and Dr. Pamela Kempton for their engagement in the development of my thesis.

I would like to thank Fredonia, Kansas Wilson County Conservation District (WCCD) director Pamela Walker and her WCCD peers for their enthusiastic willingness to help with any part of this project, including the gathering of financial support for field equipment. Pamela, as well as Zach Ecton, Rod Vorhees, and Erik Patton, took time out of their day to meet with Dr. Datta and I to discuss Salt Creek in a field trip and I thank them for that educational experience very much!

I had a lot of help in my field work. A big shout out to my South African pals Simon Goble and Eduard Uys for their gracious help in using the hand-drilled auger to retrieve soil samples on a warm day. That was hard work and they did it with a smile! Thank you to my father who helped me build my pressure transducer vessels as well as helping me install the rain gauges. A special thank you goes to the lab tech in the PaleoLab, Jennifer Roozeboom, for her patience, knowledge, and helpfulness in the particle size analysis phase of my research.

During my thesis I was blessed with an awesome full-time job in Manhattan. My coworkers were nothing but supportive and flexible, allowing me to do what I needed to in order to work on my thesis. They are great! Thanks Charlotte, Janelle, Andy, and Sean!

Finally, I would also like to thank all my scholarship and grant donors who have allowed me to relieve some of the financial burdens that come with higher education and research. The late Paul Strunk and his wife Deanna, the Schultz Memorial Fund, Wilson County Conservation District, and the Kansas Geological Foundation have all contributed to this study and I sincerely thank them.

# Dedication

This thesis is dedicated to those in Southeast Kansas who were affected by the 2007 flood and suffered from the loss of homes, businesses, and/or personal belongings. It was this flood—and the subsequent, smaller floods— that influenced my decision to study hydrology and pursue a thesis that analyzed flood events in hopes of providing more insight to the mechanisms of flooding in this area.

# Chapter 1 - Introduction

## 1.1 History of Flooding in Salt Creek Watershed

Salt Creek, whose headwaters originate west of Fredonia in the agriculture-dominated southeast corner of Kansas in Wilson County, is frequented by flood events. The 2007 flood was considered a 0.2% flood, or a 500-year flood (AMEC Foster Wheeler, 2017). The 2007 flood was produced from a 5-day rainfall event between June 27th, 2007, and July 1st, 2007. The rainfall in each day is as follows: 0.64cm, 3.38cm, 13.21cm, 29.87cm, and 0.64cm (NOAA, 2017b). The 5-day rainfall event totaled 50.27cm and in only two days. Fredonia and the surrounding area experienced rainfall that is equal to one-third of its average annual precipitation (NOAA, 2017b). Estimates of flood extent by residents and appraisers placed the peak flood water level at 5m high in the West Park, which is photographed in Figure 1.

**Figure 1:** Morning of July 1st, 2007 after nearly 30cm of rain fell overnight in an already flooded channel. This image shows the stockyards and veterinary clinic in the bottom center of the photo. Orange arrows indicate the main channel of Salt Creek as it runs through the West Park. *Image source unknown.*

A much smaller, but impactful, flood occurred on September 9th, 2016. This flood was produced from a 9.45cm overnight rainfall event (NOAA, 2017b) and was documented by photos at two different times of the day in the West Park area of the watershed. As no hourly precipitation data were available at this time, rainfall is estimated to have stopped between 4:00 a.m. to 6:00 a.m. on the morning of September 9th, 2016. At 8:00 a.m., Salt Creek reached the top of its banks, and at 12:00 p.m. flood waters stretched approximately 160m to the west side of the creek.

A third flood occurred on September 7th, 2018, in which 7.62cm fell in 2.5 hours. The day prior on September 6th, 2018, 5cm had fallen throughout the day. Before the September 6th rainfall event, Salt Creek was mainly stagnant. Detailed measurements of water level for this flood are not

available, because the field equipment had been removed from the channel at this time for monthly manual data extraction.


**Figure 2:** Image on the left is a June 2014 *Google Street View* photograph which displays the normal flow for Salt Creek. The image on the right is during the September 9th, 2016 flood event that greatly surpassed the banks of the creek in the West Park.

An interesting note is that when local Wilson County Conservation District Manager, Pamela Walker, and Fredonia Fire Chief, Zac Ecton, were asked how long it took for flood waters to recede, they both agreed that it only took only 5-6 hours for the floodwaters from the July 2007 flood to recede. This swift receding of floodwater was also noted in the much smaller September 2016 and 2018 floods.

According to informal interviews with residents, a number of large and small flood events have occurred in Salt Creek watershed besides the two recorded events mentioned above. Unfortunately, no data for these floods exist aside from the occasional photograph, and for larger events, such as the 2007 flood, appraiser flood extent measurements may exist. This gap in historical flood data, combined with limited understanding of geologic and pedologic features in the area, has left a community without a means to begin protecting themselves from future flooding through mitigation.

# Chapter 2 - Background

## 2.1 The Hydrologic Cycle

The *hydrologic cycle* is the fundamental concept of hydrology and is therefore a fundamental part of understanding flooding. The hydrological cycle involves several processes that work together to move water in its liquid (rain), gaseous (water vapor), and solid (ice) forms. Solar energy is the main driver of the hydrologic cycle, as water vapor formation and transportation are largely driven by energy from the sun (Hornberger et al., 1998). Another key driver of the hydrological cycle is gravity, the governing principle of precipitation and flow.

The hydrological cycle starts with the *evaporation* of ocean water, which accumulates in the atmosphere. This accumulation of water vapor becomes heavy and eventually falls onto continents or into the oceans as *precipitation* (rain, snow, sleet, hail, etc.). When this precipitation reaches the land surface, it is either intercepted and retained by vegetation or soaks into the soil in a process called *infiltration*. What is not infiltrated into soils flows across the surface of the Earth by the force of gravity, this excess surface flow is called *runoff*. Some of the water on the surface can be returned to the atmosphere through evaporation or *transpiration* (water returned to atmosphere via plants). The cycle then repeats.

## 2.2 Flood Risk and Prediction

A flood is commonly defined as a situation in which water surpasses the banks and flows into areas it usually does not (Adiat, Nawawi, & Abdullah, 2012; Pivot, Josien, & Martin, 2002). Flooding can occur anywhere and at any time. Floods in magnitude, frequency, and duration, with all of these depending on a multitude of factors (discussed in Section 2.4). The damages that floods cause can be extreme, causing hundreds of thousands of dollars or more in damage to infrastructure, homes, crops, and property (NOAA-NWS, n.d.).

While floods are nearly impossible to predict, organizations such as the U.S. Geological Survey (USGS) have used long-term stream gauge data as “warning systems”. These stream gauges collect real-time water level data and interpretation of these data allows for an estimate of future conditions that may result from a storm event. Unfortunately, many small streams do not have stream gauges recording live data long enough to make this estimate of future condition, or they may not have stream gauges at all, making accurate predictions of floods nearly impossible

using traditional methods. Despite this, hydrodynamic modeling software has made it possible to estimate flood conditions using regional characteristics such as topography, soils, and climate data.

### 2.2.1 FEMA Flood Maps and Flood Frequency Analysis

The 2007 flood affected not only Salt Creek but other creeks in the area as well. This flood caused many of area creeks' floodwaters to surpass the boundaries of the current Federal Emergency Management Association's (FEMA) 1% flood map (Bailey, 2016). Previously known as the "100-year flood", professionals now prefer the use of the term "1%-flood", as the general public assumed the 100-year floods occur every 100 years, although in reality, the 100-year flood occurs *on average* every 100 years (FEMA, 2004). The definition of the 1%-flood is a flood that, on average, has a probability of 0.01 to be equaled or exceeded every year (FEMA, 2004). The 1%-flood discharge is different depending on the river or stream it is associated with and may change as the regional characteristics (land-use, climate, etc.) change.

In response to the massive 2007 flood event, FEMA and the Kansas Department of Agriculture's (KDA) Division of Water Resources (DWR) created a new 1% floodplain map for Wilson County. At the time of this writing, the new floodplain map is still under review, but a draft map has been made available along with a detailed report (AMEC Foster Wheeler, 2017). To create this new floodplain map, KDA-DWR used new methodology compared to that of previous flood map creation. LiDAR imagery and rainfall-runoff models using HEC-HMS provided a more accurate estimate of the 1% floodplain. This hydrologic study was performed to develop peak discharges for the 10%, 4%, 2%, 1%, 1%-minus, 1%-plus and 0.2% annual chance storm events (AMEC Foster Wheeler, 2017). The 1%-plus and -minus storm events are determined using error bands on the precipitation estimates, and curve numbers used in the HEC-HMS model to develop the excess precipitation hyetographs (FEMA, n.d.).

Approximately 6.7km of Salt Creek channel was used in KDA-DWR's creation of the rainfall-runoff model. Table 1 lists the calculated rainfall depths and their annual chance of occurrence. Table 2 displays the product of this KDA-DWR project. It is important to note that at the time of writing this thesis, the AMEC Foster Wheeler (2017) report was only available in draft form, so minor changes may ultimately be made to the data in the final publication depending on if local residents have a conflict with the proposed floodplain map.

| Event (annual chance) | 24-Hour Rainfall Depth (cm) |
|---|---|
| 10% | 14.0 |
| 4% | 17.5 |
| 2% | 20.6 |
| 1% | 23.6 |
| 1%-minus | 20.8 |
| 1%-plus | 27.2 |
| 0.20% | 32.5 |

**Table 1**: Rainfall depth associated with the event's annual chance of occuring for Salt Creek Watershed. Data adapted from AMEC Foster Wheeler (2017).

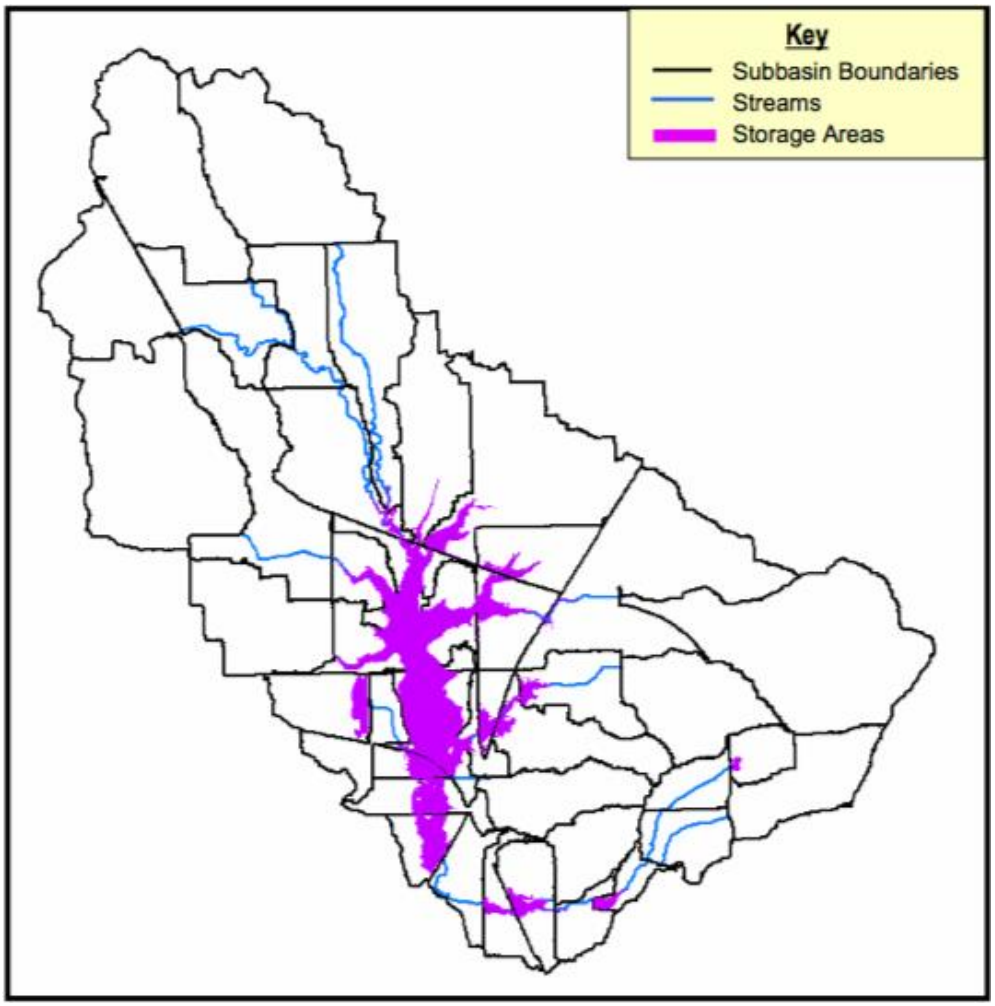


**Figure 3:** Extent of maximum water elevation of modeled storage areas during 1% chance storm event for Salt Creek Watershed. Map by AMEC Foster Wheeler (2017).

| Flooding Source and Location | Drainage Area ($km^2$) | Peak Annual Chance Discharges ($m^3/s$) | | | | | | |
|---|---|---|---|---|---|---|---|---|
| | | 10% | 4% | 2% | 1%- | 1% | 1%+ | 0.20% |
| **Salt Creek** | | | | | | | | |
| At Confluence w/ Salt Creek Tributary 1 | 49.2 | 154.0 | 196.9 | 232.1 | 234.9 | 266.9 | 304.6 | 360.9 |
| At Washington Street | 43.0 | 145.2 | 186.1 | 219.8 | 222.5 | 252.6 | 286.5 | 337.9 |
| At 1150 Road | 35.5 | 103.3 | 116.3 | 125.4 | 126.1 | 133.1 | 140.1 | 149.8 |
| **Salt Creek Tributary 1** *(location unspecified)* | | | | | | | | |
| At Mouth | 5.3 | 21.4 | 29.9 | 37.7 | 38.3 | 44.9 | 51.8 | 61.7 |
| At Cement Plant Road | 3.4 | 14.7 | 21.6 | 28.3 | 28.9 | 34.9 | 42.7 | 54.3 |
| At US Highway 400 | 1.2 | 9.3 | 12.4 | 15.2 | 15.4 | 17.9 | 21.0 | 25.7 |
| **Salt Creek Tributary 3** *(location unspecified)* | | | | | | | | |
| At Mouth | 3.9 | 39.7 | 67.7 | 92.6 | 94.6 | 118.8 | 148.3 | 190.1 |
| At Kansas and Oklahoma Railroad | 3.4 | 27.9 | 35.5 | 42.3 | 42.9 | 48.7 | 55.5 | 68.2 |
| At 15th Street | 1.5 | 14.3 | 19.1 | 23.3 | 23.6 | 27.5 | 32.3 | 39.5 |

**Table 2:** Estimated peak discharges and their respective annual chance that occur at various locations in Salt Creek. Data adapted from AMEC Foster Wheeler (2017).

## 2.3 The Role of Soils in Flooding

### 2.3.1 Soil Texture and Particle Size Distribution

Soil texture is defined as the proportions of the grain sizes sand, silt, and clay in a soil sample. There are many different classifications for these sizes, but this study will use the classification by the USDA's Natural Resource Conservation Service (USDA-NRCS, 2019) seen in Table 3. The particle size distributions of a particular soil indicate the soil texture. Particle size distributions of the soil change characteristics such as infiltration, permeability, and runoff rates. There are three main particle sizes that are represented on the gradation curve: clay, silt, and sand (Gupta, 2008). Soils with high percentages of finer particles such as clays and silts leave little pore space for water movement to occur, making infiltration and permeability slow which in turn increases runoff.

| Textural Fraction | Min Size (µm) | Max Size (µm) |
|---|---|---|
| coarse sand | 500 | 1000 |
| medium sand | 250 | 500 |
| fine sand | 100 | 250 |
| very fine sand | 50 | 100 |
| silt | 2 | 50 |
| clay | 0 | 2 |

**Table 3:** USDA-NRCS (2019) classification for grain sizes.

### 2.3.2 Antecedent Soil Moisture

Antecedent soil moisture is defined as the moisture that is in the soil before a precipitation event occurs. The runoff ratio describes the fraction of precipitation that appears as runoff, which depends largely on the antecedent soil moisture and soil moisture content must exceed a threshold before notable runoff occurs (Fryirs & Brierley, 2013). Soil moisture can occur from precipitation events, irrigation of agricultural land or lawns, or other miscellaneous events where water is applied to a surface. Alternatively, soil moisture can also occur from groundwater being pulled toward the surface through capillary action.

### 2.3.3 Infiltration vs. Runoff

The hydrologic processes of infiltration and runoff are essential to assessing flood risk (see Figure 4). Infiltration is the movement of water into soil by gravity and capillary action and is affected by viscous forces involved in the flow through soil pores as quantified in terms of permeability or hydraulic conductivity (Tarboton, 2003). Once infiltrated, this water is referred to as soil moisture (Fryirs & Brierley, 2013), as discussed in the above section. In the study of floods, infiltration rate is of particular interest. *Infiltration rate* is the rate at which water on the surface permeates into the soil. Infiltration rate is affected by factors such as antecedent soil moisture, soil type, sediment size, precipitation intensity, and slope (Fryirs & Brierley, 2013). The maximum rate at which water can percolate through the soil is known as *infiltration capacity*. Note that infiltration capacity is a rate, not a depth quantity (Tarboton, 2003). Infiltration rate and capacity are measured in the field or lab using the soil of interest. Saturated hydraulic conductivity (*Ks*) is the infiltration rate once the soil has become fully saturated and the infiltration rate is constant.

Runoff is what occurs if the amount or rate of water introduced to a surface exceeds the infiltration rate. This can be quantified by the equation:

$$R = w - f \qquad \textit{eq. 1}$$

where $R$ is the overland flow runoff rate, $w$ is surface water input rate, and $f$ is the infiltration rate (Tarboton, 2003). A graphical representation of this relationship is displayed in Figure 4. Depending on this antecedent soil moisture, runoff usually occurs during the most intense phase of rainstorms (Fryirs & Brierley, 2013).

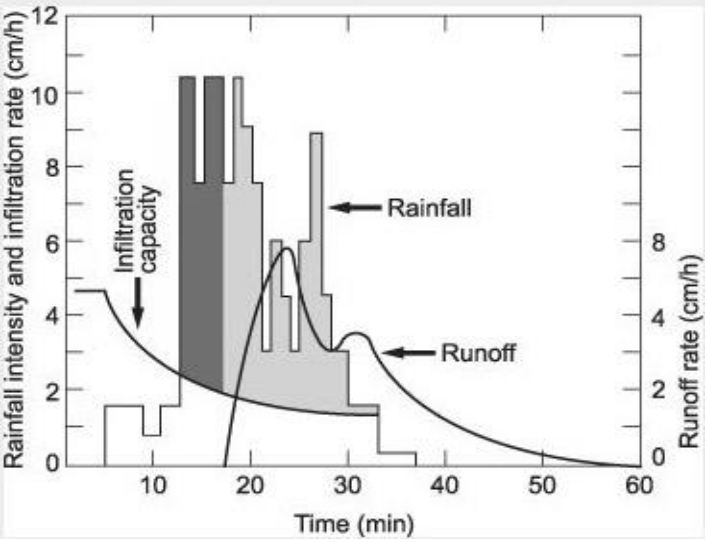


**Figure 4:** Relationship between rainfall, infiltration, and runoff modified from Dunne and Leopold (1978). The dark grey columns represent precipitation that is caught in depressions in the ground. The light grey columns represent precipitation that becomes runoff. Infiltration capacity decreases as total rainfall depth increases. Runoff rate peaks after peak rainfall intensity occurs and tapers off as rainfall halts.

#### 2.3.3.1 Ponding Time

Ponding time (also referred to as time of ponding) is the moment in time when the precipitation rate exceeds the infiltration rate and runoff begins to occur. Ponding time ($t_p$) is a function of the wetting front soil suction head ($H_f$), length of the wetting front ($L_f$), saturated hydraulic conductivity ($K_s$), infiltrability ($I$), rainfall rate ($r$), initial volumetric water content ($\theta_i$), and saturated volumetric water content ($\theta_s$). Ponding time can be estimated by the following series of equations:

$$L_f = \frac{H_f}{\left(\frac{r}{K_s}\right)-1} \qquad \textit{eq. 2}$$

$$I = L_f(\theta_s \times \theta_i) \qquad \textit{eq. 3}$$

$$t_p = \frac{I}{r} \qquad \textit{eq. 4}$$

### 2.3.4 Permeability

Soil is a permeable material, as it contains variable volumes of pore spaces that are filled with air or fluid. The permeability of soil is the ability of fluid to flow through these pore spaces in the soil. Permeability is measured as a length per unit time. The permeability of a soil is affected by the ratio of voids, distribution of inter-granular pores, and the antecedent moisture content (Elhakim, 2016). It is typical for permeability to be greater in soils that contain larger particle sizes where pore spaces are larger. Permeability in fine-grained soils is measured using a falling-head permeability test. However, it is important to note that due to the manner in which soil samples are taken (i.e. soil samples are disturbed or broken up), lab-tested permeability is not a perfect representation of the in-situ soil permeability.

Due to the nature of permeability tests and soil texture, using estimated $K_s$ values, like those in Table 4, to broadly define a "standard" $K_s$ value for a given soil texture is not useful given that $K_s$ varies by two orders of magnitude, dependig on a variaty of factors. Nagy et al. (2013) identified a number of these factors, which are listed below:

- grain orientation and shape
- quantity and connection of pore spaces (compaction, soil texture, etc.)
- uniformity coefficient
- the properties of the passing liquid (markedly viscosity),
- hydraulic gradient and Reynolds number
- migration and wash-out and wash-in of grains

| **$K_s$ Values by Texture (µm/s)** | | |
|---|---|---|
| **Texture** | **Rawls, et.al., 1982** | **USDA, n.d.** |
| sand | 32.72 | 42.34-141.14 |
| loamy sand | 8.31 | |
| sandy loam | 3.03 | 14.11-42.34 |
| loam | 0.94 | 4.23-14.11 |
| silt loam | 1.81 | |
| sandy clay loam | 0.33 | 1.41-4.23 |
| clay loam | 0.28 | |
| silty clay loam | 0.28 | |
| sandy clay | 0.17 | 0.42-1.41 |
| silty clay | 0.14 | |
| clay | 0.08 | |
| Cd horizon<br>Natric horizon | none | 0.00-0.42 |

**Table 4:** Saturated hydraulic conductivities for given soil textures. There is no "standard value" for $K_s$, as seen in this table. The $K_s$ values between publications range so greatly, it is nearly impossible to compare results with any degree of accuracy.

## 2.4 Other Factors That Affect Flood Potential

Flooding is largely caused by an excess of water that is usually produced by runoff during storm events (Section 2.3.1). However, the amount of said runoff greatly varies depending on the characteristics of an area such as climate, slope, soils, and subsurface interference (lithology and groundwater). Although flooding usually stems from unusually large precipitation events, there are various factors that contribute to the flooding potential of a stream or river. These factors can be either natural or anthropogenic (human-induced), or a combination of the two.

### 2.4.1 Climate and Climate Change

The first natural factor that affects flood potential is climate, specifically precipitation. The amount of precipitation that falls in an area is known to be heavily influenced by temperature, that is, cold air cannot hold as much water vapor as warm air (Hornberger, Raffensperger, Wiberg, & Eshleman, 1998). Cooling of an air mass usually produces saturated conditions; hence, storms tend to manifest with a decrease in temperature.

Climate change has been an increasingly significant component of flood-related research (Milly et al., 2002). In the last century, the state of Kansas has warmed by at least half a degree Fahrenheit (EPA, 2016). The implications of this slight increase in temperature are decreases in soil moisture, which lead to increases in humidity; average rainfall; and the frequency of heavy rainstorms increasing in some areas while other areas are experiencing drought (EPA, 2016; NASA, n.d.). The National Climate Assessment (2014) concluded that from 1958 to 2012, the Southern Great Plains (Kansas, Oklahoma, and Texas) have experienced a 16% increase in the amount of precipitation that falls in heavy events, which they define as the heaviest 1% of all daily events. Changing climate also changes vegetation cover, as different species have varying sensitivities to temperature and precipitation fluctuations (Fryirs & Brierley, 2013). The effects of vegetation on flood potential will be discussed in Section 2.4.4.

An interesting, yet less understood, potential contributor to climate change in southeastern Kansas is western Kansas's large use of irrigation waters from the Ogallala Aquifer. DeAngelis et al. (2010) found that during the 20th century July precipitation increased 15–30% for areas from eastern Kansas to Indiana. However, they report numerous factors that could be contributing to this statistical increase in July precipitation—namely greenhouse gases, sea surface temperatures,

and natural climate change. Moreover, it is nearly impossible to separate the responses to the different variables (DeAngelis et al., 2010).

### 2.4.2 Slope

When rain falls on a surface, the slope of that surface determines the velocity at which the rainfall runoff will descend downstream towards the channel. Increasing the slope increases the velocity, and vice versa. As the velocity increases, the ability of runoff to infiltrate into the soil decreases. This, in turn, increases the amount of runoff that enters the stream channel that then increases the chance of flooding in that channel. However, this situation can be reversed in areas with very flat topography, as ponding of runoff outside of the creek occurs which can result in flood conditions (Adiat, Nawawi, & Abdullah, 2012).

### 2.4.3 Lithology and Groundwater

Lithology is the physical characteristics of the geology of an area. Lithologic controls (i.e. geology) can influence the size of a creek's floodplain and the infiltration capacity of the soils. Groundwater is simply water that resides in permeable rock formations. The water table is the surface of the zone of saturation or the area under the surface of the earth that is saturated with water. A shallow water table, that is, a water table that is close to the surface of the earth, can increase the antecedent moisture of the soil due to capillary forces pulling water towards the surface. Therefore, the presence of a shallow water table can reduce infiltration capacity and increase runoff (Fryirs & Brierley, 2013).

### 2.4.4 Land Cover and Land Use (LCLU)

Land cover and land use (abbreviated as LCLU) greatly affect the amount of runoff and changes in LCLU can alter the ecological system (Sajikumar & Remya, 2014; Bronstert, Niehoff, & Burger, 2002). In this section, land cover (LC) refers to any kind of material at the surface of the Earth; for example, naturally occurring cover such as grasses, trees, rocks, and water, as well as unnaturally occurring cover such as roads, turf, and buildings. Land use (LU) refers to any number of uses that a particular area has. Primary examples of land use are cropland (tilled or untilled), urbanized areas (residential or industrial), forested areas, and grasslands (grazed or un-grazed by livestock).

Changes to LCLU are usually human-induced rather than natural (Sajikumar & Remya, 2014). As the world population continues to rise ("World population," 2015), natural lands are converted to fill the needs of the masses, whether it be urbanization or agriculture. Land use change often does not comply with the natural hydrologic or biochemical cycles of that area; hence, degradation of the landscape often occurs after a rapid change in land cover or use (Yusuf, Guluda, & Jayanegara, 2017). Land cover change and water availability have a cyclical pattern, meaning that changes in land cover cause changes in water availability that further change the land cover (Sajikumar & Remya, 2014).

#### 2.4.4.1 Urbanization

Urbanization is the process of making an area more urban, for example, the building of buildings, roads, sewers, and other infrastructure that allows cities to function properly. Although flooding solely due to urbanization is not usually an issue in rural areas such as Wilson County, the impacts from the existing small towns can still cause adverse effects to its watershed. Urbanization can create an increase in runoff due to the increased presence of impermeable surfaces as well as the compaction of soil as a byproduct of equipment used in the building processes. Compaction of soil leads to increased runoff (Alaui, Rogger, Peth, & Gunter, 2018).

#### 2.4.4.2 Agriculture and Industry

Agriculture and industry are well-known forces of disturbance to the natural world. Agriculture includes both farming (crops) and ranching (livestock). Industry is a broad term but includes the processing of raw goods gathered from the environment such as logging, oil and gas extraction and refinement, and mining, all of which involve land-disturbance to some extent. The significance of agriculture and industry in floods is mainly the need to remove natural land cover in order to operate. Removing land cover, as discussed in 2.4.4, increases runoff amount and velocity, contributing to larger, faster flood waters.

The Kansas economy is supported by millions of acres of small- and large-scale farming operations that are scattered throughout the state (USDA-NASS, 2019). These farms commonly produce row-crops such as corn, wheat, milo, and soybeans (USDA-NASS, 2019). The tillage practices of the cropland are up to the individual farmer, although the environmentalist movement has prompted many farmers to convert to no-till tillage practices in an effort to reduce soil erosion

and conserve water. According to the USDA (2012), in 2012 Kansas farmers practiced no-till farming more than any other state (over 42,000 $km^2$ of no-till fields). No-till farming has been a popular effort to reduce erosion of soils and soil-water evaporation in fields. It has been proven experimentally that no-till practices significantly reduce soil erosion rates as well as runoff rates (DeLaune, 2012; Volkmer, 2014). Reducing runoff rates can reduce the volume and velocity of floodwaters.

# Chapter 3 - Hypothesis and Objectives

This study was conducted to provide a greater understanding of surface inundation in Salt Creek watershed, which has a history of floods that affect local homes and businesses. This study takes a multidisciplinary approach to study flooding, using not only topographical and climatic characteristics that are commonly associated with floods, but also incorporating data on the physical characteristics of the soils and land-use change.

A relative lack of direct data related to Salt Creek necessitated the use of historical information so that flood risk can be assessed. According to the Federal Emergency Management Agency (FEMA), there are eight sources of information to aid in determining the flood risk of an area: (1) site-specific data, such as stream gaging records; (2) rainfall records; (3) historic information, such as flood marks on buildings and other structures and areas flooded; (4) newspaper accounts and diaries; (5) marking of flood levels after an event, (e.g. appraiser flood-extent measurements); (6) botanical evidence, such as scars on trees; (7) physical and geomorphic techniques; and (8) regional information, i.e., look at flood occurrences along similar streams in the area (Wright, 2007). Many of the floods within Salt Creek have not been well documented in terms of marking of floodwaters in the past.

## 3.1 Hypotheses

(1) Initial runoff conditions are poor due to impermeable clay and silt soils that were created from the underlying shale bedrock within Salt Creek watershed. It is likely that a significant portion of precipitation is transported directly into the stream as runoff.

(2) Multiple factors are affecting flood extent; including land cover and land use (LCLU) change, climate change, soil characteristics, and debris pile-ups. Some or all of these factors may influence on the extent of floods in Salt Creek.

(3) The role of ground elevation in Salt Creek may have a significant influence on the extent of floods. The ANUGA hydrodynamic model will produce simulated flooding extents for multiple precipitation intensities with the Salt Creek watershed.

## 3.2 Objectives

(1) *Conduct soil analyses of Salt Creek watershed in order to have a more accurate idea of the soil types in the area*. Currently, many of the soil physical properties within this watershed, such as saturated hydraulic conductivity ($K_s$) and the percent of clay and silt in the soil are estimated based on soil texture. Because soil type plays a significant role in the flood response of an area, an analysis of soil will be conducted. Soil analyses will consist of particle size analyses to determine soil texture and falling-head permeability tests to determine saturated hydraulic conductivity. Particle size analysis followed by permeability testing for multiple locations within Salt Creek watershed will provide useful information relating to runoff rates. Additionally, a ponding time calculation will be performed using the permeability test results.

(2) *Determine what factors are contributing to flooding in Salt Creek and, if applicable, whether these factors have changed through time through a historical data analysis*. These factors include soil, lithology, groundwater, land-use change, and climate.

(3) *Collect data on precipitation and water level within Salt Creek watershed and interpret these data to assess the relationship between precipitation intensity and duration and water levels of Salt Creek.*

(4) *Model the relationship between precipitation intensity and depth with Salt Creek's water levels using the ANUGA hydrodynamic model*. Two of the three ANUGA scenarios tested will be based on real flood events, i.e. those from 2007 and 2016. Comparisons of the ANUGA model simulations will be made to the real flood events.

During the course of this study, a fifth objective was created:

(5) While in the process of modeling the Salt Creek watershed's flood patterns, elevation characteristics created by the underlying geology of this area prompted an investigation of the Fall River's effect on the Salt Creek floods. This relationship was found late in the study, but an effort was made to introduce evidence of the relationship as well as propose

topics for future studies that would be beneficial in explaining Salt Creek's flooding behaviors.

# Chapter 4 - Study Area

## 4.1 Location

Salt Creek is a stream system located in northwest Wilson County, Kansas. Salt Creek confluences with the Plum Branch of the Fall River. Fredonia is almost completely encompassed by Salt Creek watershed. It was established in 1871 and currently hosts a population of approximately 2,000 people. The rural area surrounding Fredonia is primarily used for farming and ranching.

A creek's watershed (also called a basin or catchment) is the drainage area that flows into that stream. Watershed shape and size are influenced by the elevations and slopes of the landscape. Salt Creek watershed was delineated within the free, open-source GIS software Quantum GIS (QGIS) using a 1/3 arc-second digital elevation model (DEM) produced by the United States Geological Survey (USGS) (U.S. Geological Survey, 2017). The delineation is seen in Figure 5. Salt Creek watershed covers approximately 49.5km$^2$.

In this study, more focus will be placed on the West Park area of Salt Creek, as this area is near the outlet of the stream and flooding tends to be documented more here than anywhere else in the watershed. This area is home to the veterinarian clinic, fair grounds, meat locker, softball fields, rodeo grounds, and stockyards. The West Park section of Salt Creek is a relatively straight channel. It is unknown whether this straightness is a product of past anthropogenic channelization or whether it is a natural occurrence. Riprap (a name given to materials purposefully placed on the stream banks) in the form of large blocks of cement has been placed on the stream banks within the West Park to reduce erosion. There are three bridges and two pipelines that interact with Salt Creek in the West Park. These interactions will be discussed later in this thesis.

## 4.2 Salt Creek Water Use

Water use may impede the implementation of some flood mitigation efforts. Fortunately, Salt Creek has limited water use from humans, making it an optimal channel for flood mitigation, if desired. The bottom third of Salt Creek's main channel exhibits constant streamflow during normal, non-drought seasons (perennial stream-type characteristics) while the upper two-thirds of the channel system exhibit streamflow only during times of rainfall (ephemeral stream-type characteristics).

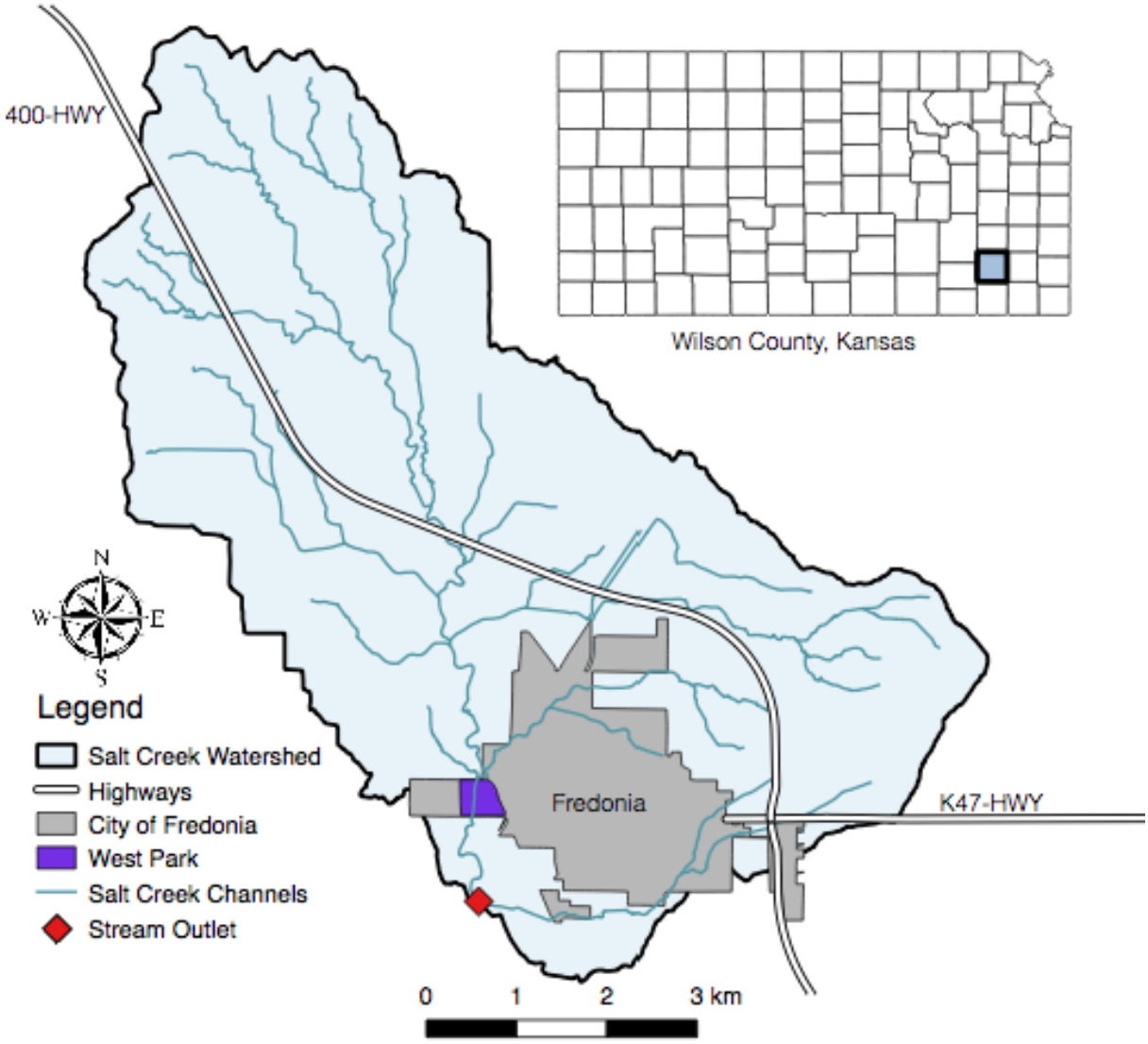


**Figure 5:** Salt Creek watershed location map.

Data on water quality are not available, although it is likely to be poor, as Salt Creek is bounded on most sides by either cropland that utilizes fertilizer, pesticides, and/or herbicides or by fields that host cattle. No water is drawn from Salt Creek for irrigation, drinking water, or other purposes. As the majority of the channels are ephemeral, wildlife such as fish are not suited to live there, making recreational fishing in those areas unfeasible. Although adequate fish habitat may exist within the southern portions of the channel from the West Park to the outlet of the stream, recreational fishing is still limited. Other recreational uses such as swimming and boating are generally impractical due to the narrow, shallow channels.

## 4.3 Climate

Climatic data for Salt Creek watershed is limited in accuracy due to the equipment used to measure the data in Fredonia. The National Oceanic and Atmospheric Association (NOAA) collects precipitation data from the Fredonia area through the use of a standard rain gauge (a glass tube) and has collected air temperature data through the use of a standard thermometer (for years 1948-1986), a maximum/minimum temperature sensor (MMTS) (for years 1986-2006), or a Nimbus temperature sensor (for years 2006-present) (NOAA, 2017b). Additionally, snow is measured by the use of snowboards (NOAA, 2017b). The data collected from the NOAA includes approximately 75% of records from January 1st, 1909 to January 1st, 2017 (Figure 6) (NOAA, 2017b). Figure 6 shows the annual precipitation from 1902 to 2016 for the Fredonia area.

Similar to other areas of the Midwest, Salt Creek watershed receives four distinct seasonal variations in precipitation and temperature. The normal rainfall, snowfall, and minimum and maximum temperatures for these seasonal variations can be seen in Table 5.

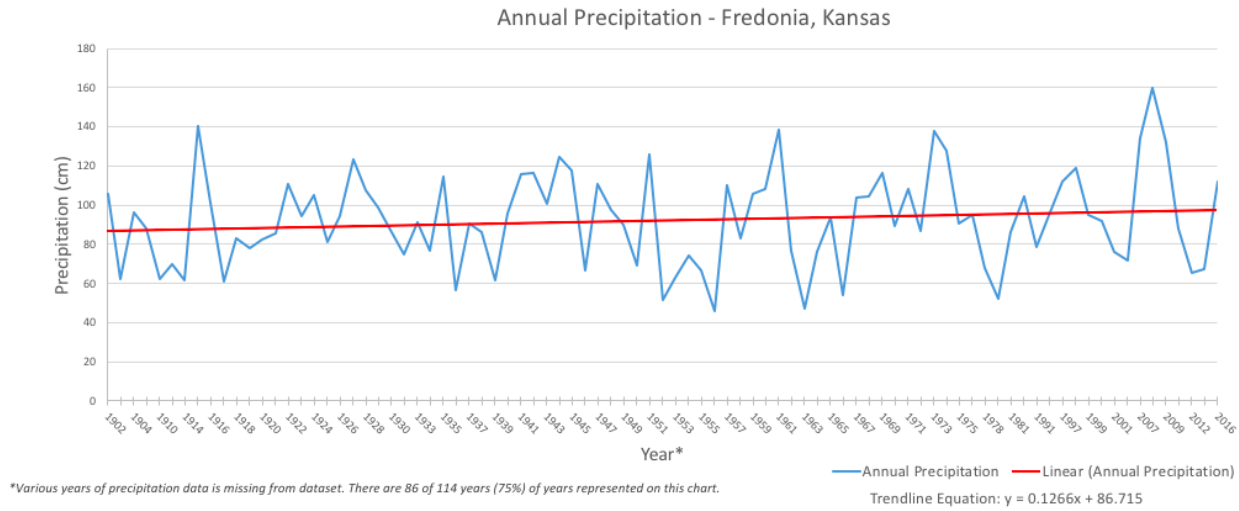


**Figure 6:** Annual precipitation data as reported by the NOAA (2017). The red trend line indicates an overall increasing trend in annual precipitation. The trend line increases by approximately 15cm from 1902 to 2016.

| Season | Month | Normal Rainfall (cm) | Normal Snowfall (cm) | Normal Tmax (ºC) | Normal Tmin (ºC) |
|---|---|---|---|---|---|
| **Winter** | December | 4.1 | 7.4 | 7.4 | -5.3 |
| | January | | | | |
| | February | | | | |
| **Spring** | March | 10.5 | 0.8 | 19.8 | 6.4 |
| | April | | | | |
| | May | | | | |
| **Summer** | June | 12.3 | 0.0 | 31.4 | 19.0 |
| | July | | | | |
| | August | | | | |
| **Autumn** | September | 9.2 | 0.3 | 21.3 | 7.3 |
| | October | | | | |
| | November | | | | |

**Table 5**: Normal climatic conditions for the four seasons in Fredonia, Kansas. Normal climate conditions are calculated from data from the years 1986 – 2010. Tmax = max temperature and Tmin = minimum temperature. Data from NOAA (2017).

## 4.4 Physiographic Region

Physiographic regions or provinces are geographic areas that are defined by geomorphology, geology, and climate. Salt Creek watershed is located in the physiographic region Osage Cuestas. The Osage Cuestas physiographic region is characterized by east-facing escarpments (cuestas) created from uplift and erosion and are contrasted by flat areas and rolling hills (Kansas Geological Survey, 1999). The cuestas have alternating layers of sandstone, limestone, and shale; however, limestone is the dominant rock type. Chert gravel deposits are common in the Osage Cuesta region, likely the result of past limestone erosion (Kansas Geological Survey, 1999). The cuestas can be seen in the far north area of the watershed in Figure 7.

## 4.5 Elevation and Slope

Elevation in Salt Creek watershed ranges from a maximum of 323.0m in the northern area of the watershed and a minimum of 255.7m in the southern area of the watershed. See Figure 7. The maximum slope is 10.8º and the minimum slope is 0.14º as calculated using QGIS. Elevation peaks primarily in the northernmost and easternmost areas of the watershed. It is likely that the limestone in the easternmost high elevation area is due to the presence of limestone (Figure 8).

The northernmost high elevation area may be due to the presence of limestone, however the geologic map shown in Figure 8 is fairly coarse in resolution at this scale.

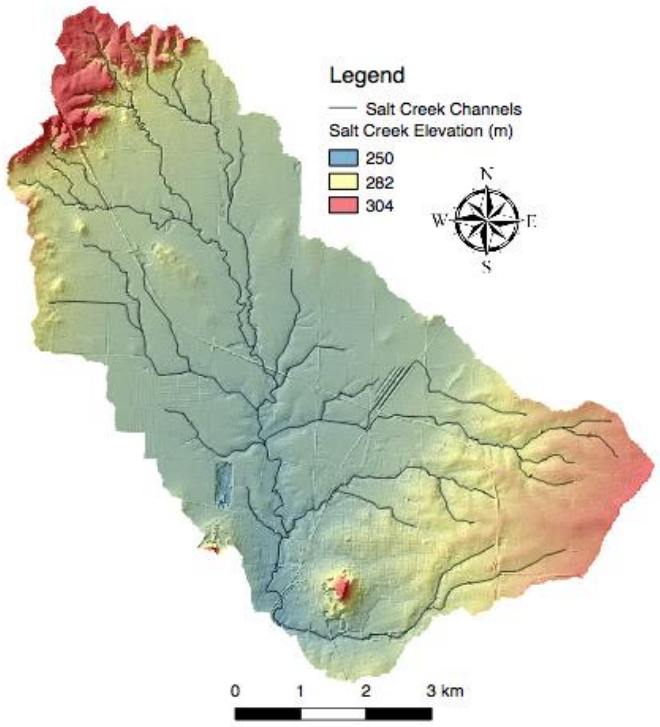


**Figure 7:** Salt Creek watershed elevation with an underlying hill-shade layer to detail terrain.

## 4.6 Geology and Groundwater

The geological map of the study area can be seen in Figure 8. The underlying lithology of Salt Creek is mainly in the Douglas Group's Stranger Formation (~82.8%) with eastern tributaries that extend into the Stanton Limestone of the Lansing Group (~16.5%) (Kansas Geological Survey, 1999). The Stranger Formation and Stanton Limestone are both from the Pennsylvanian System. The Stranger Formation is composed of alternating layers of limestone and shale members and one sandstone member, with shale members being significantly thicker (Kansas Geological Survey, 1999). Where Salt Creek exists south of the West Park, alluvium becomes prominent along the creek.

There are two, prominent limestone and sandstone mounds (known locally as the West and East Mounds, or the Twin Mounds) located near the outlet of the watershed that are not reflected in the geologic map in Figure 8, but can be seen in the DEM in Figure 7 (the mound to the west is only partially located in the watershed). Mounds such as these are relatively uncommon in the region.

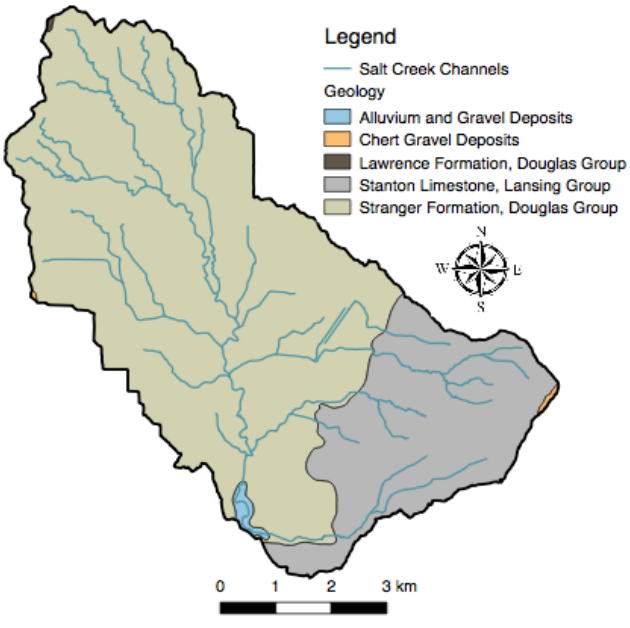


**Figure 8:** Geologic map of Salt Creek watershed. Data from Kansas Geological Survey (2017).

The water table in Salt Creek watershed ranges in depth from 60cm to 213cm below the surface (Kansas Geological Survey, 2018; Swanson, 1989; Soil Survey Staff, 2017). The USGS *Web Soil Survey* (WSS) tool is a free, online resource for finding technical soil data for an area within the United States. The water table depths for Salt Creek watershed are included within the WSS database. The water table, according to the WSS, refers to a saturated zone in the soil that lasts for more than one month (Soil Survey Staff, 2017). WSS estimates the depths to water table by using observations of the water table at selected sites and on evidence of a saturated zone, mainly redoximorphic features, in the soil (Soil Survey Staff, 2017). Approximately 79% of the soils in Salt Creek watershed have a depth to water table of ≤61cm and the remaining 21% of soils have a depth to water table of >200cm (Soil Survey Staff, 2017). According to Kumar and Malik (1990), capillary rise of water in soils with hydraulic conductivity values of 0.5μm/s can reach a height of 141cm above the water table. Because the soils in Salt Creek watershed are mainly silt and clay based, capillary action is stronger as cohesion and adhesion of water molecules is stronger in smaller-grained soils which leads to increased soil moisture above the water table (Boeker & van Grondelle, 1995). Additionally, in fine-grained soils, capillary rise can allow soil to "climb" up to four meters into the soil above the water table (Boeker & van Grondelle, 1995), which in the case of Salt Creek could mean a constant presence of antecedent moisture in the top layers of soil. As described in Section 2.3.2, this antecedent moisture decreases infiltration rate and increases runoff.

## 4.7 Soils

Data for soil type, parent material, and hydrologic soils groups were extracted from the WSS system. Maps for these are seen below in Figures 9, 10, and 11. Soils type descriptions are provided in Table 6. Soil type mainly consists of a mixture of silt loams and clay loams. The most common soil type in the watershed is Woodson silt loam, 0-1% slope (8957), which encompasses approximately 43% of the watershed. As described by Swanson (1989), the Woodson series is generally made up of deep, somewhat poorly drained soils that are very impermeable. The top 20cm (A-horizon) of the Woodson series is typically a silt loam and any deeper than 20cm tends to be a silty clay (Swanson, 1989). Kenoma silt loam, 1-3% slope makes up 10% of the watershed. The Kenoma series is very similar to the Woodson series, in that it is highly impermeable and has a silt loam A-horizon with deeper depths consisting of silty clay textures.

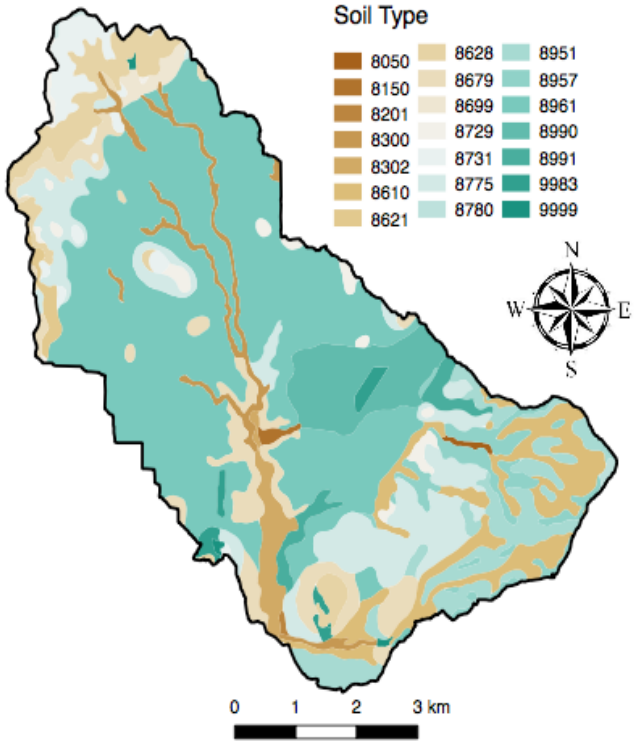


**Figure 9:** Soil type map of Salt Creek watershed.
Data from Soil Survey Staff (2017).

| Symbol | Description |
|---|---|
| 8050 | Girard silty clay loam, 0 to 1 percent slopes, frequently flooded |
| 8150 | Lanton silt loam, 0 to 2 percent slopes, occasionally flooded |
| 8201 | Osage silty clay loam, 0 to 1 percent slopes, occasionally flooded |
| 8300 | Verdigris silt loam, channeled, 0 to 2 percent slopes, frequently flooded |
| 8302 | Verdigris silt loam, 0 to 1 percent slopes, occasionally flooded |
| 8610 | Apperson silty clay loam, 1 to 3 percent slopes |
| 8621 | Bates loam, 1 to 3 percent slopes |
| 8628 | Bates-Collinsville complex, 7 to 20 percent slopes |
| 8679 | Dennis silt loam, 1 to 3 percent slopes |
| 8699 | Dennis-Dwight silt loams, 1 to 5 percent slopes |
| 8729 | Eram silt loam, 1 to 3 percent slopes |
| 8731 | Eram silt loam, 3 to 7 percent slopes |
| 8775 | Kenoma silt loam, 1 to 3 percent slopes |
| 8780 | Kenoma-Olpe complex, 3 to 7 percent slopes |
| 8951 | Wagstaff silty clay loam, 1 to 3 percent slopes |
| 8957 | Wagstaff-Shidler complex, 1 to 8 percent slopes |
| 8961 | Woodson silt loam, 0 to 1 percent slopes |
| 8990 | Zaar silty clay, 0 to 1 percent slopes |
| 8991 | Zaar silty clay, 1 to 3 percent slopes |
| 9983 | Gravel pits and quarries |
| 9999 | Water |

**Table 6:** Soil type descriptions for Figure 9. Descriptions from Soil Survey Staff (2017).

Parent material for Salt Creek watershed's soils coincides with the geology of the area. Higher elevations in the northwest and the South Mound have parent material that consists of mixture of sandstone and shale. The eastern-southeastern portion of the watershed is uniformly limestone. A sizable section of the watershed's soils is derived from silty or clayey alluvium. Figure 10 shows the parent material.

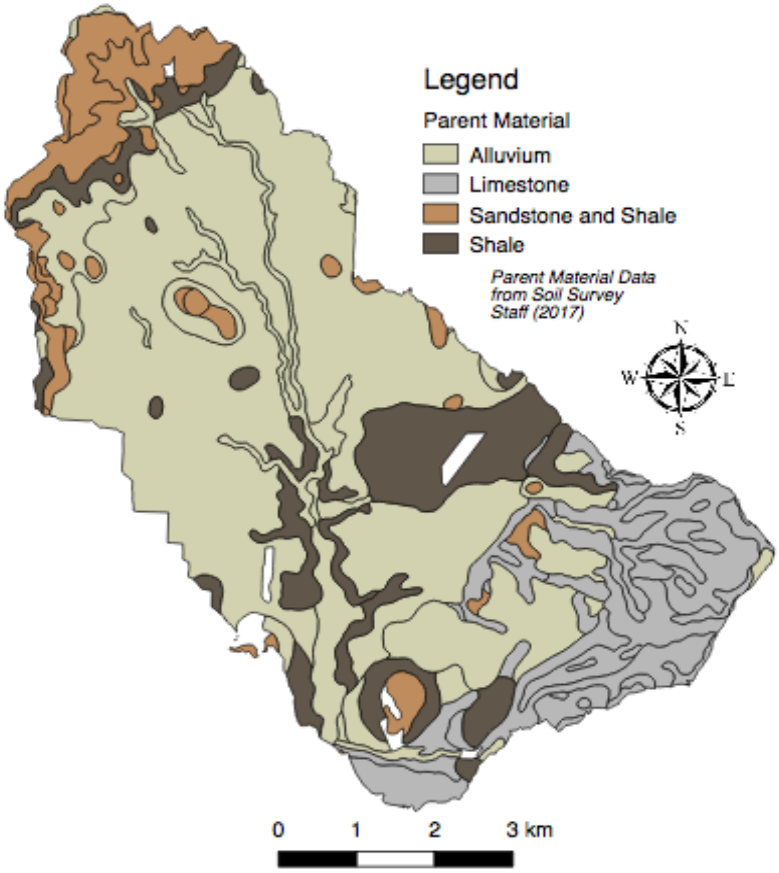


**Figure 10:** Map of parent material of soils in Salt Creek watershed. Data from Soil Survey Staff (2017).

Hydrologic soil groups (HSGs) are a characterization of soil (A, B, C, or D) that is determined by the ability of water to transmit through a layer of soil that has the lowest hydraulic conductivity (Natural Resource Covservation Service, 2009). The groupings are assigned by factors such as soil type and texture and degree of swelling when saturated. Slope is not taken into account when assigning HSGs. HSGs are, in essence, a way to describe the runoff potential of a particular soil. The groupings A, B, C, and D each have a separate estimated runoff potential, with

A having the lowest runoff potential and D having the highest runoff potential. In Salt Creek watershed, HSG D represents 86% of the watershed, meaning that a large portion of the watershed has a high runoff potential. HSGs B and C/D are prevalent around in and around the creek itself. Figure 11 shows the hydrologic soil groups.

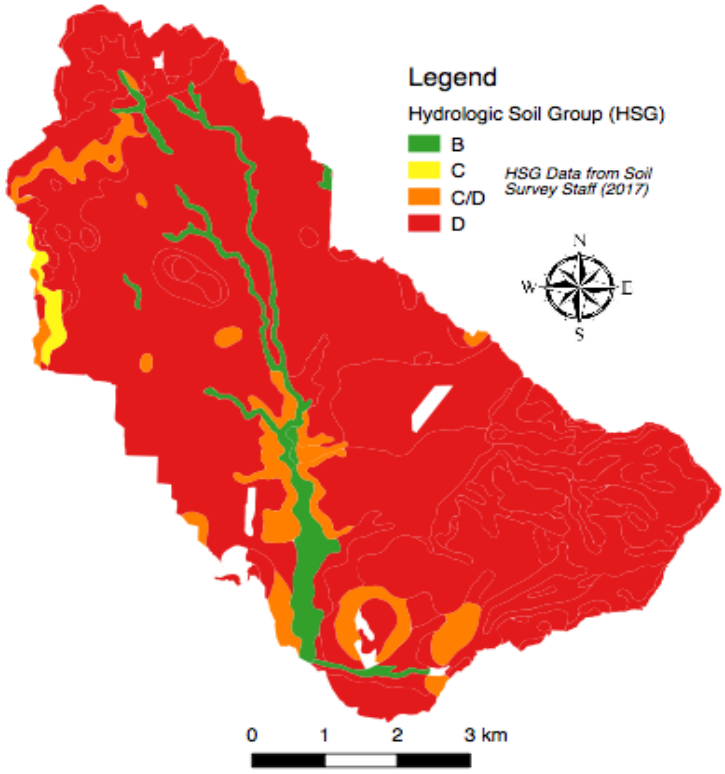


**Figure 11:** Map of hydrologic soil groups of Salt Creek watershed. HSG B represents 5%, HSG C represents 1%, HSG C/D represents 7%, and HSG D represents 86%. White areas do not have HSG data. Data from Soil Survey Staff (2017).

## 4.8 Land Cover and Land Use (LCLU) Change

As mentioned in Section 2.4.4, LCLU changes affect flooding potential. Assessing the changes in LCLU in the past can help predict the changes to LCLU in the future. This allows analysts to estimate what physical changes to soils properties (such as infiltration rates) could be expected in the future (Bronstert, Niehoff, & Burger, 2002). LCLU data used in this report are from the Kansas Land Cover Pattern (KLCP) dataset created by the Kansas Biological Survey (KBS) and Kansas Applied Remote Sensing (KARS) program and sourced from KansasGIS.gov. Figure 12 displays these datasets for Salt Creek watershed for the years 1990, 2005 and 2015. Analyses of the LCLU patterns within QGIS yielded the results shown in Table 7 and Table 8.

Using knowledge of the area, it can be hypothesized what influenced the changes in LCLU from 1990 to 2015. Urban land has decreased as the rural City of Fredonia has decreased in population. Urban openland has increased, likely due to the opening of a hydraulic fracturing "mine" that was located in the northeast section of Fredonia which used a considerable amount of land for deposition of the mined materials. Cropland has increased by utilizing land that was once grassland. Woodland has increased, especially around Salt Creek's main channel, and may be due to the rapid spread of invasive species such as cedar trees. Riparian areas appearing on either side of a stream channel can hold precipitation and store floodwaters (Hey & Philippi, 1995), therefore reducing total flood extent downstream to some degree (Ogawa & Male, 1986). Water has increased due to the creation of a limestone quarry east of Fredonia and a possible increase in the number of ponds constructed for recreational or stock-watering use. There may be a difference in resolution of the data as technology has improved; although this is difficult to account for it should be considered. Due to the somewhat minor changes in LCLU, there is no conclusive evidence that LCLU has contributed to increasing flood extents.

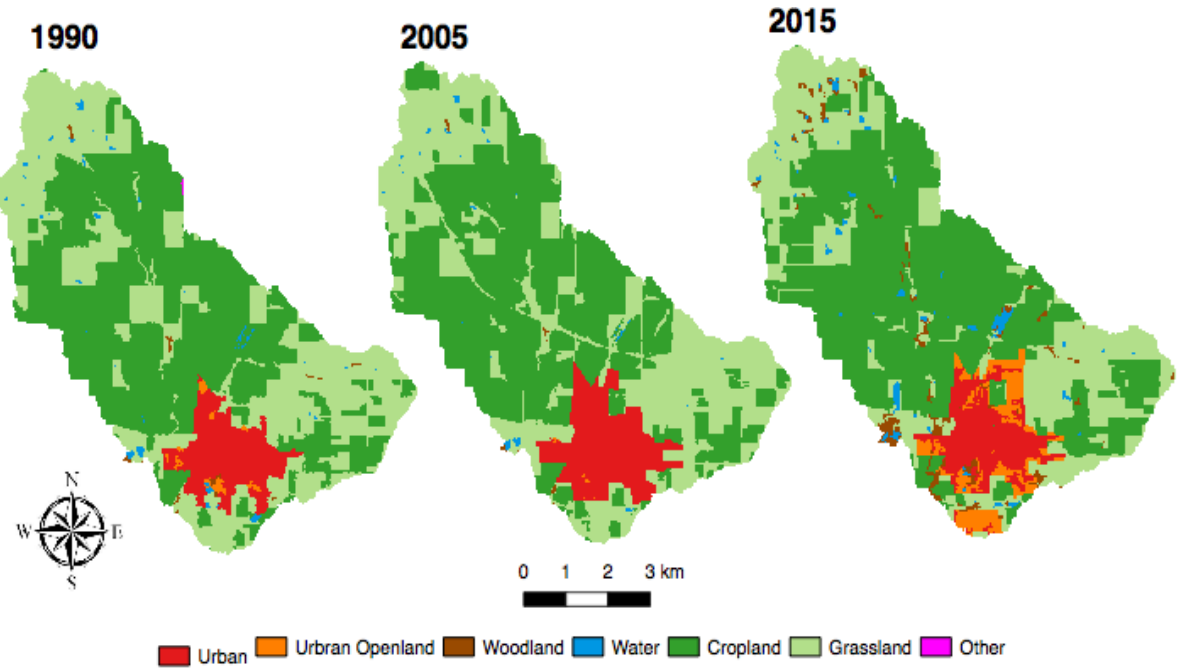


**Figure 12:** LCLU patterns for the years 1990, 2005 and 2015.

| Land Use | 1990 | | 2005 | | 2015 | |
|---|---|---|---|---|---|---|
| | *Area (km^2)* | *% of Area* | *Area (km^2)* | *% of Area* | *Area (km^2)* | *% of Area* |
| Urban | 3.9 | 7.8% | 3.4 | 6.9% | 3.7 | 7.4% |
| Urban Openland | 0.2 | 0.5% | 1.4 | 2.9% | 2.1 | 4.2% |
| Cropland | 25.9 | 52.3% | 25.2 | 50.9% | 26.8 | 54.1% |
| Grassland | 19.0 | 38.3% | 18.1 | 36.5% | 15.1 | 30.4% |
| Woodland | 0.2 | 0.3% | 0.8 | 1.6% | 1.2 | 2.4% |
| Water | 0.3 | 0.6% | 0.6 | 1.1% | 0.7 | 1.5% |
| Other | 0.0 | 0.0% | 0.0 | 0.0% | 0.0 | 0.0% |

**Table 7:** Land-use changes in Salt Creek Watershed.

| Percent Land-Use Change from 1990 - 2015 | |
|---|---|
| Urban | -0.5% |
| Urban Openland | 3.7% |
| Cropland | 1.8% |
| Grassland | -7.9% |
| Woodland | 2.1% |
| Water | 0.8% |
| Other | 0.0% |

**Table 8:** LCLU change from 1990 to 2015 in Salt Creek watershed. Grassland has considerably decreased while urban openland, cropland, and woodland areas have increased.

# Chapter 5 - Materials and Methods

## 5.1 Assessment of Streamflow Obstructions

In this report, streamflow obstructions are defined as any kind of obstacle in the stream that does or has the potential to significantly affect the flow of water through the channel. Examples of this in Salt Creek include bridge stability structures (pillars) and active or inactive pipelines. These stream obstructions alone may not necessarily affect streamflow at all times; however, they have strong potentials to collect passing debris such as tree limbs, leaves, and trash. Accumulation of debris on these stream obstructions has the ability to back-up or congest water upstream of them (Guo et al., 2007). Another effect this can have on the stream is causing a circulation of water to occur at the base of the debris pile that erodes bottom sediments to create deeper pools (Sullivan et al., 1986; Montgomery et al., 2003). Emphasis on will be placed on streamflow obstructions in channels that are south of 400-Highway. This is because the storage areas of Salt Creek, as seen in Figure 3, occur primarily south of 400-Highway.

### 5.1.1 Salt Creek Debris Removal Project

In 2013, local agronomist and rangeland management specialist Ethan Walker conducted a study in which he observed the debris impacts within Salt Creek (Walker, 2013). In his informal report, he identified thirteen areas within the creek that had heavy debris pile-ups. In response to this report, a team of local contractors and environmentalists choose one area of the main channel that had a debris pile-up and removed the pile. This effort cleared that section of the creek and restored flow. This successful venture prompted more conversation about clearing the channel and tributaries of debris to allow for the uninhibited flow of flood water. We predict that this could be a temporary solution to minimize the flood extent in some sections of Salt Creek.

## 5.2 Water-Level Data Collection

Prior to this study, there have been no attempts to record water-level data for Salt Creek. To collect real-time water-level data, two Solinst Levelogger Junior Edge pressure transducers were installed in the West Park area of Salt Creek. The Levelogger Junior Edge pressure transducer has an accuracy of ±0.1% FS and automatically compensates for temperature when logging

readings (Solinst Canada Ltd., 2017). The pressure transducers are denoted as PT-1 and PT-2 for the purpose of identification within this report. PT-1 was installed in July 2017. PT-2 was installed upstream of PT-1 in September 2017. PT-2 is placed approximately one meter upstream from a bridge that had accumulated a large amount of debris, mainly tree limbs, trash, and leaves. See Figure 14, which shows the placement of the pressure transducers labeled PT-1, PT-2, and BL. PT-1 is 379m downstream of PT-2. BL is 188m west of PT-2.

According to a conversation with Solinst technicians, it is acceptable to lay the Levelogger horizontally, instead of vertically, in the water. The vessels for the Leveloggers consisted of a small tube of PVC pipe with two end caps. One end cap was glued to the pipe. The pipe was perforated using a drill to allow for water flow inside the pipe. The Levelogger was inserted into the pipe and capped. The pipe was then zip-tied to a block. A hole was dug in the bed of Salt Creek so that the pressure transducer could lay as flush as possible with the bed of the stream. This process was completed for both pressure transducers. This method of installation is not ideal, as it requires wading into the stream to fetch the pressure transducer. This was especially true for PT-2 which had turbid, waist-deep water. The most common method of installation for pressure transducers is using a long, perforated PVC pipe attached to a bridge and using a string to pull the pressure transducer up and down the pipe. This mode of installation, however, raised concerns due to the fact that Salt Creek has a reputation for carrying debris that could damage the housing pipe. The housing for the Barologger consisted of a “treehouse” with an open face and a hook that the Barologger hung from. See Figure 13 for picture of the housing structures.

The Solinst Levelogger Junior Edge pressure transducers automatically collect measurements of absolute pressure (atmospheric pressure + water pressure). To compensate for atmospheric pressure, a Solinst Barologger Edge pressure transducer was installed against a tree near PT-1 and PT-2. The Barologger Edge has an accuracy of ±0.007 PSI and automatically compensates for temperature when logging readings (Solinst Canada Ltd., 2017). The Barologger Edge is denoted as BL in this study. To compensate for atmospheric pressure, the data from BL was first converted to the water column equivalent in meters by multiplying the reading in PSI by 0.703 (Solinst Canada Ltd., 2017). The water column equivalents are then subtracted from the time-paired Levelogger reading to attain a water height. Finally, to compensate for the height of the Levelogger vessels from the bed of the stream, 0.076m is added to the atmospheric pressure compensated water height.

All pressure transducers were set to record pressure measurements every three minutes. If possible, the pressure transducers had data extracted from them every month during the observation period. Occasionally, high water or bad weather would inhibit extraction, but this was not a problem as the pressure transducers could store a large set of data before becoming full. Data from the water level readings was imported into Excel for interpretation.

Pressure transducers cannot withstand freezing water, as it can cause harm to internal electronics. Due to this, BL and PT-1 were removed from the stream in November. PT-2 was removed in October, as the water was much deeper, making it more difficult to reach in cold temperatures.


**Figure 13:** Pressure transducer vessels. The vessel on the left houses the Levelogger and the treehouse on the right houses the Barologger Edge.

## 5.3 Precipitation Data Collection

To attain more accurate measurements of precipitation and precipitation intensity, two HOBO Data Logging Rain Gauges (model RG3-M) were installed within Salt Creek watershed. HOBO Data Logging Rain Gauges use a tipping-bucket mechanism in which one tip of the bucket occurs for each 0.2mm of rainfall. Each bucket tip is detected through the use of magnets, and each tip is then recorded automatically. The calibration accuracy of the RG3-M is ±1.0% or up to 2cm per hour. The maximum rainfall rate the RG3-M can record is 12.5cm per hour. Like the pressure transducers, the rain gauges were removed from the field in late November 2017 to protect them from freezing temperatures that could damage the electronics or mechanisms. Two HOBO rain

gauges placed in different areas of the watershed ensured that spatial variability of precipitation events could be accounted for. The rain gauges were mounted on posts and activated in August 2017. The rain gauges are labeled as HOBO-1 and HOBO-2. HOBO-1 is located within the City of Fredonia and HOBO-2 is located north of the town. The locations of the HOBO rain gauges can be seen in Figure 14.

There were four instances of HOBO rain gauge equipment errors, failures, or accidents during the five-month observation period. HOBO-1 experienced an unknown error that resulted in a failure to record a storm event that occurred on August 17, 2017. This error was an isolated incident, as all other storm events were recorded successfully. HOBO-2 experienced a battery failure on the data logger on August 8, 2017. The battery was replaced and the data logger resumed recording. However, the HOBO-2 data logger experienced a second failure in which a replacement battery did not resolve the issue, resulting in a loss of all data from HOBO-2 after September 2, 2017. It was thought that during a storm event in which little to no rain fell, but severe winds blew, the top funnel of the HOBO-2 was blown off. This may have been a cause of the electronic malfunction. Only one set of precipitation measurements were needed to compare Salt Creek water levels and rainfall intensity.

## 5.4 Soil Collection and Analysis

### 5.4.1 Sample Collection

While WSS data provide a useful tool, the resolution of these data is insufficient at the scale of the Salt Creek watershed. Many soil datasets within WSS are generalized or estimated, so it may not be entirely accurate for the area. More detailed soil analyses of the watershed were required to provide better understanding of the soil properties and how they might affect flooding. Multiple soil samples depths were taken from ten separate sites within the watershed to assess particle size and permeability (Figure 14). Ten sample sites will provide enough information to improve the soil physical property datasets currently available.

Sample sites were selected based on geographic location and land-use, so that many different types of soil could be represented. After site locations were determined, the samples were all collected on September 23$^{rd}$, 2017. Samples were all collected on September 23$^{rd}$, 2017. Firstly, the top layer of soil (approximately 5cm) and any debris was removed from the area to be sampled. This ensured as little as possible organic material was present in the sample. After the top layer

was removed, the sampling process began. Samples were taken by a hand-drilled auger at depths of up to 152cm, with an average depth of 110cm. The auger was drilled into the soil until full. The soil in the auger was considered one sample and was placed in a plastic bag that was labeled with the site number and depth. A total of 79 sample bags were collected. Because the soil analyses to be conducted were not chemical in nature, the samples were not required to be stored in any special conditions.

Sample depths used for analyses were chosen so that shallow (<50cm), middle (<50cm and <85cm), and deep (>85cm) soils were represented at each site, if possible. Due to the fact that silty and clayey soils can be compact and become too strenuous to drill through, the deepest sample depth varied from site-to-site. When the clay-rich layer was struck, drilling had to cease.

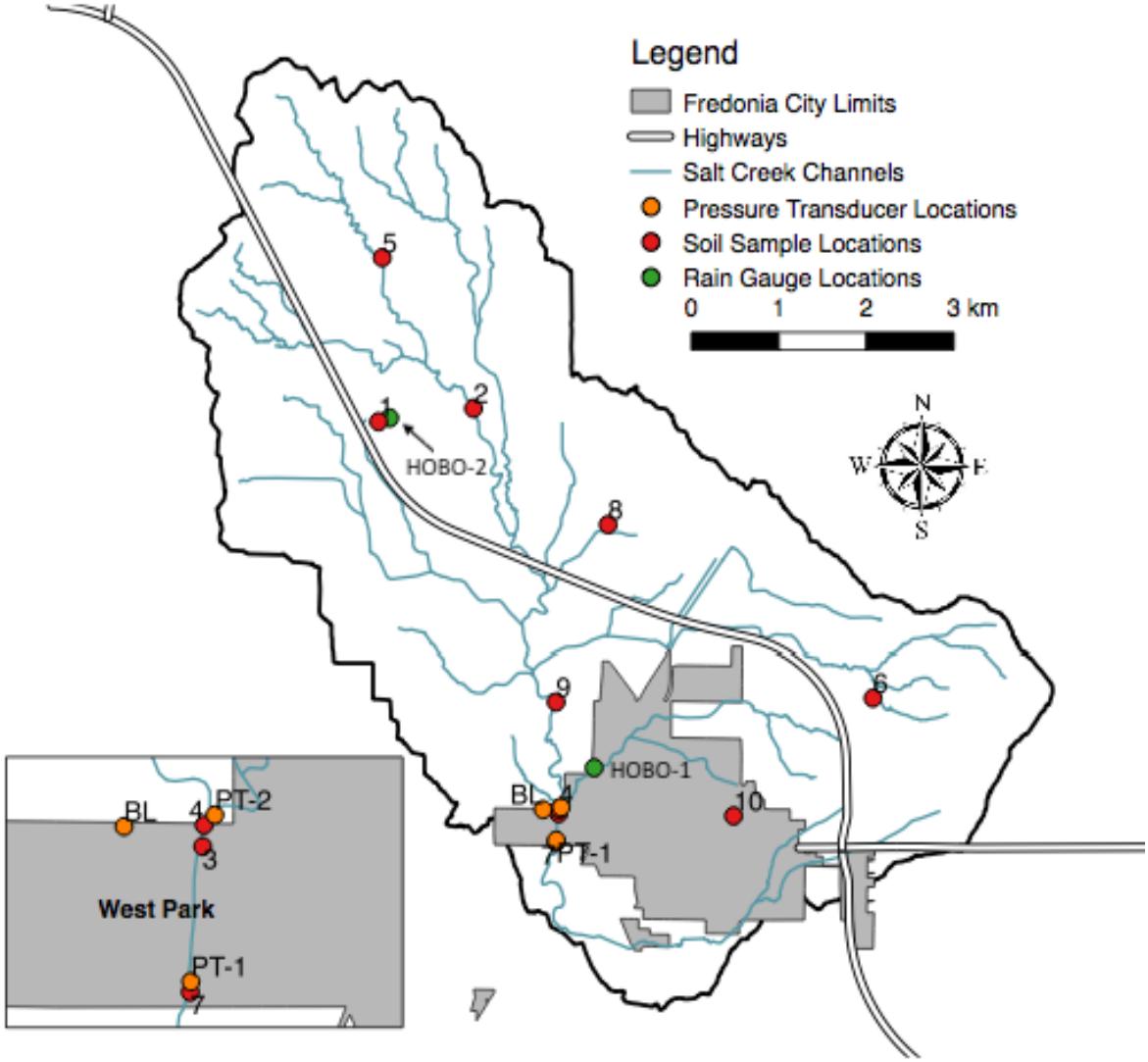


**Figure 14:** A map of the field instruments and soil sample locations within Salt Creek watershed.

Additionally, sites 2, 4, and 7 were located near the water of Salt Creek and only one depth was taken due to the invasion of water into the hole after the sample was retrieved. The depths that were chosen for analyses are listed in Table 9.

| Soil Samples (cm) | | | | | | | | | |
|---|---|---|---|---|---|---|---|---|---|
| **Site 1** | **Site 2** | **Site 3** | **Site 4** | **Site 5** | **Site 6** | **Site 7** | **Site 8** | **Site 9** | **Site 10** |
| 5 to 18 | 41 to 46 | 5 to 15 | 97 to 102 | 10 to 28 | 10 to 25 | 74 to 81 | 18 to 30 | 20 to 25 | 23 to 38 |
| 53 to 61 | | 72 to 79 | | 43 to 64 | 53 to 64 | | 74 to 84 | 69 to 79 | 56 to 71 |
| 112 to 132 | | 142 to 147 | | 122 to 132 | 127 to 132 | | 84-97 | 86 to 91 | 122 to 132 |

**Table 9:** Sample depths chosen for analysis. Depths in blue had only particle size analyses conducted and depths in green had both particle size analyses and permeability testing completed.

### 5.4.2 Particle Size Analyses

Particle sizes analyses (PSA) were conducted on all twenty-four sample depths. The test was conducted using a Malvern Mastersizer 3000 laser particle size analyzer, which measures the laser diffraction of a particulate. Approximately 4-grams of a sample was placed in a cup and diluted and mixed with 15mL of DI water. Diluted samples were placed in an ultrasonic bath for twenty minutes. The ultrasonic bath uses water and ultrasound which vigorously shakes the samples so that the aggregates break apart (Birrell, 1966). The sample was then pipetted into the Hydro EV receptacle—a beaker filled with 500mL of DI water in which the Mastersizer 3000 receives sample—until an obscuration percentage of 10-15% was reached. The Mastersizer 3000 then measured the particle sizes three times and averaged each run. This was repeated for each sample.

Some samples depth volumes were too small for the permeability tests and had to be combined with a bag of an adjacent sample depth in order to have enough volume to run the permeability tests described in Section 5.4.3. Adjacent sample depth bags also had PSA tests completed. A total of three adjacent sample depths were selected for PSA analyses:

- Site 1: 18-34cm. To be combined with sample depth Site 1, 5-18cm.
- Site 5: 28-43cm. To be combined with sample depth Site 5, 43-64cm.
- Site 6: 50-53cm. To be combined with sample depth Site 6, 53-64cm.

If a PSA yielded results that seemed uncharacteristically large (i.e. having a large reading of course sand in a sample that it was evident did not have a large volume of coarse sand via a hand test), or if the results did not reflect a relative similarity the permeability test's hydraulic conductivity for that sample, a PSA test was rerun. A total of five tests were rerun to correct the

results of the PSA, as the original results concluded with a soil texture that did not appear accurate given the feel of the soil with a finger test as well as the permeability test results:

- Site 3: 72-79cm
- Site 5: 122-132cm
- Site 8: 74-84cm
- Site 9: 20-25cm
- Site 9: 69-79cm

#### 5.4.2.1 Possible Sources of Inaccuracy in the Particle Size Analyses

The results of the PSA analysis suggest that the method is prone to error, at least for the samples analyzed as part of this study. The reason for the inaccuracy is unknown, but may be due to clay aggregates that could not be disaggregated prior to or during sample analysis. This inaccuracy will be further discussed in Section 7.1.

### 5.4.3 Permeability Test

For soils with a high percentage of fine particles, a falling-head test is used to calculate a value of permeability (Chegeniazadeh & Nikraz, 2011). For this study, a falling-head test was conducted using a Humboldt Constant Head Permeameter, which was modified to be used for the falling-head test. Modification of the permeameter involved plugging two of the four valves on the permeameter, so that there was only one inflow tube at the bottom and one outflow tube at the top of the permeameter.

Preparation for the falling-head tests involved two steps: (1) soil samples were air-dried on trays until most antecedent moisture had evaporated and (2) the dried samples were crushed to smaller pieces with a hammer so that they could be compacted into the permeameter. Crushing the sample did not reduce the grain sizes, instead, it was only used to reduce the occurrence of large, aggregated clumps of soil. Once crushed, the sample was placed in the permeameter, stopping to compact the sample regularly as it was input. The cap was placed on the permeameter and the outflow tube attached. The inflow tube was attached to the valve at the base of the permeameter.

To conduct the falling-head test, the sample was first fully saturated with water via the inflow tube until water ran steadily out of the outflow tube. Then the inflow valve was turned off

and a measurement was taken for the initial head. The inflow valve was opened to allow for flow of water and every sixty seconds a measurement of head was taken for a total of 180 seconds. When three minutes had been reached, the inflow valve was shut, and the final head was measured. Hydraulic conductivity was then calculated using the equation:

$$K = \left(\frac{A_t L}{A_c(t_f - t_i)} \times ln\frac{H_f}{H_i}\right) \times 10000 \qquad \textit{eq. 5}$$

where $K$ is hydraulic conductivity, $A_t$ is the area of the tube, L is the length of head within permeameter cylinder, $A_c$ is the area of the permeameter cylinder, $t_f - t_i$ is the change in time between measurements (sixty seconds in this experiment), $H_f$ is the final head, and $H_i$ is the initial head. The resulting $K$ has the units µm/s. The constant variables in the equation for this permeameter were:

- $A_t$ = 0.45cm$^2$
- $A_c$= 126.64cm$^2$
- $L$ = 15.24cm

Substituting these constants into equation 5 gives the equation used to calculate saturated hydraulic conductivity in all permeability tests for this study:

$$K = \left(\frac{(0.45)(15.24)}{(126.64)(t_f - t_i)} \times ln\frac{H_f}{H_i}\right) \times 10000 \qquad \textit{eq. 6}$$

For each soil sample chosen for permeability testing, three measurements of head were taken, one every 60 seconds until 180 seconds had passed. $K$ was calculated for each of these measurements and the average $K$ value in µm/s for that sample was calculated.

#### 5.4.3.1 Possible Sources of Error in Permeability Tests

Falling-head permeability tests proved difficult to conduct. A common problem during testing was that after saturation of the sample within the permeameter, water would make pathways along the wall of the permeameter causing water to flow uncharacteristically fast through the sample. Fortunately, this problem was easily identifiable, and testing was stopped if it occurred.

This problem was not easily remedied. The first attempt to remedy was to compress the sample within the permeameter to compact it and fill in water pathways. This often caused the sample to be too compact, and water could not flow through. If this happened, the sample had to be removed, re-dried, re-crushed, and re-tested. Precautionary measures, such as hammering the dried sample into the smallest aggregates possible, as well as more thoroughly compacting the dry sample in the permeameter, appeared to decrease the occurrence of these water pathways. Therefore, possible sources of error for permeability tests conducted in this study include water pathways that caused too-fast rates of flow through the sample and compaction that was either too compact or not compact enough. It is recommended that in future studies in this area, in situ permeability tests are conducted to provide permeability rates for undisturbed soils.

### 5.4.4 Estimation of Ponding Time

To estimate values for initial volumetric water content, $\theta_i$, Figure 15 was used. Field capacity is the water content (also called soil moisture) that remains in the soil after all excess water has been drained and no downward movement of water is occurring. It can take 2-3 days for field capacity to be reached as the clay-rich soils drain (Cornell University, n.d.). Permanent wilting point is when the moisture in the soil requires too much energy for the plant roots to pull that moisture away from the soil particles, causing the plants to begin wilting. Both field capacity and permanent wilting point increase as the average soil texture becomes finer-grained as seen in Figure 15. For the purposes of this project, a soil texture of clay loam will be used as it has the closest value to the average calculated $K_s$ values found in this study (see Table 4 for $K_s$ values for a given soil texture and Section 6.3.2 for calculated $K_s$ values). The value for field capacity and permanent wilting point will be assumed at 0.35$m^3m^3$ and 0.15$m^3m^3$, respectively (see Figure 15). Soil Survey Staff (2017) had average values similar to these within the top 30cm of soil in Salt Creek watershed. The value

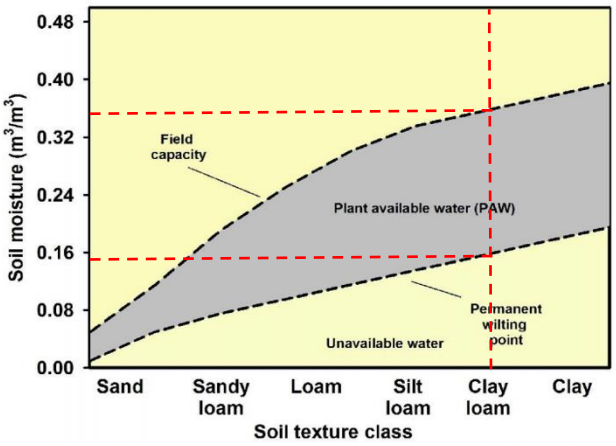


**Figure 15:** Soil moisture as a function of the soil textural class. Figure by Zotarelli, Dukes and Berreto (n.d.). Red lines indicate the values for clay loam.

for $\theta_s$ for all calculations will be 0.45$m^3m^3$, as this would be a typical value for saturated clay loam soils.

Ponding time calculations were completed for the following scenarii using the ponding time equations 1, 2, and 3 found in Section 5.4.4:

(1) The initial soil conditions are dry, as if there have been several weeks of no rain in the summer (typical for this watershed). $\theta_i$ = 0.15$m^3m^3$ and $\theta_s$ = 0.45$m^3m^3$
    a. 3.73cm per hour (2007 flood)
    b. 2.54cm per hour
    c. 1.12cm per hour (2016 flood)

(2) Initial soil conditions are saturated, as if there was a substantial rain event within the previous 2-3 days prior. $\theta_i$ = 0.35$m^3m^3$ and $\theta_s$ = 0.45$m^3m^3$
    a. 3.73cm per hour (2007 flood)
    b. 2.54cm per hour
    c. 1.12cm per hour (2016 flood)

## 5.5 ANUGA Hydrodynamic Model

ANUGA is a free, open-source hydrodynamic model released in 2006 (https://anuga.anu.edu.au/). ANUGA stands for Australia National University (ANU) and Geoscience Australia (GA), who are the creators of the model. ANUGA is written in the Python coding language. At its core, ANUGA uses shallow water flow equations in 2D to model channel flow and flood inundation (Roberts, Nielsen, Gray, Sexton, & Davies, 2015). ANUGA was chosen for this project because it is capable of simulating flooding and its flexibility with adding new operators.

ANUGA is not as well-known as models like HEC-RAS, but is capable of completing the same tasks one would use HEC-RAS for. In fact, Van Drie, Simon, and Schymitzek (2008) have identified that models such as HEC-RAS are not always appropriate to use, as they are not capable of addressing 2D flow or momentum specific problems. The core of ANUGA is the fluid dynamics module, called `shallow_water`, which is based on a finite-volume method for solving the Shallow Water Wave Equations as solved by Mungkasi & Roberts (2013). The study area is specified and represented by a mesh of triangular cells that represent the topography. By solving

the governing equation within each cell, water depth and horizontal momentum are tracked over time.

### 5.5.1 Model Inputs

#### 5.5.1.1 Elevation and Friction

The base digital elevation model (DEM) used with ANUGA was procured from USGS's *The National Map* database (United States Geological Survey, 2017). It is a 1/3 arc-second ArcGrid DEM. The USGS DEM was clipped to encompass all of Salt Creek watershed. The resulting model output includes some areas on the outer boundaries that is not part of Salt Creek watershed due to a need to reduce the number of nodal points within ANUGA for the sake of model efficiency. Figure 16 shows the model domain versus Salt Creek watershed boundary.

DEMs do not always remove bridges from the water courses to show the bed of the stream rather than the elevation of the bridge. This creates artificial embankments through which water cannot pass. There were several spots where this occurred within Salt Creek, most noticeably along 400-Highway north of Fredonia. This was corrected using a culvert operator which allows for the transfer of water through a tube-like structure of specified dimensions.

A friction coefficient (Manning's *n*) is applied to the domain to simulate the natural resistance of water flowing across terrain. The coefficient was set to 0.035, which is the specified value for a floodplain composed of pasture and farmland (Chow, 1959).

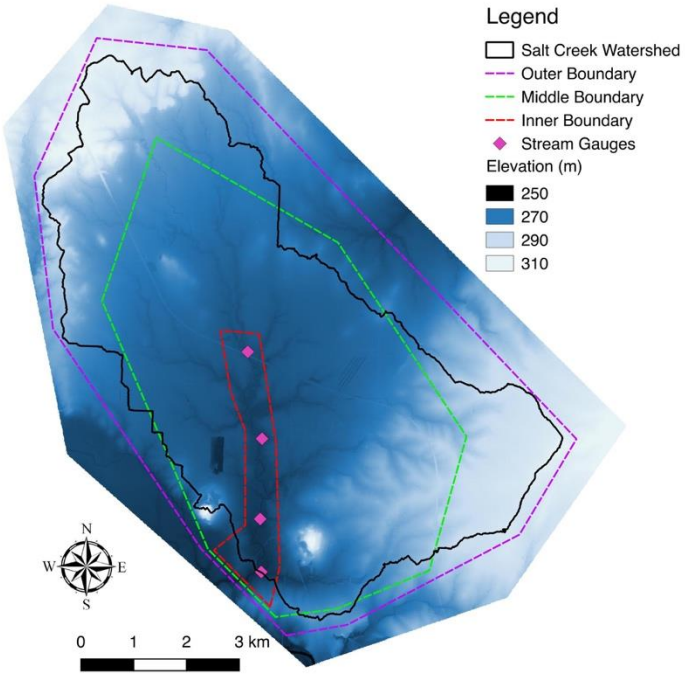


**Figure 16:** ANUGA domain versus Salt Creek watershed boundary. Hydrograph locations are represented by pink dots. The outer, middle, and inner boundaries allow for changes in triangle sizes to be made within those boundaries. Triangle sizes are smallest in the inner boundary and larger in the outer boundary.

#### 5.5.1.2 Boundary Conditions

Boundary conditions of the domain were set to:

```
=========================================================================
min_elev = domain.quantities['elevation'].vertex_values.min()
Bd = anuga.Dirichlet_boundary([min_elev - 1, 0., 0.]) #at outlet
Br = anuga.Reflective_boundary(domain)                #on all other sides
=========================================================================
```

A Dirichlet boundary condition specifies constant values for stage, x-momentum and y-momentum at the boundary (Roberts et al., 2015). Specifying the stage to be `min_elev - 1` allowed water to leave the domain, effectively acting as an outlet. A Reflective boundary condition keeps water from leaving the domain. Using the boundary conditions above, the domain outlet was specified as a Dirichlet boundary and all other boundaries were made Reflective.

#### 5.5.1.3 Rainfall Operator

A rainfall operator was needed in order to apply rain. An example of the rainfall operator code (combined with the model time) is:

```
=========================================================================
from anuga.operators.rate_operators import Rate_operator

initial_rate = 0.0000031 #meters/second
rain_operator = Rate_operator(domain, rate = initial_rate)

timestep = 300 #seconds
for t in domain.evolve(yieldstep = timestep, finaltime = 24*3600):
      print domain.timestepping_statistics()
      if t > 3600*8:
              rain_operator.set_rate(rate = 0.0)
=========================================================================
```

In this particular example, ANUGA has been directed to apply water (rain) to the entire domain at a rate of 0.0000031m/s for 3,600*8 seconds (eight hours), then after eight hours, the rate will be reduced to 0.0m/s for the duration of the run. As seen in this example, the ANUGA model requires time to be in seconds and any depths, areas, or volumes to be measured in meters, square meters, or cubic meters.

### 5.5.2 Model Outputs

During the ANUGA model run, `stage` is calculated using `rainfall_operator` and the DEM. The `stage` is the absolute height of water, i.e. water level (depth) + elevation of the ground. The `depth` is calculated through the equation `depth = stage – elevation` within the script. This calculated `depth` value is what is used as output. The values of `stage`, `elevation`, `x-momentum`, and `y-momentum` were recorded at a timestep of 300 seconds. There were a total of 288 timesteps at the conclusion of a 24-hour simulation.

The ANUGA model produced two types of output: (1) a .sww file that contained all output, such as `stage`, `elevation`, `x-momentum`, `y-momentum`, and `depth`, and (2) an Excel list of depths for each timestep for a specified "gauge" location. A "gauge" is simply a geographic point that is created with coordinates of where the desired hydrograph locations are in the watershed. There were four gauges chosen to produce hydrographs in each scenario (Figure 16). Using the program Paraview, the output can be viewed as a video of water depth over time. Additionally, water velocity and direction can be viewed if desired.

### 5.5.3 Scenarii Tested

A total of three tests were conducted using ANUGA: two to simulate the flooding that occurred in Salt Creek watershed during 2007 and 2016 and one to simulate a flood in between the intensity of the prior mentioned tests. ANUGA's essential function was to estimate what precipitation patterns (intensity and duration) closely reproduce the flooding extent seen in Salt Creek during the floods of 2007 and 2016. All three tests had rainfall falling on the domain for a total of 8 hours. This was an estimate of the local precipitation patterns, which tended to have precipitation events occur overnight.

Test 1: The first test is mainly for the purposes of assessing whether the model will produce results that are realistic for this watershed by attempting to recreate the 2007 flood event mentioned in Section 1.1. This test models the estimated results of a 3.73cm/hour rainfall for a total of 8 hours, with a total of 29.84cm of rainfall over this time period. 3.73cm/hour is the estimated precipitation rate for this flood event on the night of June 30, 2007 and morning of July 1, 2007 (NOAA, 2017b).

Test 2: The second test models the results of a 2.54cm/hour rainfall for a total of 8 hours, with a total of 20.32cm of rainfall over this time period. This is a hypothetical flood event.

Test 3: The third test models a simulation similar to the 2016 flood event. This test models the results of a 1.12cm/hr rain for a total of 8 hours, with a total of 8.96cm of rain over this time period. 1.12cm/hour is the estimated precipitation rate for this flood event on the night of September 9, 2016 (NOAA, 2017b).

### 5.5.4 Assumptions Within the ANUGA Model

There are several assumptions that are made during application of the ANUGA model that were necessitated by the duration of this study.

(1) There is no water present in the stream system at the initiation of the model run. As seen in the field, the majority of Salt Creek's channels are ephemeral, and it is difficult to know the base conditions (i.e. water levels prior to the precipitation event) in which the 2007 and 2016 flood occurred due to water level readings not being accounted for prior or during to these flood events.

(2) Base conditions assume 100% runoff of rainfall input. Because the saturated hydraulic conductivity values calculated in Section 6.3.2 were so slow, it was assumed the runoff lost to infiltration in the simulations would be negligible.

(3) The rainfall rate is spatially and temporally equal across the domain in any given scenario.

(4) There is no drag or friction of water induced by contact with vegetation, as there will be no vegetation operator implemented in the model. To this, it is also assumed 100% of rainfall reaches the soil surface runs off, that is, there is no canopy interception or loss of water to evaporation or infiltration.

(5) The urban area of the watershed (town of Fredonia) does not have defined buildings or roadways that manipulate overland flow.

# Chapter 6 - Results

## 6.1 Field Observations

### 6.1.1 Identified Streamflow Obstructions

From 400-Highway going south, and including the 400-Highway bridge, there are seven bridges along the main channel. Of these, there are six road bridges and one railroad bridge. All road bridges are relatively un-impactful; however, the railroad bridge has a support pillar located in the center of Salt Creek. This pillar was observed with a small collection of tree limbs and leaves located around the base, although at this time the stream was at a comparatively lower discharge due to dry conditions.

From 400-Highway, there are several pipelines that cross Salt Creek's main channel. Although local community members did not know why the pipelines within the creek are exposed, they may have once been buried beneath the creek and many years of stream incision has exposed the pipelines. There are two exposed pipelines within the West Park area of Salt Creek. One of these, which lies directly beneath the Madison Street bridge, has collected a large amount of debris (Figure 17). The pipeline, according to officials, is likely to be a water pipe that is approximately 0.45m in diameter. The pipeline was originally supported by two cemented rock pillars that are on the banks on both sides of the stream. It appears that, at some point in time, the pipeline began to bend or bow, and in response, a third cemented rock pillar was built directly in the center of the stream. This has caused debris to built-up on the north side of the pipeline. The second pipeline is located approximately 260m downstream and, although it does not have support structures, debris still collects adjacent to it. At the time of observation, this pipeline was clear of debris.

**Figure 17:** Madison Street bridge and pipe displaying a large amount of debris collection. PT-2 was located on the other side of the debris pile from where the photographer is standing.

## 6.2 Relationship between Precipitation and Salt Creek Water Level

During the precipitation observation period from July 26, 2017, to November 19, 2017, precipitation occurred on twenty-six days. Figure 18 shows the rainfall events in Salt Creek during the observation period as recorded by HOBO-1. HOBO-2's reading of August 16, 2017, was included, as it was not read by HOBO-1 as described in Section 5.3. The total rain recorded during the observation period was 28cm. This was above average precipitation for summer and autumn (21.5cm) compared to the data in Table 5. The largest rain event was 89.2-mm, which occurred on August 16, 2017, as recorded by HOBO-2. During a part of this storm event, 60.8-mm of rain fell in just under two hours. Figure 19a-c displays the water level and precipitation measurements for several events captured by the rain gauges and pressures transducers.

The observation period for PT-1 was July 15, 2017 to November 19, 2017. During the observation period for PT-1, the average height of water was 19.33cm with a standard deviation of 14.54cm. The maximum water level was 175.55cm and the minimum water level was 10.09cm. The observation period for PT-2 was September 2, 2017 to October 8, 2017. PT-2 had a shorter observation period due to being procured later than PT-1. It was removed from the field earlier than PT-1 due to oncoming cold weather making it more difficult to reach PT-2 as it was in deeper water. During the observation period for PT-2, the average height of water was 81.05cm with a standard deviation of 6.53cm. The maximum water level was 104.52cm and the minimum water level was 63.82cm. It is likely that the standard deviation of PT-1 is so high due to it recording more precipitation events than PT-2, as their observation periods differed.

We can conclude from the data gathered during the observation period that antecedent moisture in the soil from a prior precipitation event creates much steeper increases in the hydrograph. As to be expected, a more intense precipitation event (i.e. a high rate of rainfall) also creates steeper peaks in the hydrograph. A shorter duration precipitation event with a high precipitation intensity will result in a steep increase on the hydrograph followed by an immediate steep decrease in the hydrograph. Peak water levels at PT-1 occurred between 5-7 hours after peak precipitation intensity. A relationship between water level and precipitation for PT-2 was difficult to establish due a shorter observation period.

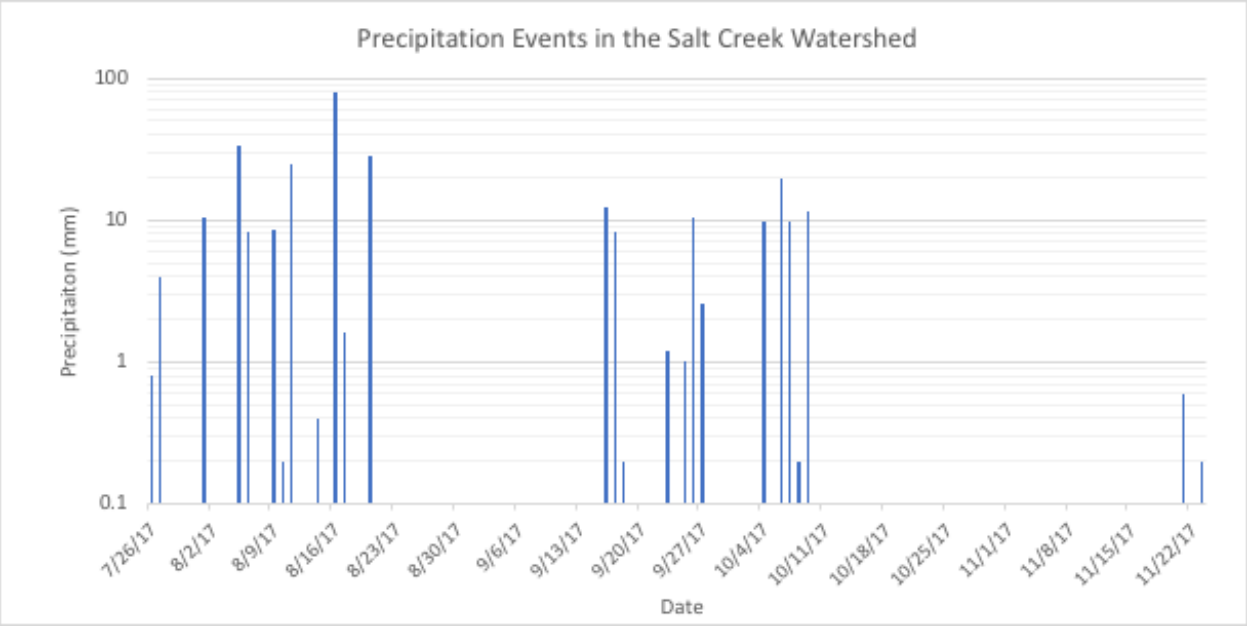


**Figure 18:** Precipitation events in Salt Creek watershed during the observation period. Note that the y-axis is in log-scale. Most events occurred in August, September, and the first part of October.

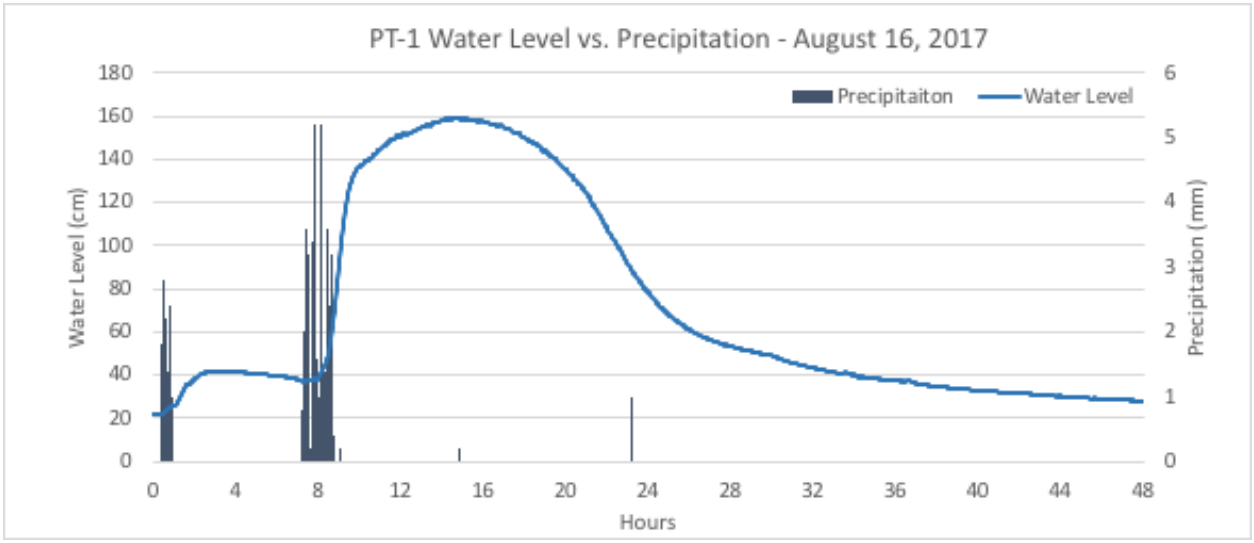


**Figure 19:** This figure displays the changes in Salt Creek's water level in response to varying intensities of precipitation. The rain gauges recorded a rainfall event on August 11th of 24.6mm, meaning that the soil moisture prior to the August 16th storm event was high. This high intensity storm resulted in a sudden rise in the water level, from 38.1cm to 134.5cm in 1.9 hours. The water level peaked 7 hours after peak intensity and then gradually fell to normal levels over the following 38 hours.

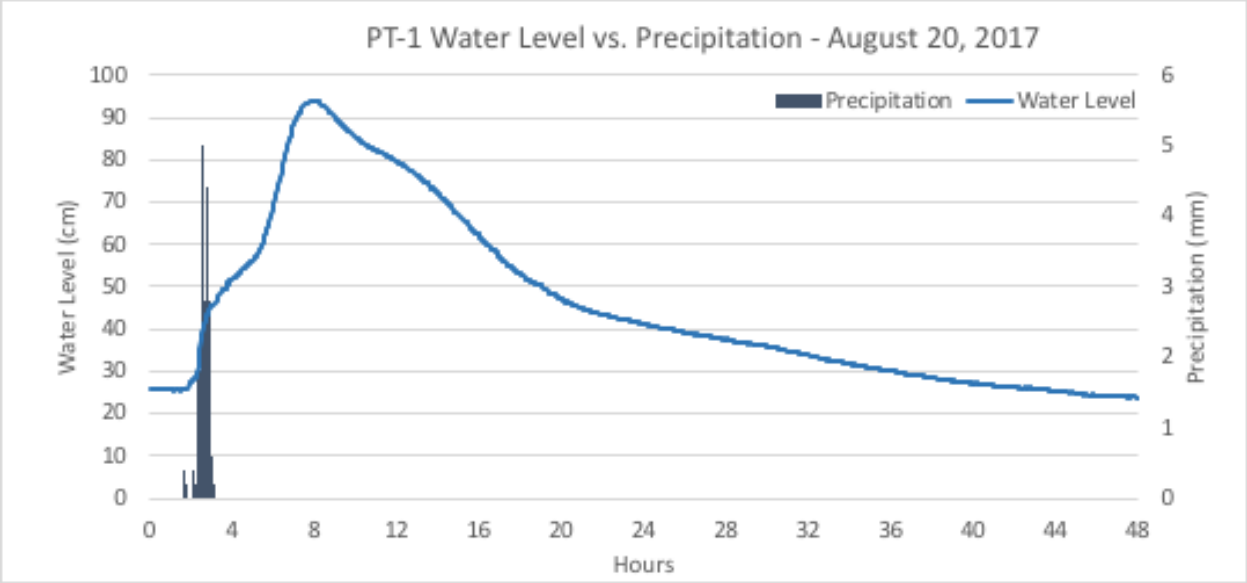


**Figure 20:** Water level increased sharply at the same time precipitation fell, indicating that the majority of the precipitation may have fallen near PT-1. This could also be caused by high runoff rates from pre-saturated soils from the August 16 event. A second peak in water level occurs approximately 5 hours after peak precipitation intensity was reached. The peak dropped off much faster than the peak seen in Figure 19a, likely due to the fact that this precipitation event had a shorter duration.

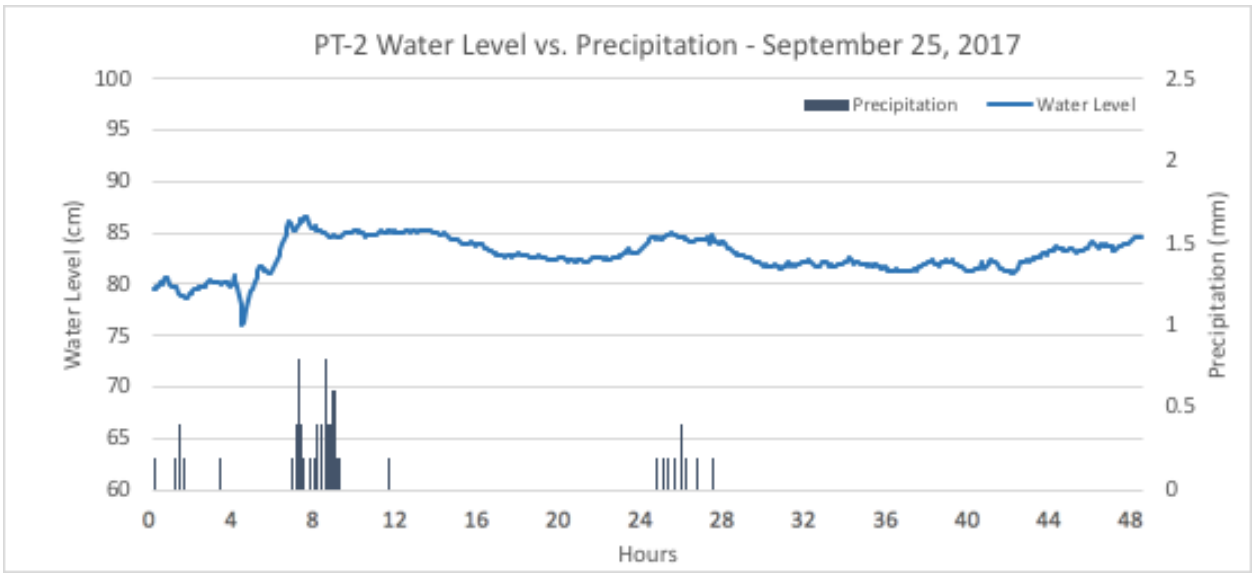


**Figure 21:** This much smaller storm event at PT-2 had a spike in water level at hour 7, which is around the same time that the heavier precipitation was falling.

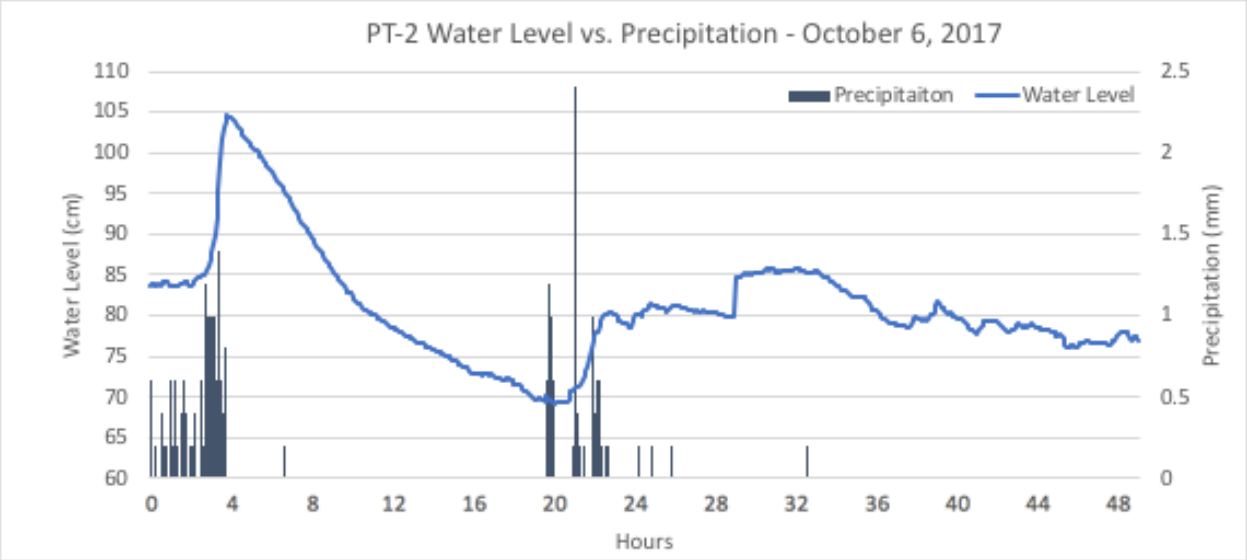


**Figure 22:** This event also has a water level that increased sharply at the same time precipitation was being recorded, again indicating saturated soils or that the precipitation likely fell in a close proximity to PT-2.

## 6.3 Soil Analyses Results

### 6.3.1 Particle Size Analyses Results

The particle size analysis using the Mastersizer 3000 yielded the results shown in Figure 23-32. Using the USDA's *Soil Texture Calculator* online tool, soil texture for each sample depth was determined (United States Department of Agriculture, 2018). Soil texture classification is shown in Appendix A, A.13-A.20. Out of twenty-four samples, sixteen (67%) were classified as a silty loam, three (13%) were classified as silty clay loam, two (8%) very fine sandy loam, and one (4%) each for silt, coarse sand, and coarse sandy loam. Table 10-12 described the average composition of the soils by soil depth and Figure 33 shows the average compositions in a chart. Figure 33 shows the average composition by depth and site in a chart.

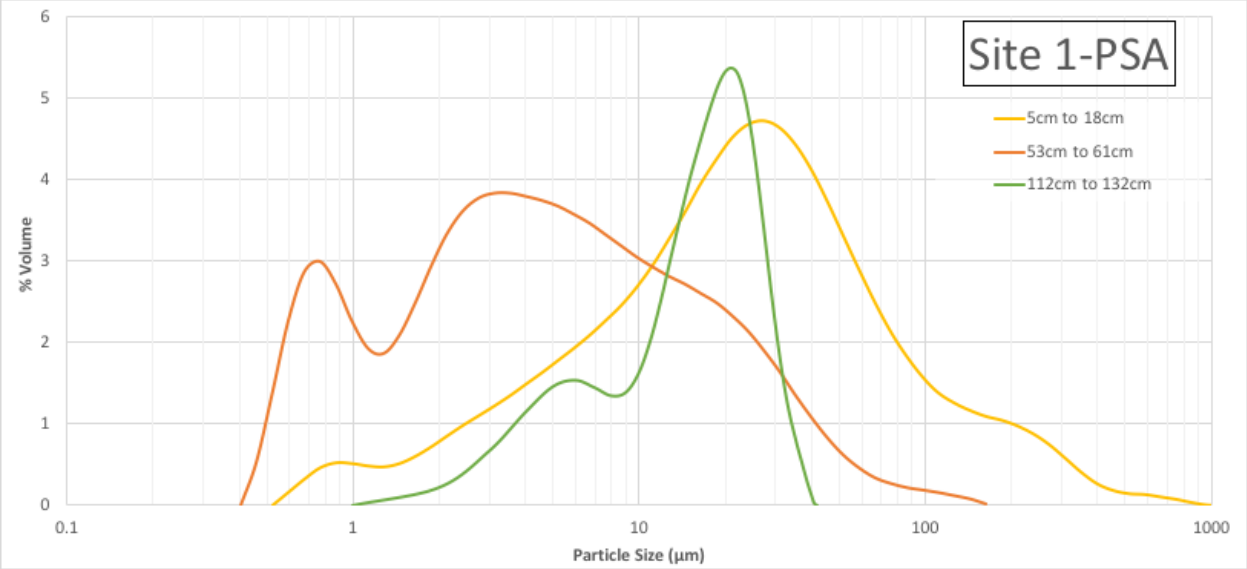


**Figure 23:** Particle size distribution of Site 1 soil samples. Site 1 had shallow and deep depths which had coarse grains than the middle depth.

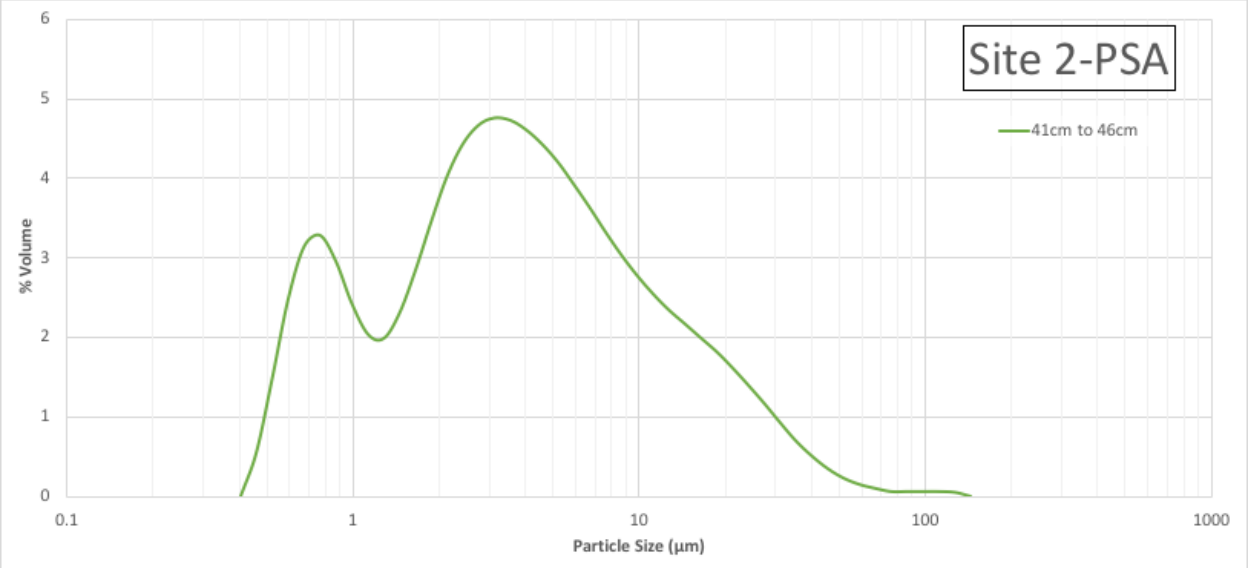


**Figure 24:** Particle size distribution of the Site 2 soil sample.  Site 2 had a more significant volume of silt.

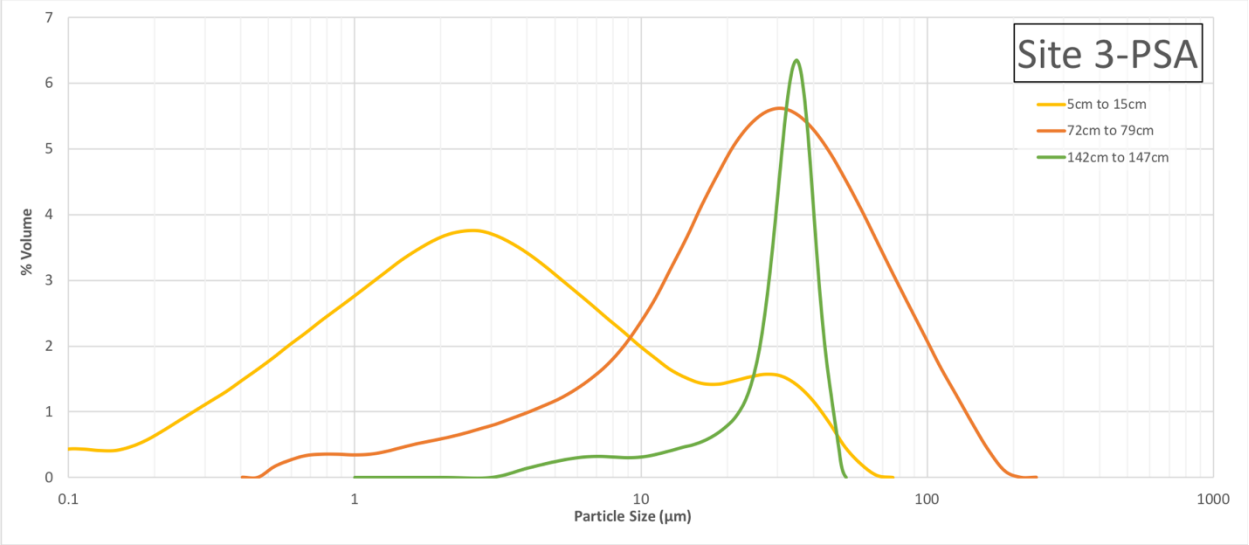


**Figure 25:** Particle size distribution of Site 3 soil samples. Site 3 had a large volume of coarser particles in the middle and deep depths and a more clay and silt rich shallow depth.

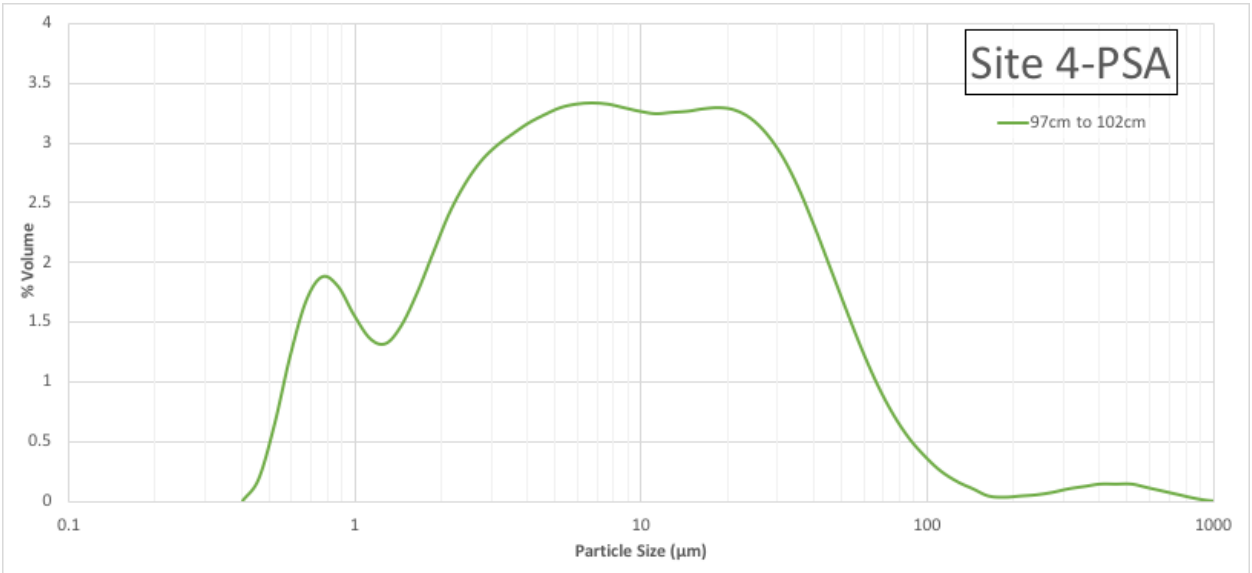


**Figure 26:** Particle size distribution of the Site 4 soil sample. Site 4 had a larger volume of silt and fine-grained sand.

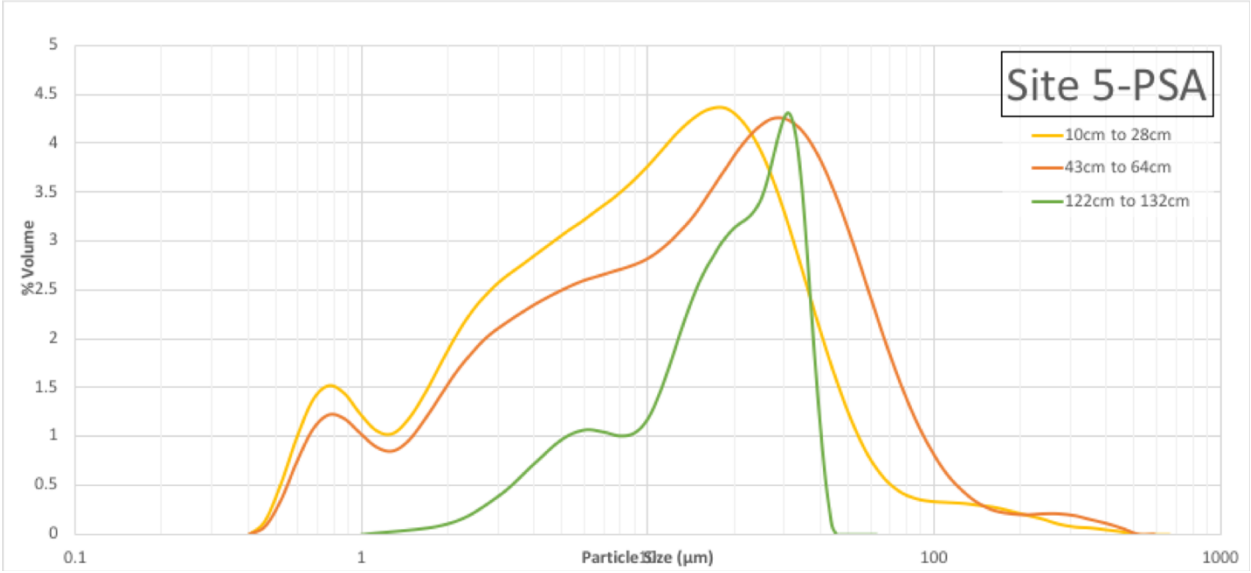


**Figure 27:** Particle size distribution of Site 5 soil samples. Site 5 was relatively uniform in its particle sizes in all depths compared to that of other sites. Particles sizes tended to be silt to fine-grained sand.

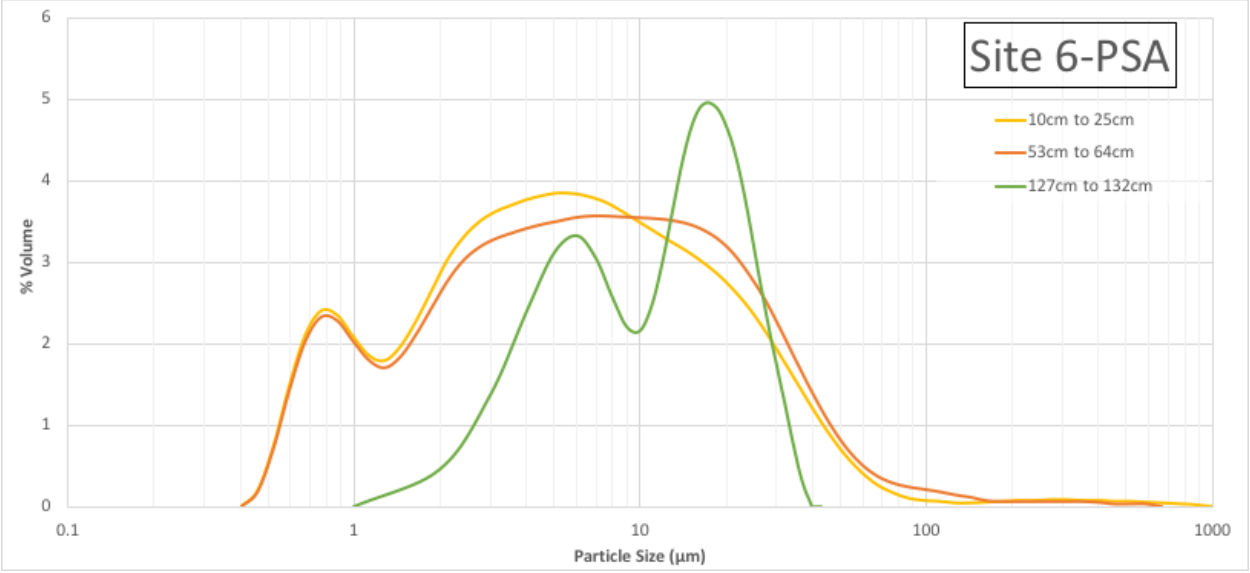


**Figure 28:** Particle size distribution of Site 6 soil samples. The shallow and middle depths are very uniform, with a deep depth displaying more silt and less clay.

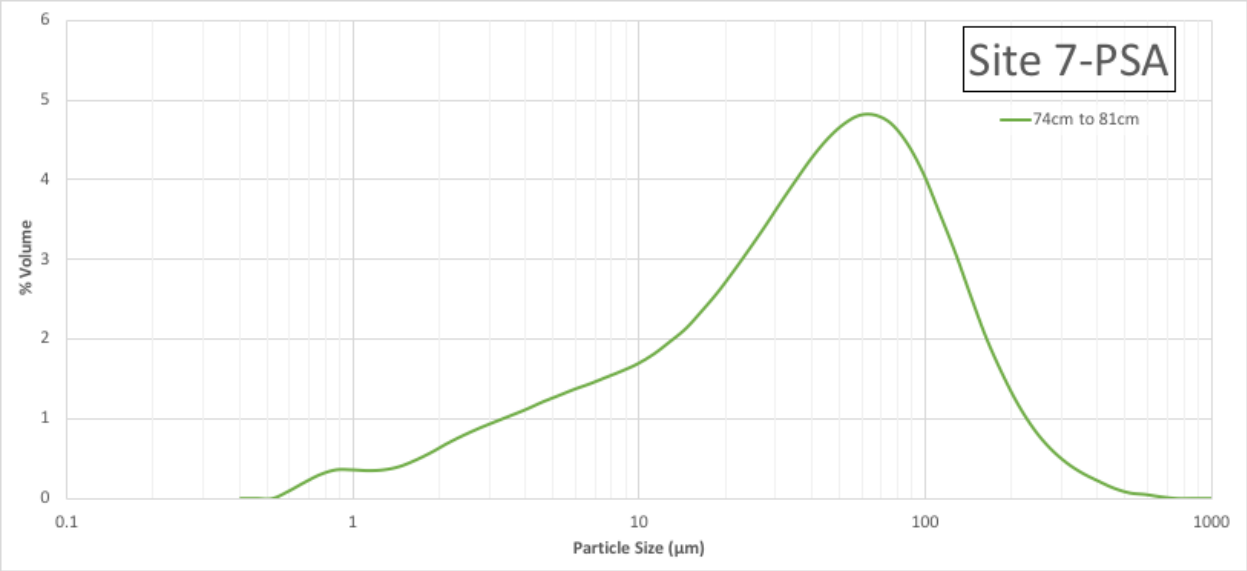


**Figure 29:** Particle size distribution of the Site 7 soil sample. Site 7 had a significant volume of fine-grained sand compared to other samples.

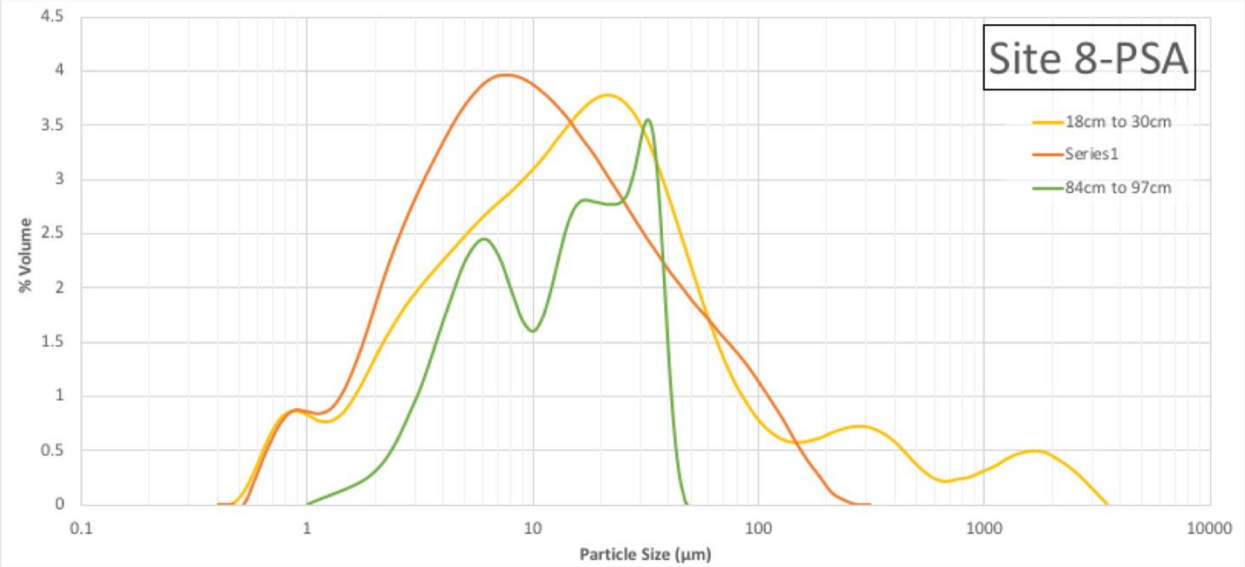


**Figure 30:** Particle size distribution of Site 8 soil samples. Site 8 was fairly uniform, with the concentration of particles sizes mainly in the silt range. The shallowest depth displayed a small volume of coarse sands.

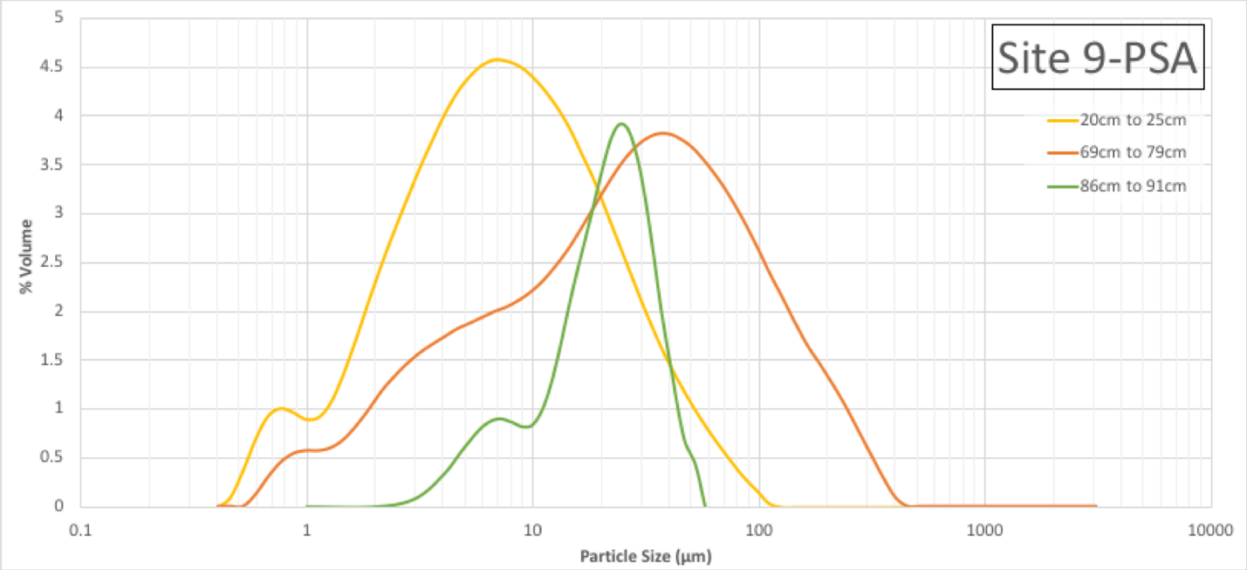


**Figure 32:** Particle size distribution of Site 9 soil samples. Site 9 depths consisted of shallow and deep depths displaying a large volume of silt and a middle depth with a larger volume of fine- to medium-grained sand.

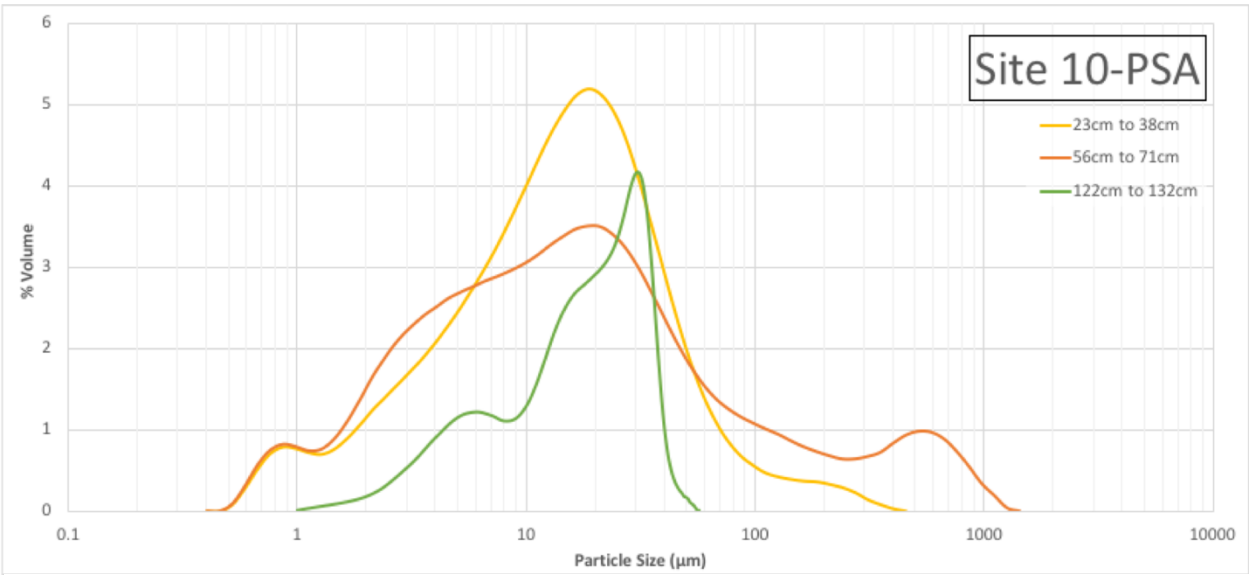


**Figure 31:** Particle size distribution of Site 10 soil samples. Site 10 particles sizes tended to be silty with a small volume of fine-grained sand.

| Statistics for the Shallowest Sample Depths (<50cm) | | | | |
|---|---|---|---|---|
| **Grain Size** | **Average %** | **Standard Deviation** | **Maximum %** | **Minimum %** |
| coarse sand | 0.83% | 2% | 4.91% | 0.00% |
| medium sand | 1.69% | 2% | 5.39% | 0.00% |
| fine sand | 3.97% | 4% | 10.57% | 0.21% |
| very fine sand | 7.53% | 5% | 14.17% | 1.68% |
| silt | 76.0% | 7% | 85.32% | 65.8% |
| clay | 9.99% | 6% | 21.90% | 4.13% |

**Table 10:** Particle size analysis statistics for soil sample depths of less than 50cm.

| Statistics for the Middle Sample Depths (>50cm and <85cm) | | | | |
|---|---|---|---|---|
| **Grain Size** | **Average %** | **Standard Deviation** | **Maximum %** | **Minimum %** |
| coarse sand | 0.56% | 2% | 4.70% | 0.00% |
| medium sand | 1.00% | 1% | 3.8% | 0.00% |
| fine sand | 5.22% | 5% | 14.0% | 0.11% |
| very fine sand | 12.3% | 11% | 32.1% | 0.66% |
| silt | 68.1% | 9% | 78.6% | 48.4% |
| clay | 12.9% | 10% | 29.0% | 2.90% |

**Table 11:** Particle size analysis statistics for soil sample depths of more than 50cm and less than 85cm.

| Statistics for the Deepest Sample Depths (>85cm) | | | | |
|---|---|---|---|---|
| **Grain Size** | **Average %** | **Standard Deviation** | **Maximum %** | **Minimum %** |
| coarse sand | 0.06% | 0% | 0.40% | 0.00% |
| medium sand | 0.33% | 1% | 1.60% | 0.00% |
| fine sand | 1.83% | 3% | 7.14% | 0.00% |
| very fine sand | 6.89% | 7% | 22.9% | 0.09% |
| silt | 76.2% | 6% | 83.7% | 67.3% |
| clay | 14.7% | 8% | 29.8% | 2.64% |

**Table 12:** Particle size analysis statistics for soil sample depths of more than 85cm.

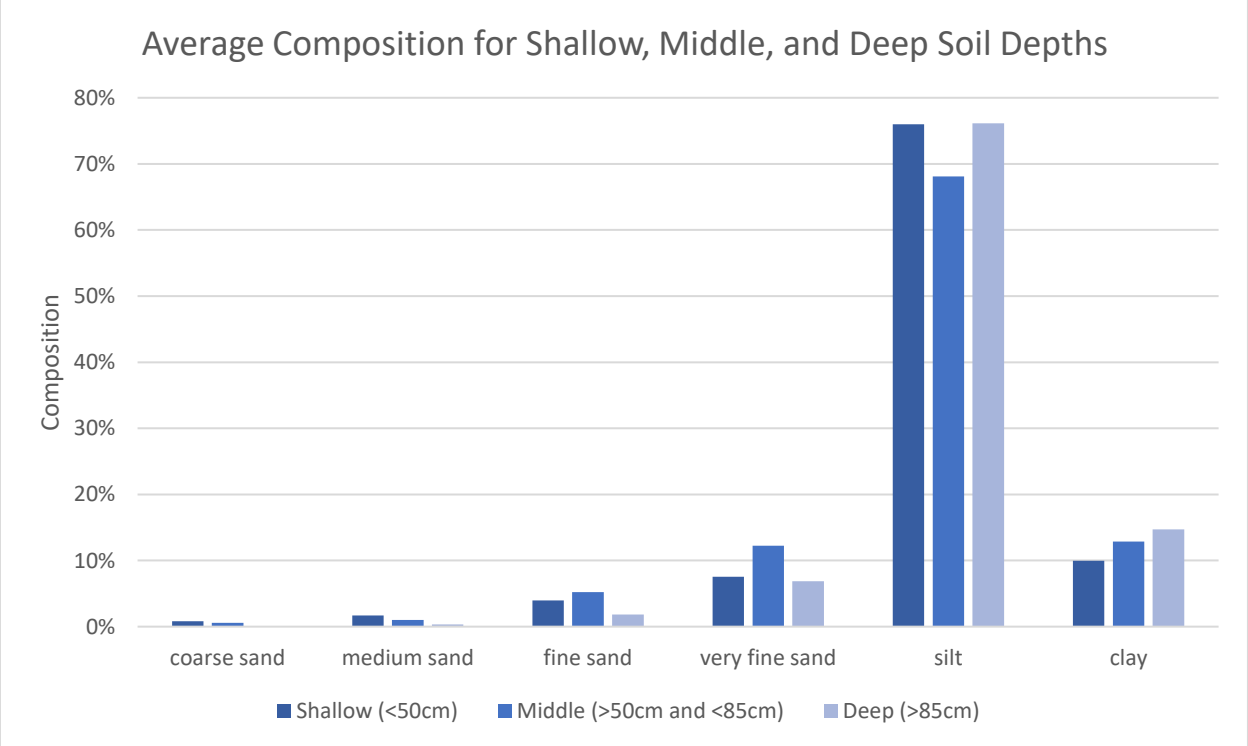


**Figure 33:** Average composition of the soil in Salt Creek watershed by depth. Shallow (<50cm), middle (>50cm and <85cm), and deep (>85cm) depths are represented.

### 6.3.2 Permeability Test Results

Using Equation 6, the saturated hydraulic conductivities were calculated for each permeability test. Figure 34 summarizes the resulting saturated hydraulic conductivities determined using the falling-head permeability test. The details of each permeability test are shown in Table 13.

$K_s$ values appear to decrease with decreases in depth at Site 1, Site 3, Site 5, and Site 9. This decrease is especially substantial in Site 1 and Site 9, where the decrease in $K_s$ from more shallow to more deep is 0.28µm/s and 0.73µm/s, respectively. This could likely be due to the hand-drilled auger coming into a closer proximity to the impermeable soil layer. According to Figure 23, Site 1: 5-18cm has an average particle size that is larger than Site 1: 112-132cm. According to Figure 31, Site 9: 69-79cm has an average particle size that is larger than Site 9: 86-91cm. The two sites with the lower $K_s$ values also have more homogenous particle sizes versus their shallower counterparts.

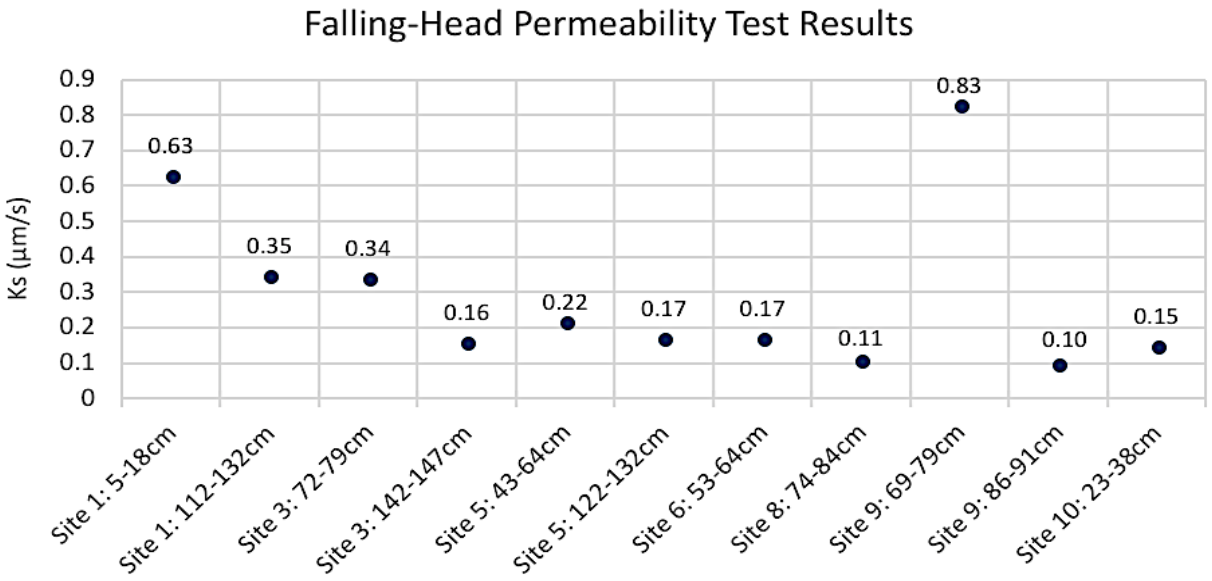


**Figure 34:** Falling-head permeability test results.

| Site | Depth, cm | Soil Texture | $t_0$, sec | $t_f$, sec | $h_0$, cm | $h_f$, cm | $K_s$, $\mu$m/sec | $K_s$ avg , $\mu$m/sec | Notes | Ratio |
|---|---|---|---|---|---|---|---|---|---|---|
| site ID | depth of sample | | initial time | final time | initial head height | final head height | sat. hyd. cond. | sat. hyd. cond. | | |
| 1 | 5 to 18 | silt loam | 0 | 60 | 100 | 92.7 | 0.68 | 0.63 | Must be combined with 18-34cm bag | Proportions: |
| | | | 60 | 120 | 92.7 | 86.4 | 0.64 | | | 5 to 18cm: 459.95g |
| | | | 120 | 180 | 86.4 | 81.1 | 0.57 | | | 18-34cm: 150.176g |
| 1 | 112 to 132 | silt loam | 0 | 60 | 95.6 | 91.6 | 0.39 | 0.35 | - | - |
| | | | 60 | 120 | 91.6 | 87.9 | 0.37 | | | |
| | | | 120 | 180 | 87.9 | 85.1 | 0.29 | | | |
| 3 | 72 to 79 | silt loam | 0 | 60 | 98.8 | 95.1 | 0.34 | 0.34 | - | - |
| | | | 60 | 120 | 95.1 | 91.7 | 0.33 | | | |
| | | | 120 | 180 | 91.7 | 88.3 | 0.34 | | | |
| 3 | 142 to 147 | silt loam | 0 | 60 | 88.6 | 87.1 | 0.15 | 0.16 | - | - |
| | | | 60 | 120 | 87.1 | 85.4 | 0.18 | | | |
| | | | 120 | 180 | 85.4 | 83.9 | 0.16 | | | |
| 5 | 43 to 64 | silt loam | 0 | 60 | 97.5 | 95.1 | 0.22 | 0.22 | Must be combined with 28-43cm bag | Proportions: |
| | | | 60 | 120 | 95.1 | 93.0 | 0.20 | | | 28-43cm: 315.52g |
| | | | 120 | 180 | 93.0 | 90.7 | 0.23 | | | 43-64cm: 396.75g |
| 5 | 122 to 132 | silt loam | 0 | 60 | 97.4 | 95.7 | 0.16 | 0.17 | - | - |
| | | | 60 | 120 | 95.7 | 93.9 | 0.17 | | | |
| | | | 120 | 180 | 93.9 | 92.1 | 0.17 | | | |
| 6 | 53 to 64 | silt loam | 0 | 60 | 99.7 | 97.9 | 0.16 | 0.17 | Must be combined with 40-53cm bag | Proportions: |
| | | | 60 | 120 | 97.9 | 96.1 | 0.17 | | | 40-53cm: 356.63g |
| | | | 120 | 180 | 96.1 | 94.3 | 0.17 | | | 53-64cm: 355.86g |
| 8 | 74 to 84 | silt loam | 0 | 60 | 96.3 | 94.6 | 0.16 | 0.11 | - | - |
| | | | 60 | 120 | 94.6 | 93.6 | 0.10 | | | |
| | | | 120 | 180 | 93.6 | 92.7 | 0.09 | | | |
| 9 | 69 to 79 | silt loam | 0 | 60 | 97.5 | 88.7 | 0.85 | 0.83 | - | - |
| | | | 60 | 120 | 88.7 | 81.2 | 0.8 | | | |
| | | | 120 | 180 | 81.2 | 74.0 | 0.84 | | | |
| 9 | 86 to 91 | silt loam | 0 | 60 | 99 | 97.8 | 0.11 | 0.10 | - | - |
| | | | 60 | 120 | 97.8 | 96.7 | 0.1 | | | |
| | | | 120 | 180 | 96.7 | 95.7 | 0.09 | | | |
| 10 | 23 to 38 | silt | 0 | 60 | 94.6 | 92.7 | 0.18 | 0.15 | - | - |
| | | | 60 | 120 | 92.7 | 91.1 | 0.16 | | | |
| | | | 120 | 180 | 91.1 | 89.9 | 0.12 | | | |

**Table 13:** Falling-head pearmeability test results.

## 6.4 Calculated Ponding Time

Calculated ponding times are shown in Figure 35a-c. Ponding times are a function of the calculated $K_s$ values from Table 13, wetting front soil suction head for the respective $K_s$ values according to Rawls, Brakensiek, & Saxton (1983), and precipitation intensity. See Appendix A.21-A.26 for the values used in the charts. Figure 35a (1.12cm/hour) exhibits a different y-axis as the ponding times were, on average, 82% longer compared to Figure 35b (2.54cm/hour) and 92% longer compared to 35c (3.73cm/hour). The shorter times to ponding calculated here are indicative of soils that would have runoff occuring very soon during high intensity precipitation events.

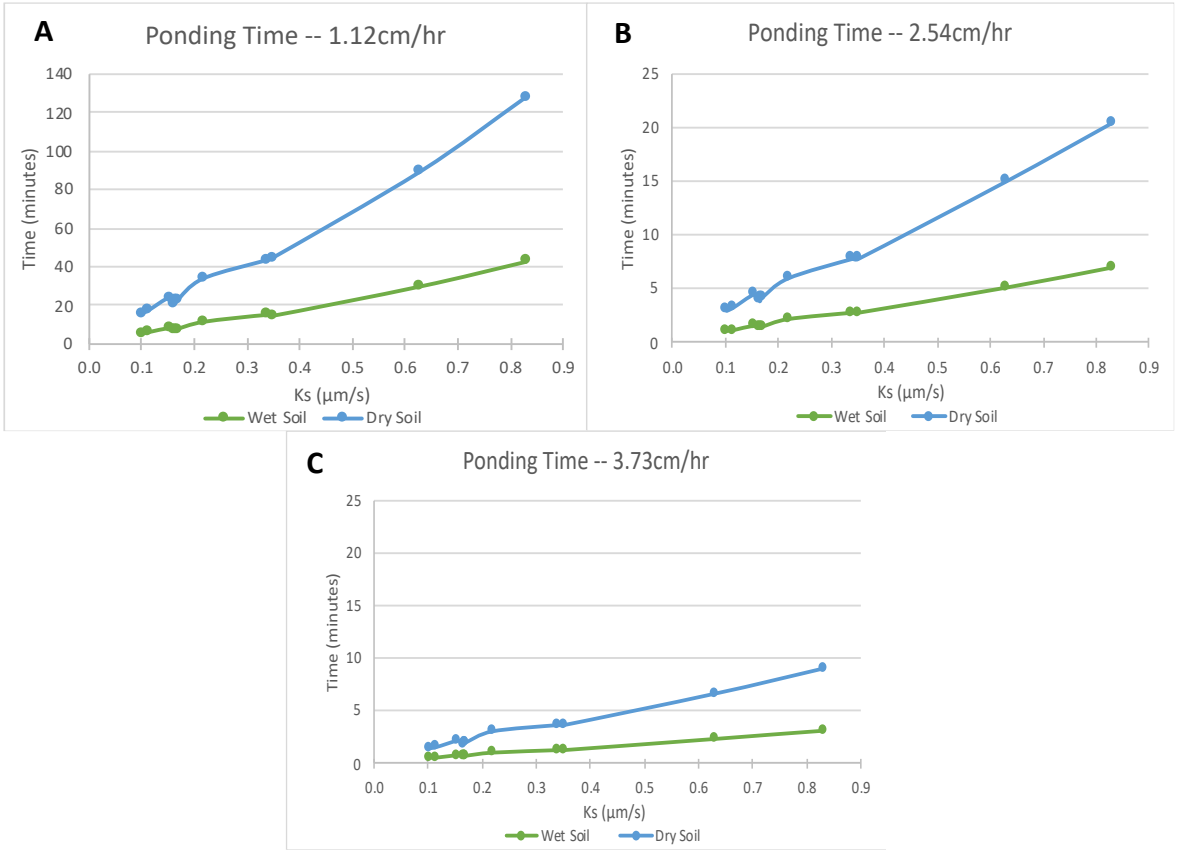


**Figure 35a-c:** Ponding time results as a matter of rainfall intensity (in cm/s) and $K_s$ (in µm/s). Note that Figure 23A has a different y-axis due to having a larger ponding time compared to Figures 23a and 23b.

## 6.5 ANUGA Model Results

The following sections display the results of the ANUGA model simulation of the three 24-hour flood scenarios: Test 1 with a precipitation intensity of 3.73cm/hour (2007 flood

simulation), Test 2 with a precipitation intensity of 2.54cm/hour, and Test 3 (2016 flood simulation) with a precipitation intensity of 1.12cm/hour.

### 6.5.1 ANUGA Test 1 Results

Using historical photographs, appraiser estimates, and anecdotal reports from local residents, the water level during the 2007 flood was estimated to be approximately 5m above the bed of Salt Creek in the West Park. Using NOAA (2017b) precipitation data for this storm event, a rainfall rate of 0.0000104m/s (3.73cm/hour) was established. This rate was applied over the domain for 8 hours (as there is no hourly data for the storm event, it is a safe assumption that the majority of the precipitation fell overnight). Figure 36 is a line chart depicting the water levels through time during the 24-hour simulation for each gauge. The maximum extent of the floodwaters for Test 1 is shown in Figure 37.

Water in all simulations tend to be stored in the main Salt Creek channel south of 400-HWY. Storage also occurs in a tributary near the southern portion of the watershed. Storage areas on the edge of the domain can be diregarded as they are not part of the Salt Creek watershed.

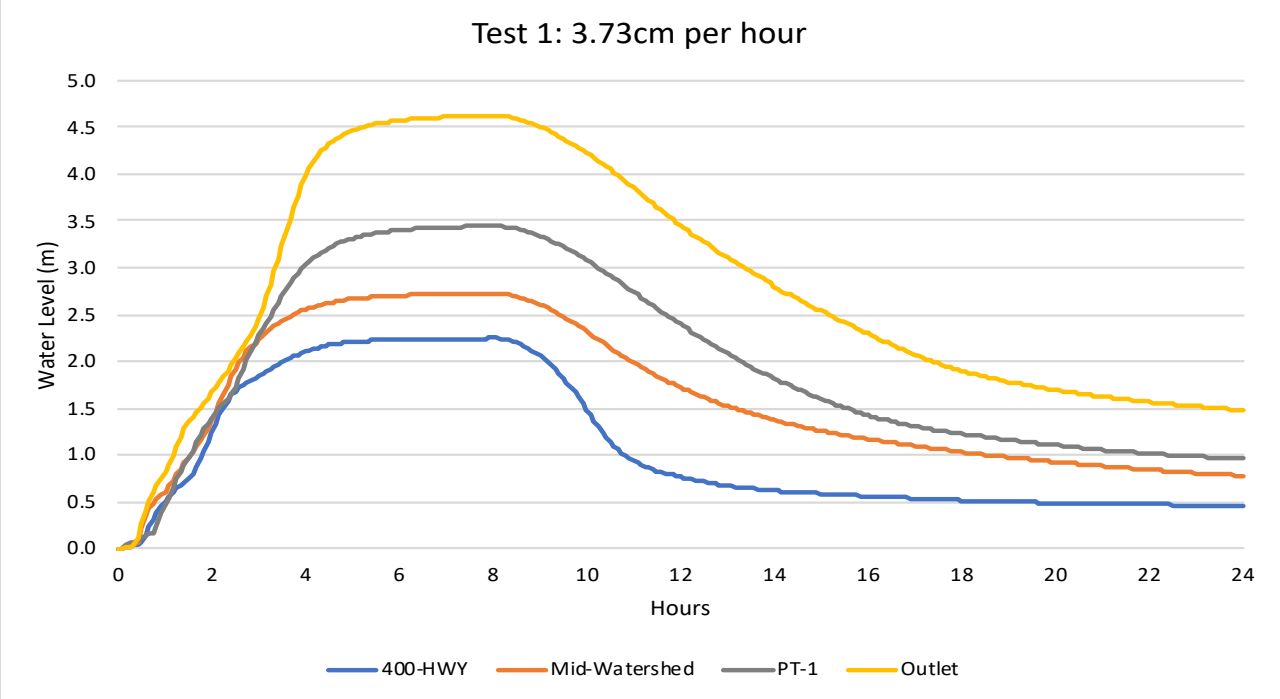


**Figure 36:** Results of the ANUGA Test 1 simulation of the 2007 flood at Salt Creek. 400-HWY reaches a peak water level of 2.25m, Mid-Watershed reaches 2.72m, PT-1 reaches 3.45m, and Outlet reaches 4.62m. 400-HWY experiences a steeper decline in water level after 8 hours.

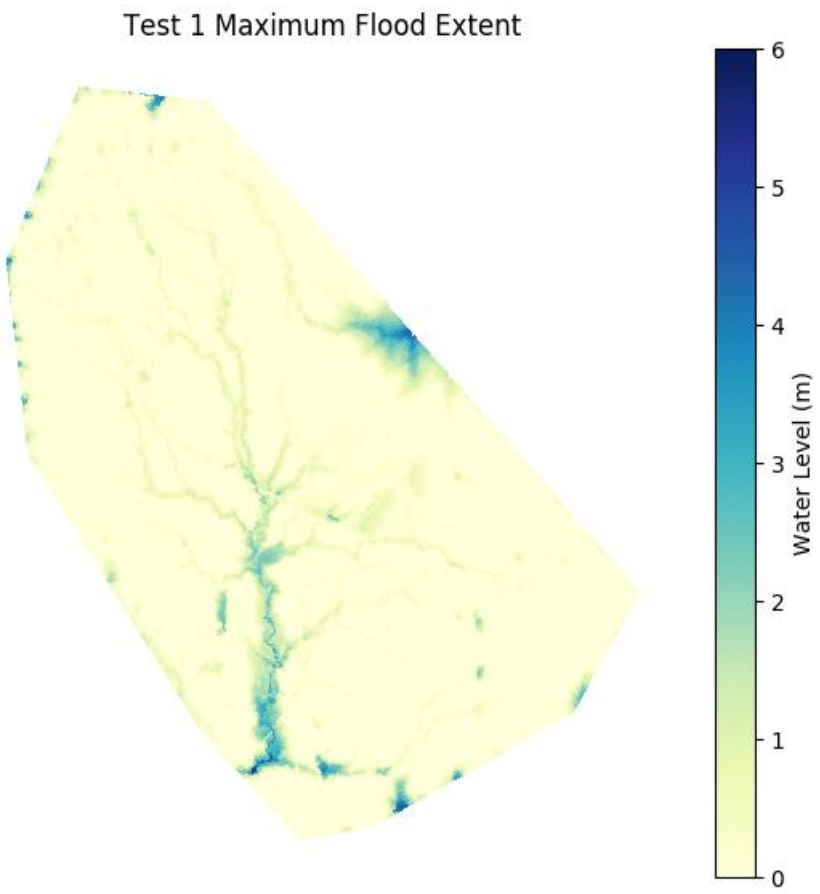


**Figure 37:** Maximum flood extent of the Test 1 ANUGA simulation. Image taken at 9 hours. The main extent of flooding occurs in the lower portions of the main channel. Water levels in the upper reaches north of 400-Highway do not exceed 1.5m.

### 6.5.2 ANUGA Test 2 Results

Figure 38 is a line chart depicting the water levels through time during the 24-hour simulation for each gauge. The maximum extent of the floodwaters for Test 2 is shown in Figure 39.

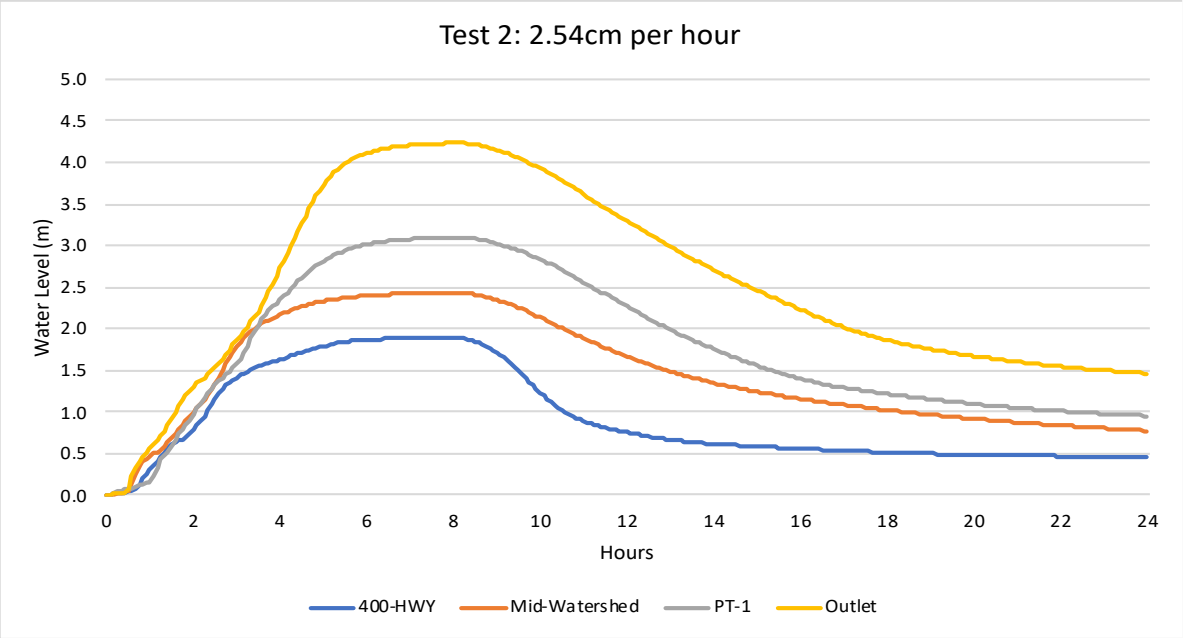


**Figure 38:** Results of the ANUGA Test 2 simulation. 400-HWY reaches a peak water level of 1.89m, Mid-Watershed reaches 2.43m, PT-1 reaches 3.10m, and Outlet reaches 4.23m. 400-HWY again experiences a steeper decline in water level after 8 hours.

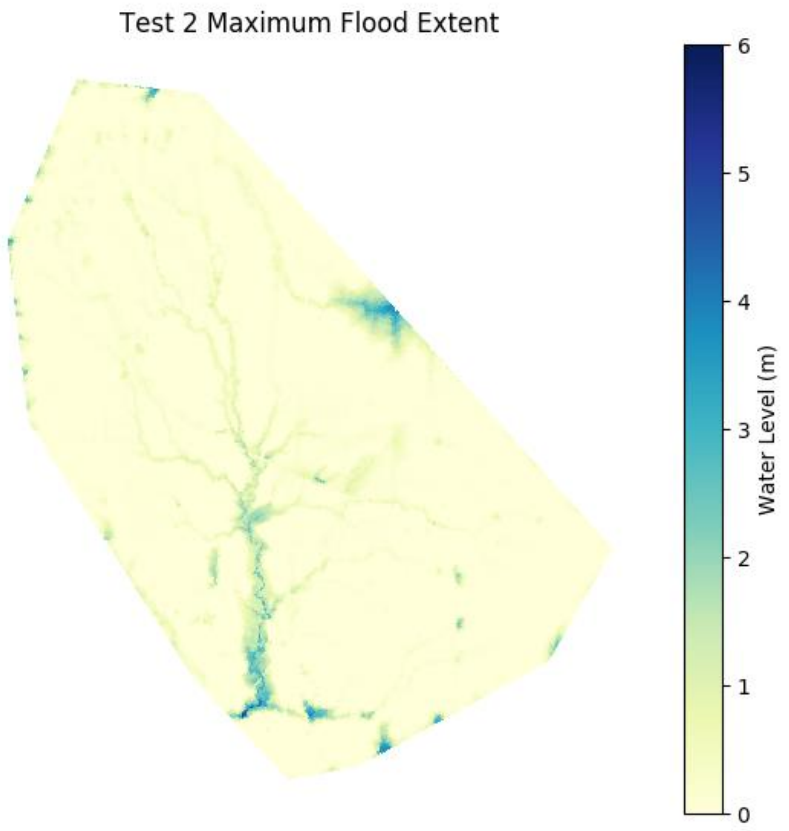


**Figure 39:** Maximum flood extent of the Test 2 ANUGA simulation. Image taken at 8 hours. This simulation had a 10% lower maximum water levels than Test 1 at the stream gauges.

### 6.5.3 ANUGA Test 3 Results

Based on photographs and anecdotal reports from local residents, the water level during the 2016 flood was approximately 3m above the bed of Salt Creek in the West Park. Using NOAA (2017b) precipitation data for this storm event, a rainfall rate of 0.0000031m/s (1.12cm/hour) was established. This rate was applied over the domain for 8 hours. Figure 40 is a line chart depicting the water levels through time during the 24-hour simulation for each gauge. The maximum extent of the floodwaters for Test 3 is shown in Figure 41.

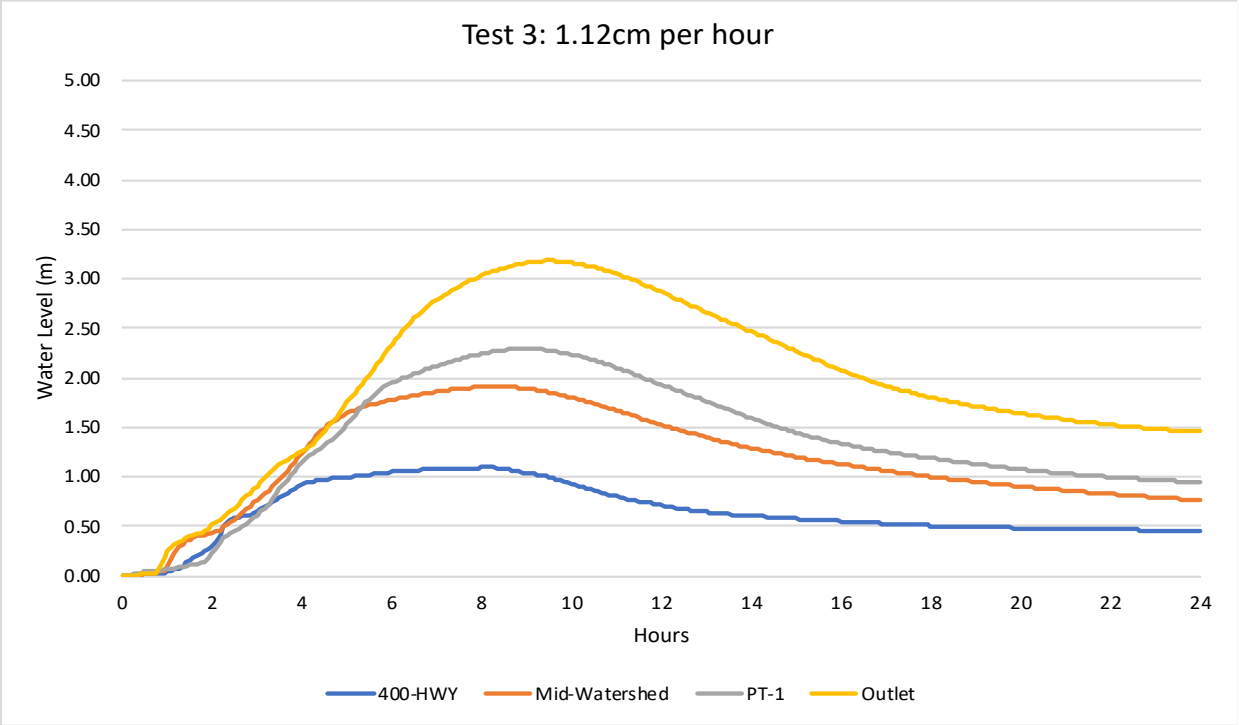


**Figure 40:** Results of the ANUGA Test 3 simulation of the 2016 flood at Salt Creek. 400-HWY reaches a peak water level of 1.10m, Mid-Watershed reaches 1.91m, PT-1 reaches 2.29m, and Outlet reaches 3.18m. 400-HWY again experiences a steeper decline in water level after 8 hours.

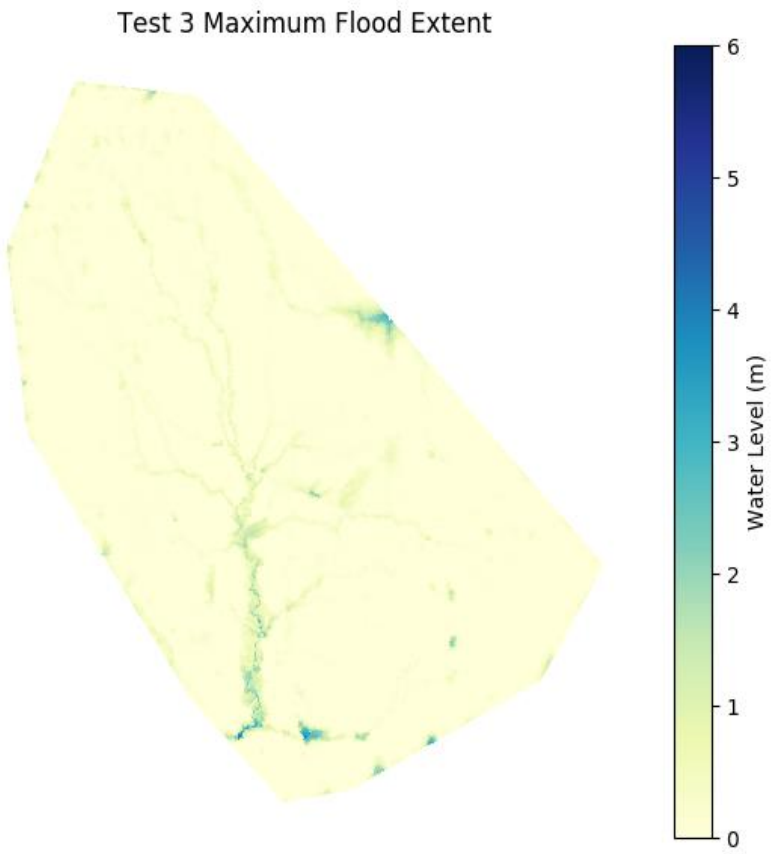


**Figure 41:** Maximum flood extent of the Test 3 ANUGA simulation. Image taken at 8 hours. This simulation had a 26% lower maximum water levels than Test 2 at the stream gauges.

# Chapter 7 - Discussion

## 7.1 Climate and LCLU Change

The current datasets available from the NOAA for the Salt Creek area are not based on local field measurements of climate, as many times they are based on satellite conditions instead of in situ precipitation and temperature measurements. They are therefore inadequate indicators of climate change for the purposes of this study. DeAngelis et al. (2010) suggest that irrigation in western Kansas has caused a 15-30% increase in precipitation in July during the 20$^{th}$ century. Similar logic may apply to the increase in flood occurrences in Salt Creek. More localized, and perhaps more frequent, analyses of LCLU changes in this area may help to confirm or disprove this hypothesis. A strong correlation between LCLU and runoff rate and volume has been documented (Sajikumar & Remya, 2014), and in an area such as Salt Creek, knowing how LCLU patterns are changing could provide insight to where flood mitigation efforts should be focused. Using this information, there is no conclusive evidence that the frequency of flooding has increased in the last ten years.

## 7.2 How Soil Properties Led to a Better Understanding of Flooding in Salt Creek

As hypothesized, soil types in Salt Creek watershed are dominated by fine-grained, low permeability soils that would cause a significant amount of runoff during a precipitation event. However, even accounting for the uncertainties in the PSA analyses through qualitative assessment, there was significantly more silt and less clay in all of the soil samples tested than anticipated prior to sampling. The average soil particle size distribution by percentage was 73.4% silt and 12.5% clay, with a combined average sand percentage of 14.1%.

Tested saturated hydraulic conductivities were very small. The average across all tests was $K_s$ = 0.29µm/s. Comparing these $K_s$ results with Swanson's (1989) results for the corresponding series, it is seen that tested $K_s$ in Salt Creek Watershed are slightly lower than Swanson's (see Table 14). However, Swanson's $K_s$ values are generalized estimates based on soil structure, porosity, and texture; according to their methodology in the report (Swanson, 1989). Even at the fastest estimated $K_s$ value (4.2µm/s from Swanson (1989) study), it implies only 1.5cm of rainfall

can infiltrate in one hour, and the smallest value (0.10µm/s from the present study) implies that only 0.04cm can infiltrate in one hour.

| Soil Type | Depth (cm) | $K_s$ Range (µm/s) Swanson (1989) | $K_s$ Range (µm/s) Salt Creek |
|---|---|---|---|
| Verdigris silt loam | 0-20 | 1.4 - 4.2 | - |
| | 20-152 | 1.4 - 4.2 | 0.10-0.83 |
| Kenoma silt loam | 0-23 | 1.4 - 4.2 | - |
| | 23-61 | < 0.42 | 0.15 |
| | 61-117 | 0.42 - 1.4 | - |
| Woodson silt loam | 0-20 | 1.4 - 4.2 | - |
| | 20-71 | < 0.42 | 0.17-0.22 |
| | 71-152 | 0.42 - 1.4 | 0.11-0.17 |
| Apperson silty clay loam | 0-20 | 1.4 - 4.2 | - |
| | 20-71 | 1.4 - 4.2 | 0.17 |
| | 71-152 | 0.42 - 1.4 | - |

**Table 14:** Lab test permeability of various soils within Salt Creek compared to estimated *Ks* range by Swanson (1989).

There was an obvious discrepancy between the results of the permeability and PSA tests wherein the $K_s$ values calculated from the permeability tests did not reflect excepted values based on the soil textures calculated with the PSA. Although Table 4 must be used with caution when comparing $K_s$ values, Rawls et.al. (1982) will be used to compare results of the falling-head test results with the PSA results. The PSA tests classified 24 of 28 (86%) of samples as a silt loam, with a mean silt content of 73.4% and mean clay content of 12.5%. A silt loam, according to Rawls et.al. (1982), has an estimated $K_s$ of 1.81µm/s. The average $K_s$ for silt loams calculated in this study was 0.31µm/s.

Rawls et.al. (1982) determined the $K_s$ values through a series of equations given the soil texture of the sample. Swanson (1989) estimated the $K_s$ values given the soil texture that was assigned to the sample after analyses. Because both of these studies did not lab- or field-test $K_s$, but rather, relied soley on the soil texture assigned to the sample. As seen in Table 4, $K_s$ ranges assigned to each soil texture substantially vary between the two studies. It is difficult to evaluate the accuracy of the $K_s$ values derived from the falling-head tests, as there is no published literature on field- or lab-tested $K_s$ values in Salt Creek watershed prior to this study. One source of the lower saturated hydraulic conductivity of the lab tested samples could be due to the extra

compaction that was needed to inhibit the formation of water pathways along the sides of the permeameter. This action could have affected available pores that would likely be present in the field. Despite this, these lab-tested $K_s$ values correlated relatively well with Swanson (1989) estimations (Table 12). However, with the tested $K_s$ being one order of magintude less from Rawls et.al. (1982) values for silt loams suggests that either the soil texture determined by the PSA tests were in error or that the $K_s$ values measured in the falling-head permeability tests had may not accurately represent in situ soils.

According to the WSS and a Wilson County soil survey (Swanson, 1989), silt and clay volumes in this watershed are estimated to be >40% and >30%, respectively. In contrast, the volume of silt and clay indicated by the PSA tests in this study were commonly >70% and <15%, respectively. Swanson (1989) estimates clay contents of independent soil series and depths, and, depending on the soil series, places estimates of clay content at 16-60% amoungst soil series in this watershed— far above the lab measured clay content from this study. However, Swanson identified most the samples as silt loams, even though the estimated clay percentages were higher than what would normally be considered a silt loam (0-30% clay) (United States Department of Agriculture, 2018). Given these discrepancies, we suggest that even though the diluted soil samples were placed in an ultrasonic bath to break apart aggregates, tightly-bound clay aggregates were not broken apart completely. This source of error was also noted by Birrell (1966). The aggregation of the clays in the soil could be caused by a high organic matter content, which has been shown to decrease the clay dispersibility (Nelson, et. al., 1999). The Mastersizer 3000 would record these aggregates as if they were one grain or particle, and therefore record them as a silt particle, or in more extreme cases, a sand particle. Therefore, the results of these PSAs may be skewed to reflect higher percentages of silt and sand than they actually have. It is very difficult to break apart these aggregates, but in future studies subjecting the samples to a longer duration in the ultrasonic bath, as well as an acid bath to decrease organic matter, would be beneficial for producing more accurate particle size representation for soils in this area.

Because PSA determines the soil texture, most of the soils were defined as silty loams. Using the calculated $K_s$ values and the Rawls et. al. (1982) $K_s$ values for a given soil texture as seen in Table 4, the soil textures in this watershed are much more likely to be categorized as silty clay loams, clay loams, or silty clay— all of which better represent the high clay content estimated by Swanson (1989) and the measured $K_s$ values in Salt Creek watershed. These soil textures are

much closer to what was expected of the soils in the area and are likely to be a more accurate depiction of the actual soil textures and clay contents in Salt Creek watershed.

Ponding time calculations revealed estimates of when water will begin to pool at the surface. A longer ponding time is preferred as this means more water is infiltrating rather than running off. The ponding times were completed on wet and dry soils for the three precipitation intensities used in this study. As expected, the higher $K_s$ values determined in this study returned longer ponding times, as water can infiltrate more quickly in these environments relative to the smaller $K_s$ values. For both the wet and dry soil ponding times, 1.12cm/hour precipitation intensity had a longer period of time before ponding occurred. Ponding times for 1.12cm/hour were calculated to be 82% longer when compared to 2.54cm/hour and 92% longer when compared to 3.73cm/hour under both soil conditions. The differences in ponding time between the wet and dry soils for the same precipitation intensity was as follows: dry soil ponding times were 67% longer than wet soils for 1.12cm/hour, 66% longer for 2.54cm/hour, and 66% longer for 3.73cm/hour.

## 7.3 Maximum Flood Extents as Simulated by ANUGA

ANUGA's primary function was then to simulate the flood extents of the 2007 and 2016 floods using either a 3.73cm/hour or 1.12cm/hour precipitation intensity, respectively, for 8 hours; a Manning's n of 0.035 (floodplain with row crops as determined by Chow (1989)); and an domain with elevation data. The most valuable information ANUGA provided was estimated stream gauge measurements, specifically measurements simulating water depths at PT-1, as most actual water depth information was gathered at this location. Table 15 shows the maximum water levels reached at each gauge point during the three ANUGA simulations. Table 16 shows the percent change between the maximum water levels from Table 15. Table 16 reveals that there is a significantly smaller increase in maximum water level between Test 1 and Test 2 compared to that of Test 2 and Test 3. This could be due to the relative flatness of this area, which forces water to spread laterally (increasing extent) rather than vertically (increasing depth) during flood events that are larger than the 2-year flood.

| Water Level (m) of Tests 1, 2, & 3 | | | | |
|---|---|---|---|---|
| | **400-HWY** | **Mid-Watershed** | **PT-1** | **Outlet** |
| **Test 1** | 2.25 | 2.72 | 3.45 | 4.62 |
| **Test 2** | 1.89 | 2.43 | 3.10 | 4.23 |
| **Test 3** | 1.10 | 1.91 | 2.29 | 3.18 |

**Table 15:** Maximum water levels for Tests 1, 2, and 3 from the ANUGA simulations. PT-1 is highlighted as this gauge has the most real-life data attached to this location allowing comparisons to be made.

| | **400-HWY** | **Mid-Watershed** | **PT-1** | **Outlet** |
|---|---|---|---|---|
| **% Change Between Tests 1 & 2** | 16% | 11% | 10% | 8% |
| **% Change Between Tests 2 & 3** | 42% | 21% | 26% | 25% |
| **% Change Between Tests 1 & 3** | 51% | 30% | 33% | 31% |

**Table 16:** Percent change of the maximum water level between the three ANUGA simulations. Percent change is calculated by a variation of the equation: 1 – (Test 2 Max / Test 1 Max) * 100, using the gauge data from Table 15. These percentages show that the changes between Tests 1 and 2 were less than that between Test 2 and 3.

Simulation results were directly compared to photographs and PT-1's field data, all of which reside in the West Park. Peak water levels during the 2007 and 2016 floods at the West Park were estimated to be 5m and 3m, respectively, according to historical photographs and anecdotal reports from residents. However, ANUGA results for these simulations resulted in peak water levels of 3.45m and 2.29m, respectively, at PT-1. After multiple simulation runs with various code alterations (such as changing boundary conditions and maximum triangle size), it was apparent that the water levels in Salt Creek during flood events could not effectively be replicated by ANUGA using the boundary conditions and rainfall rates specified. Peak water levels were consistently lower than what was experienced in reality. Stephen Roberts, ANUGA co-developer, was contacted to ensure that all model inputs and codes were executed correctly. He validated that the model was working properly and offered that the addition of culverts and a smaller maximum area per triangle might aid in producing higher water levels. Culverts were added and triangle sizes were adjusted as suggested, although this only caused minor increases in maximum water levels.

ANUGA was originally developed for the use of tsunami simulation, but papers have expressed how it has application for other types of inundation scenarios such as inland flooding (Van Drie, et. al., 2008; Mungkasi & Roberts, 2013). Van Drie et. al. (2010) stated they were able to successfully and consistently replicate measured flood levels in a 25km$^2$ catchment. This study

has shown ANUGA can be used to simulate inundation due to rainfall in inland 50km$^2$ watersheds; however, the accuracy of the results has to be evaluated carefully.

## 7.4 Theorized Impacts of the Fall River on Salt Creek by ANUGA and GIS

The lower-than-expected peak water levels predicted by the ANUGA simulations are most apparent in the 2007 flood simulation. One explanation for this discrepancy may be found in the influence of the nearby Fall River on Salt Creek water levels during extreme precipitation events. The Fall River flows from the northwest to the southeast and has a change in elevation of 200m from the upper reaches to the outlet. Figure 30 shows the location of the Fall River watershed as well as the elevation of the soil surface above sea level.

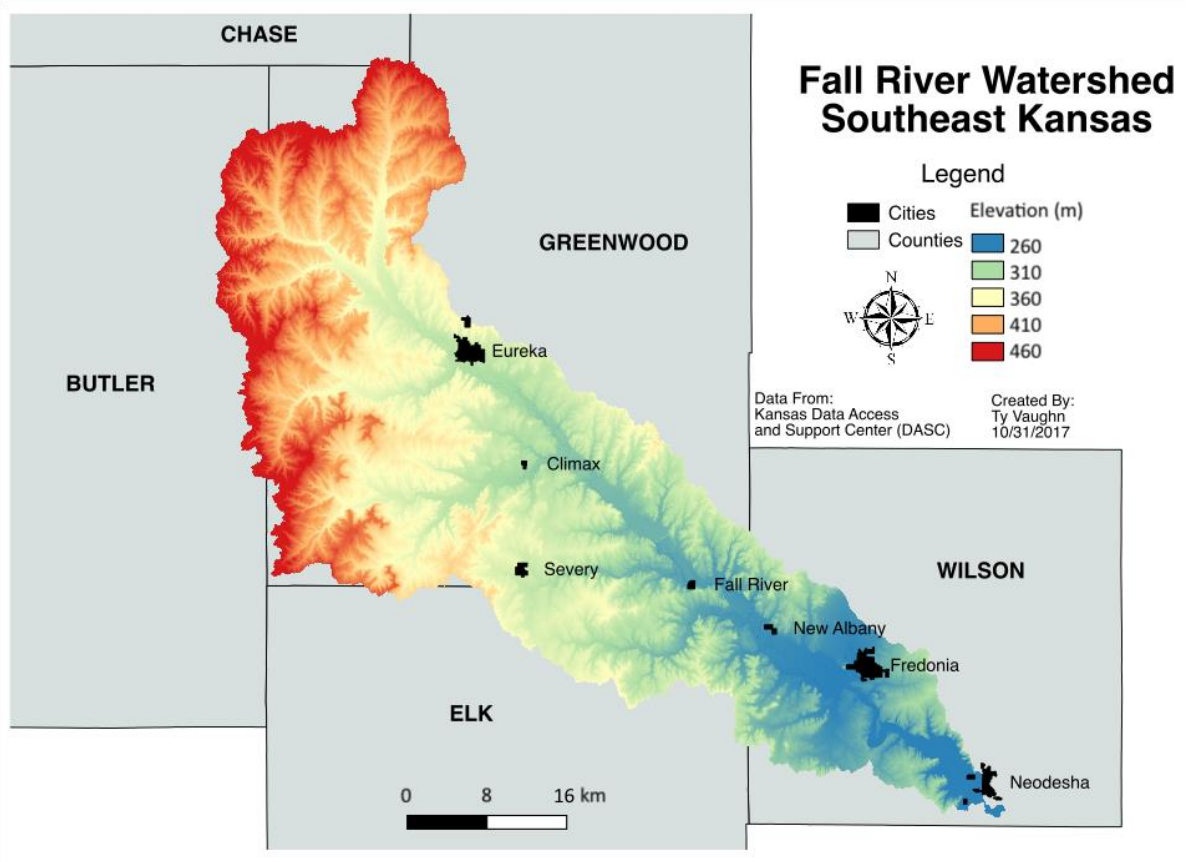


**Figure 42:** Fall River watershed elevation map. Fredonia is located near the southwest portion of the watershed.

An interesting occurance of geological constraints on the Fall River's floodplain is seen just south of Salt Creek. Much of the Fall River flows across sedimentary bedrock that is easily erodable, such as shale and sandstone. However, a layer of limestone appears south of Fredonia

that has caused a visible constriction of the alluvial floodplain— from a large 2,621m to only 579m in width. See Figure 43 for the geologic map of the Fall River.

An USGS stream gauge (ID# 07169500**)** is located 2km south of Fredonia on Harper Road bridge. The drainage basin at this stream gauge has an area of 2,142km$^2$. The National Weather Service (2018) keeps records of historic crests (maximum water level heights) that have occured at this gauge site throughout recorded history (various devices and techniques were used to measure these crests before the installation of a standard USGS stream gauge). The 2007 flood tops the list, reaching a maximum crest height of 12.5m. This crest is 1.5m higher than the next highest crest, which occurred in 1945.

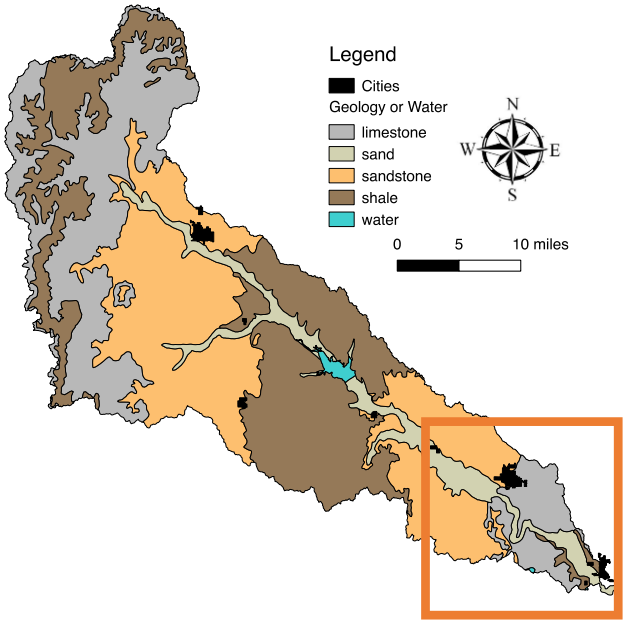


**Figure 43:** Fall River geologic map with data from Kansas DASC (2018). The red box indicates the area of interest as where sandstone in the form of the Stranger Formation, Douglas Group (see Section **Error! Reference source not found.** for geologic details) meets the Stanton Limestone.

Floods of this magnitude can often wreak havoc on tributaries. Due to the the restricted nature of the Fall River floodplain at this location, combined with the high intensity, long duration precipitaiton events, we hypothesize that the volume of water in the Fall River exceeded the storage capacity of the narrow floodplain at this location. Therfore, water spread out laterally and backedup into nearby tributaries, i.e. Salt Creek.

Historical photographs taken throughout the Fall River's watershed show that the Fall River watershed also experienced extensive flooding similar to that of Salt Creek during the 2007 flood. Salt Creek joins with Plum Branch of the Fall River, which then joins with the Fall River 2.3km upstream of the USGS stream gauge (Point B). This confluence with the Fall River has an elevation of 253m. The confluence of the Plum Branch of the Fall River and Salt Creek has an elevation of 256m (Point C). This is an elevation difference of 3m. See Figure 44.

Compared to the surrounding topography, Salt Creek watershed has a very simliar elevation to the Fall River floodplain where the two converge. Rainbow Creek watershed, located

directly south of Salt Creek watershed, as shown by the red box in Figure 45, also has a similar elevation.

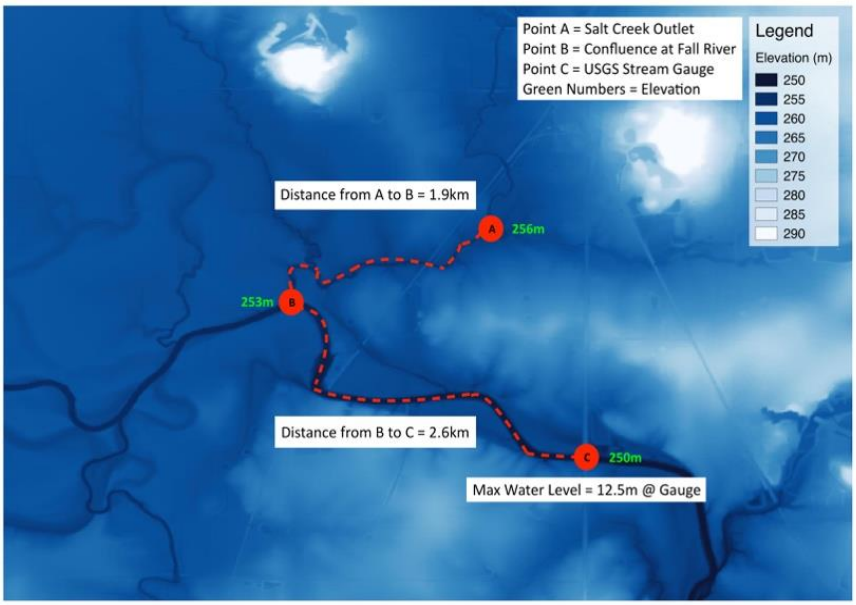


**Figure 44:** Distances between the Fall River USGS stream gauge (Point A), and Salt Creek's outlet (Point C). The green numbers are the elevations of the channel beds. The maximum water level of 12.5m is what occurred during the 2007 flood.

It is plausible that due to the combination of a unique Fall River floodplain constriction and high intensity, long duration precipitaiton events, that the large volume of water trying to flow down the Fall River was overcoming the ability of the narrow floodplain to transmit the flow within the Fall River and therfore water began to back up into Salt Creek's channel, effectively including it as a part of the floodplain. However, flooding in Salt Creek is not only the result of from the Fall River, as demonstrated in the Septemeber 9th, 2016 flood. There was only a maximum water level of 6.3m at the Fall River stream gauge (National Weather Service, 2018) from this event. It appears that, in this case, the flood events at Salt Creek depend more on precipitaiton patterns (location, intesity, duration, and total depth) than on the Fall River's water levels. However, this does not invalidate the original thought that during large precipitation events, the Fall River could essentially push water into *or* prevent water from flowing out of Salt Creek.

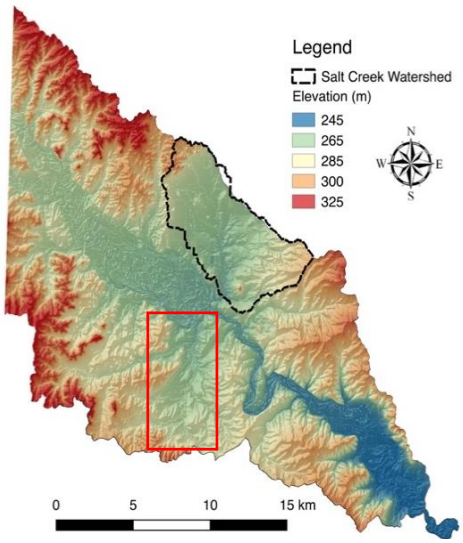


**Figure 45:** Salt Creek watershed's elevation is very similar to the floodplain of the Fall River. The area enclosed by the red box shows a similar elevation to the floodplain.

### 7.4.1 Water Surface Elevation and Flood Extent

There were no official measurements of the 2007 Salt Creek flooding. Appraisers attempted to make a map of flood extent (Kansas DASC, 2018); however, there were areas in this appraiser flood map that were depicted as not flooded when they were documented as flooded by photographs and resident tesimony, leading to a questioning of this map's accuracy. Judging from a photograph of the West Park area taken from the West Mound on July 30 (Figure 1), an estimate of the peak water level was placed at approximately 5m. This estimate corraborates the water level estimates of residents.

To visualize the possible extent of thirteen water surface elevations across the confluence area of the Fall River and Salt Creek, QGIS was used to create an inundation map which describes the areas inundated at the specified waters surface elevation (WSE). Figure 46 shows thirteen estimates of flood extent based purely on the WSE specified. The green dot in the lower right-hand corner is the stream gauge at Fall River, which has an elevation of 250m a.s.l. The WSEs started at 256.5m a.s.l. (Fall River water is contained in the channel) and, moving in 0.5m increments, ended at the peak WSE of the 2007 flood at 262.5m a.s.l. (250m bed elevation at the stream gauge + 12.5m recorded water level) (National Weather Service, 2018). Areas higher in elevation than the specified WSE are shown in red while areas equal to or lower in elevation than the specified WSE are shown in blue (Figure 46). Blue areas will inundated with water at that water surface elevation.

The following are important observations of Figure 46:

- **258.5m WSE:** Water is beginning to leave the Fall River channel near the stream gauge and flow into the floodplain. Water is also moving into the floodplain near Salt Creek's outlet. At this WSE, the stream gauge at the Fall River reaches moderate flood stage (National Weather Service, 2018).
- **259.0m WSE:** Flooding worsens in the Fall River channel near the stream gauge and Salt Creek's outlet. Flooding is beginning to occur in other tributaries to the Fall River.
- **259.5m WSE:** The part of the Fall River channel that resides in limestone has a floodplain that is fully inundated to some degree. Very noticeable flooding occurs near Salt Creek's outlet and in tributaries to the Fall River.

- **260.0m WSE**: Much of the Fall River floodplain that has shale and limestone bedrock has become inundated. The entire West Park is now experiencing flooding. Flood extent appears to expand more more-so upstream in Salt Creek, and rather expanding laterally. This is likely due to the sandstone mounds that are bounding either side of the outlet.
- **260.5m WSE:** Flooding worsens in the Fall River's floodplain and floodwater continues to spread upwards into Salt Creek's channel.
- **262.5m WSE:** This is a close approximation of the flood extent of the 2007 flood. The entire portion of the Fall River floodplain shown in this LiDAR image is inundated.

According to the National Weather Service (2018), the Fall River at the Fredonia stream gauge reaches moderate flood stage at a water level of 8.2m and major flood stage at 11m. Figure 46 shows that at a water level of 9m at the Fall River stream gauge, Salt Creek's lower floodplain begins to be affected by floodwater from the Fall River.

### 7.4.2 Using ANUGA to Model the Impacts of the Fall River on Salt Creek

Modeling the impacts of the Fall River's floodwater on Salt Creek based on the full scale of the Fall River watershed is beyond the scope of this study, as it would require greater computing power than currently available. Instead, we have attempted to model this by modifying the reflective boundary conditions of the Salt Creek domain in the ANUGA model, i.e. to simulate how the Fall River may impact Salt Creek during a large flood event. Three tests were conducted: Tests 4a, 4b, and 4c (see Figure 47-Figure 49). All the inputs were identical to Test 1 (2007 flood simulation), including rainfall intensity and duration. The only change for the Test 4 group was to implement a reflective boundary (Br) at the outlet at a specified time during the event.

Test 4a had the outlet turn reflective at the 4-hour mark, Test 4b at the 6-hour mark, and Test 4c at the 8-hour mark. The reflective outlet was an effort to simulate an event in which water could not escape from Salt Creek after the specified number of hours was reached, therefore acting as if water from the Fall River was a barrier. The outlet was kept as a reflective boundary for the full duration of the model run (24 hours) so that the timing of peak water level could be determined. In reality the Fall River's water levels would not be static through time, and this could change the

output of Salt Creek during a flood event. The simulations yielded the hydrographs in Figure 47-Figure 49

In Figure 47-Figure 49, the gauge at 400-HWY is the only gauge which begins to have a receding of water level after rainfall ceases. It appears that the 400-HWY is not affected by the reflective boundary at all, peak water level is almost identical at this gauge between all three tests. It is hypothesized that the 400-HWY gauge is at a point upstream in Salt Creek where it is not affected at all by backup floodwater. Test 4b produced water levels that were similar to those of the 2007 flood. These results suggest that if a large-scale flood event, similar to that of the 2007 flood occurred, it is possible that six hours after the precipitation event begins, Salt Creek floodwaters may not be able to escape the watershed and therefore induce an increase in the flood extent. However, this is hypothesis will need further modeling and field analyses completed to fully understand the mechanisms of flooding here.

This does not mean that flooding in Salt Creek requires backflow of floodwaters from the Fall River in order to occur. As seen in the September 2016 flood event, Salt Creek flooded when the stream gauge at the Fall River only read 6.3m, or a water surface elevation of 256.3m. At this stage, the Fall River can easily contain its flow and would not have backed up into Salt Creek. Therefore, flooding in Salt Creek also appears to depend on precipitation patterns such as precipiration intensity, depth, and location. However, this does not provide an explanation for the unaccounted for water levels from the Test 3 ANUGA simulation, which had water levels 0.7m off from real flood extent estimates. Potentially, the precipitation event this storm experienced may have lasted for a shorter amount of time with a higher precipitation intensity, which would have created a steeper, taller hydrograph.

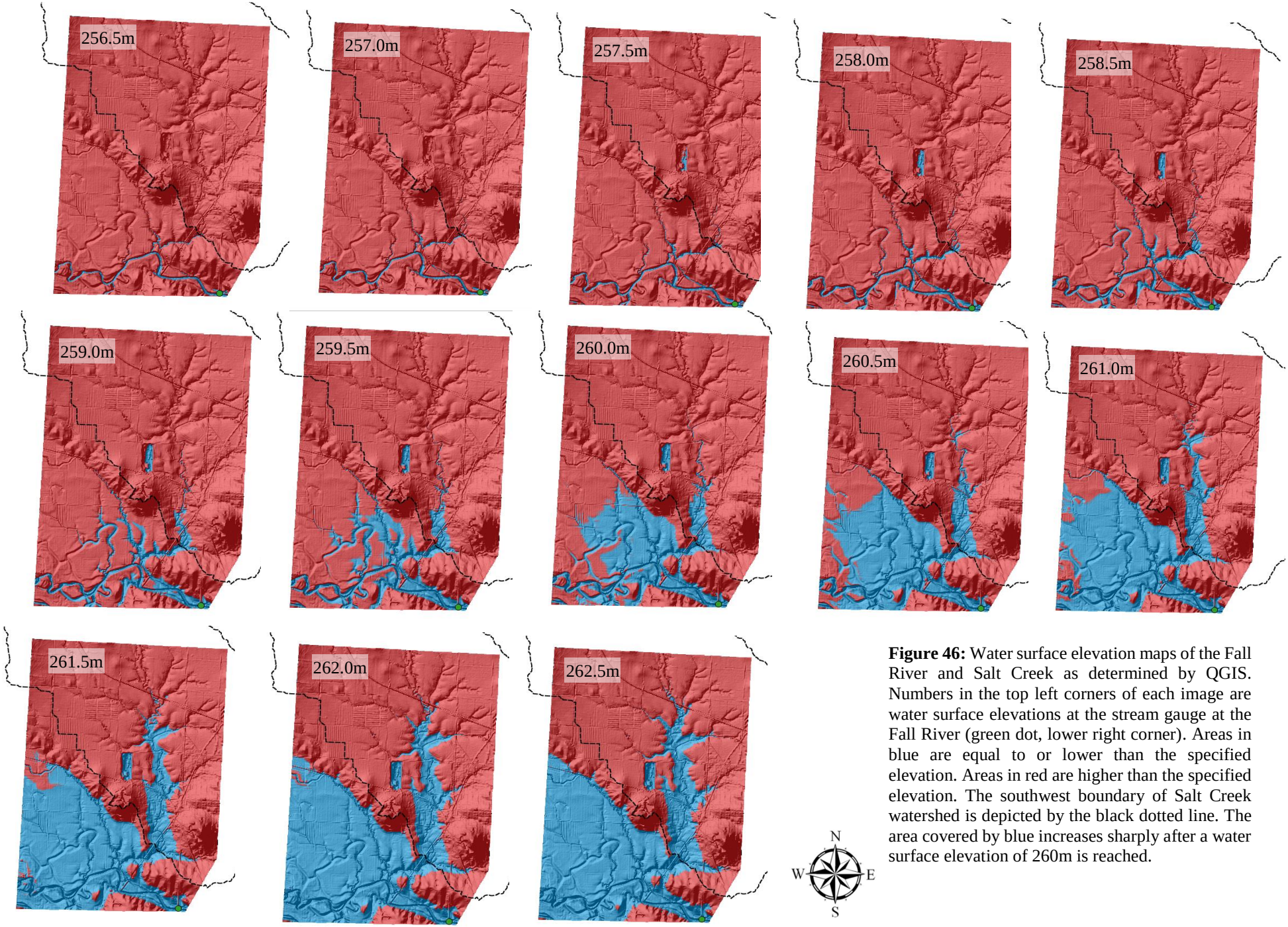


**Figure 46:** Water surface elevation maps of the Fall River and Salt Creek as determined by QGIS. Numbers in the top left corners of each image are water surface elevations at the stream gauge at the Fall River (green dot, lower right corner). Areas in blue are equal to or lower than the specified elevation. Areas in red are higher than the specified elevation. The southwest boundary of Salt Creek watershed is depicted by the black dotted line. The area covered by blue increases sharply after a water surface elevation of 260m is reached.

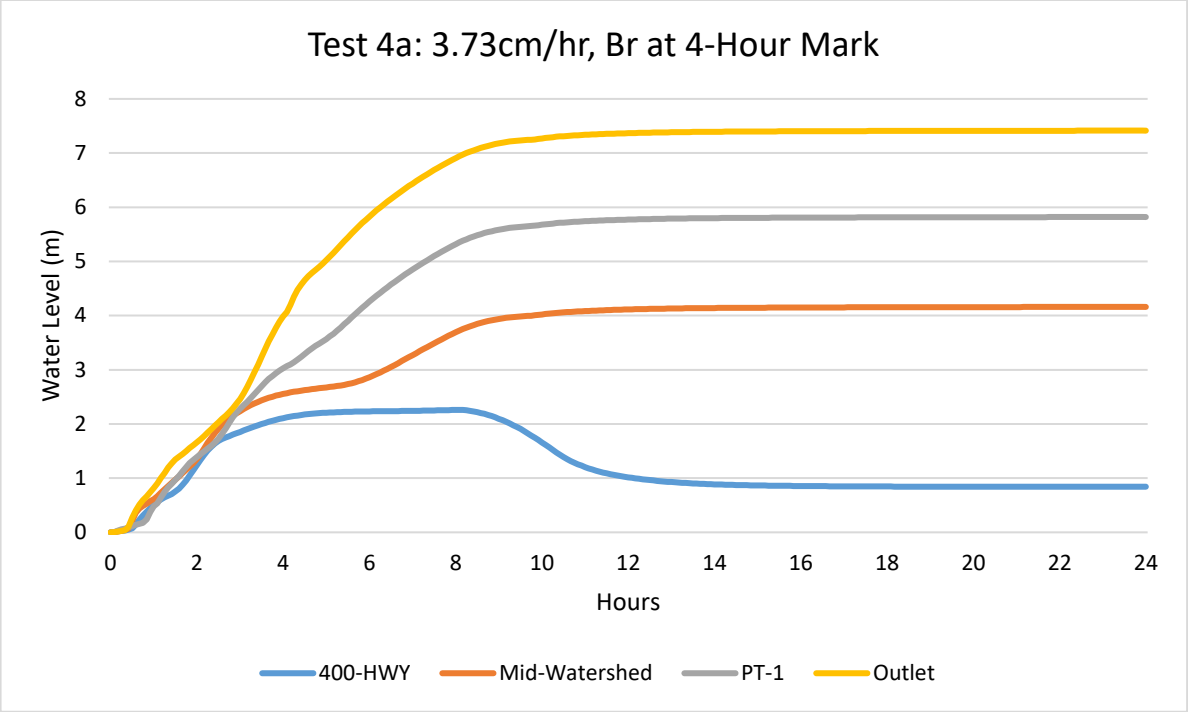


**Figure 47:** Test 4a. Outlet switches to a reflective boundary (Br) at the 4-hour mark. 400-HWY reaches a peak water level of 2.26m, Mid-Watershed reaches 4.16m, PT-1 reaches 5.82m, and Outlet reaches 7.41m.

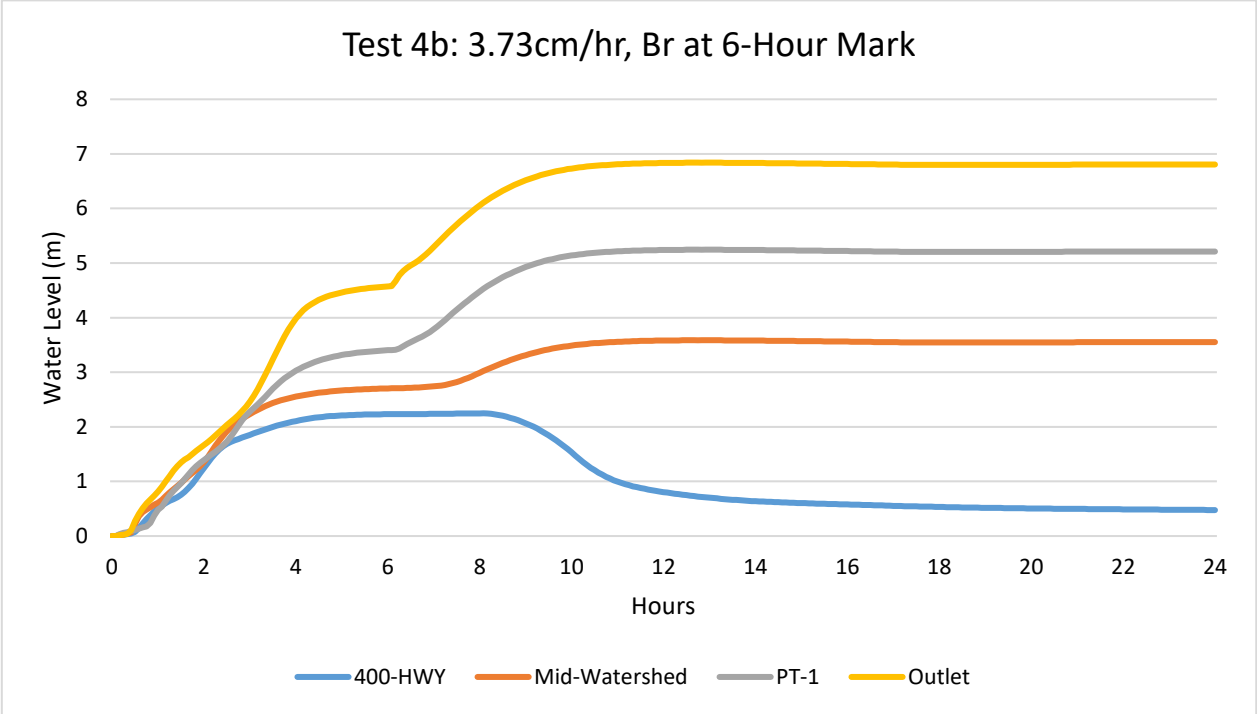


**Figure 48:** Test 4b. Outlet switches to a reflective boundary (Br) at the 6-hour mark. 400-HWY reaches a peak water level of 2.25m, Mid-Watershed reaches 3.59m, PT-1 reaches 5.24m, and Outlet reaches 6.84m.

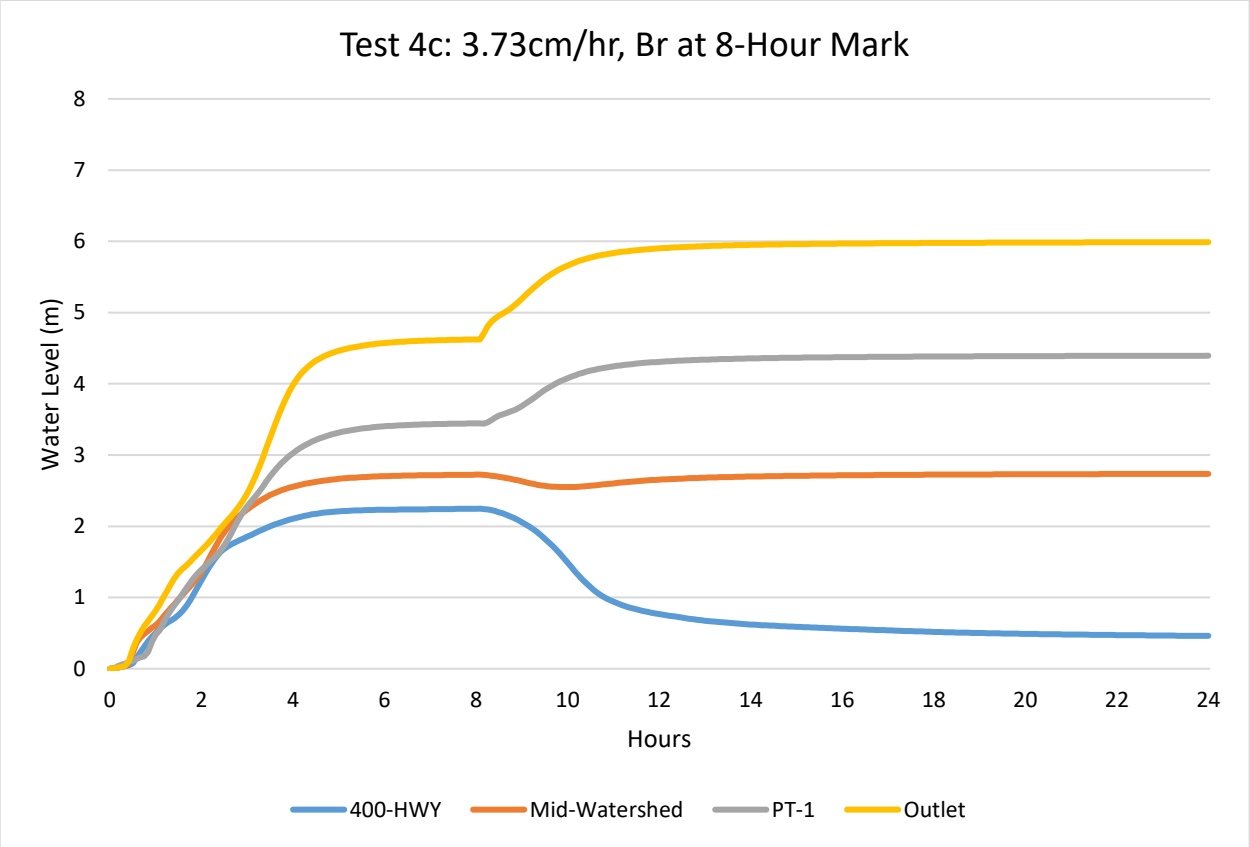


**Figure 49:** Test 4c. Outlet switches to a reflective boundary (Br) at the 8-hour mark. 400-HWY reaches a peak water level of 2.25m, Mid-Watershed reaches 2.74m, PT-1 reaches 4.39m, and Outlet reaches 5.99m.

## 7.5 Suggestions for Future Studies on Salt Creek

Soil analyses in the field (i.e. in situ) would greatly benefit the understanding of how soil physical properties affect flooding within Salt Creek watershed. In situ infiltration and permeability tests throughout the watershed would reduce the amount of deviation that occurs from disturbed samples like those taken with the hand-drilled auger. Including soil physical properties such as infiltration rate and a domain with frictional resistence assigned by land cover (Manning's *n*) would be advantageous to further analyze how these factors affect Salt Creek's flood extent. To further this, modeling changes in these two factors to predict how Salt Creek flood extents will change with changes in land cover an infiltration rate.

The addition of debris flow and stream blockages in these simulations would benefit the model by assessing whether or not these have a noticable affect on the Salt Creek's flood extents and flow patterns. It is hypothesized that the inclusion of stream blockages likely would have cause

the water level of the channel upstream of the bloackage to be higher than the water level of the channel dwnstream of the bloackage.

By implementing realtime precipitation data into the model and comparing the simulation results to actual water levels of Salt Creek during the same precipitation event, a model can be validated for use on more hypothetical precipitation events to aid in the determination of flood extents for a multitude of precipitation intesities, depths, and storm durations.

Results of this study show that geologic conditions contribute to the frequency and intensity with which Salt Creek floods. However, more data are needed to prove the Fall River's impact on the Salt Creek. A watershed-scale model of the Fall River would aid in this evaluation— something which ANUGA has not presently been validated to do due to the size of the Fall River watershed. The geologic constraints on the Fall River's floodplain south of Fredonia present an unusual situation for flooding within Salt Creek watershed that would be well suited for a modeling study that can handle the large scope. Modeling different precipitation patterns, both spatially and temporally, across the Fall River watershed and assessing how these different patterns affect the flooding of Salt Creek would be valuable.

An additional study could be revolved around the Fall River Lake, which is situated 25.5km upstream of the stream gauge on Harper Road. The lake was built in 1949 with the main purpose of flood control. The Fall River Lake has experienced excessive sedimentation, and is estimated to lose half of its capacity in 2045 if management plans are not enforced (Rahmani et al., 2018). Capacity loss in the lake could result in higher water levels downstream of the lake due to less water being able to be held behind the dam. Assessing the impact of the capacity loss on the flooding patterns of the Fall River, and subsequently flood patterns of Salt Creek, would be an excellent topic of interest.

# Chapter 8 - Conclusion

The results of this study provide a comprehensive analysis of Salt Creek watershed in order to evaluate the reasons for flooding in the area. There was no conclusive evidence siting an increase in flood frequency in Salt Creek watershed, however, Salt Creek appears to have a landscape in which flooding conditions are prime, mainly due to the soil properties such as fine-grained soil textures created from the underlying shale bedrock that decrease saturated hydraulic conductivity and, consequently, decrease infiltration rates. Falling-head permeability tests detailed the inability of water to infiltrate quickly into these soils. The average saturated hydraulic conductivity ($K_s$) determined from the permeability tests was 0.29μm/s. This means that water can infiltrate at an average rate of 0.1cm/hour in fully saturated soils. Soil testing by particles size analysis (PSA) confirmed the presence of fine-grained soils. The particle size analysis found that, on average, the soils are composed of 73.4% silt and 12.5% clay, with an average total sand percentage of 14.1%. Between the three depths of soil samples (shallow, middle, and deep), the shallow and deep samples have >83% silt while the middle depth are 78.6% silt. The middle depths are, on average, more sandy than the shallower or deeper depths.

PSA and falling-head permeability tests suggest different clay contents for the soils. The low $K_s$ values derived from the permeability tests suggest clay content is higher than determined via the PSA tests. This was likely caused by a lack of pretreatment to the soil before the PSA, such as an acid bath to rid of organic matter. Although an ultrasonic bath was used on the diluted soil samples prior to the PSA, further pretreatment might have reduced any occurrence of aggregated soil particles, leading to an increased percentage of clay in the results. Of the soils analyzed, 86%are classified as silt loams, based on the PSA, but they may be better classified as clay loams or silty clay based on the permeability test results. Using the permeability results, estimated ponding times were calculated using the equations listed in Section 5.4.4 along with the saturated hydraulic conductivities calculated in this study. Ponding times varied depending on the precipitation intensity and the saturated hydraulic conductivities, and ranged from 1 to 128 minutes for dry soil and 0.5 and 43 minutes for wet soil.

Precipitation events occurred on 26 days during the field observation period of water levels and precipitation, and of those that occurred, none produced any flooding. Of those 26 days, only 7 days produced precipitation totals over 10mm or more. Using data from two pressure transducers

and two tipping bucket rain gauges placed in the field, it was deduced that at PT-1 in the West Park, peak water levels occurred between 5-7 hours after peak rainfall intensity.

Three ANUGA simulations were conducted to assess flood extents of Salt Creek during three precipitation intensities: 1.12cm/hour, 2.54cm/hour, and 3.73cm/hour. The maximum extents of each simulation at PT-1 were 2.29m, 3.15m, and 3.45m, respectively. The ANUGA hydrodynamic model produced underwhelming flood extents that did not match the extents of the flood events they simulated. The simulated maximum flood extent at PT-1 of the 2007 flood using ANUGA was 3.45m, which is 1.55m less than what photographs and anecdotal evidence suggests occurred. Additionally, the simulated maximum flood extent at PT-1 of the 2016 flood using ANUGA was 2.29m, which is 0.71m less than what photographs and anecdotal evidence suggests occurred.

A key discovery from this research is the role flooding in the Fall River may have on the flood extent of Salt Creek during large precipitation events. When the Fall River watershed receives a substantial rainstorm, the resulting floodwaters may back up into Salt Creek's floodplain—or at least prevent flood waters from within Salt Creek from escaping. The geology surrounding the confluence of Salt Creek and the Fall River has created a funnel effect that, when the smaller, limestone portion of the floodplain is overwhelmed with floodwater, the floodwaters begin to backup into the larger, shale portion of the floodplain of which Salt Creek is a part. The low elevation of Salt Creek watershed combined with this funnel affect creates an ideal area for flooding during high intensity, widespread precipitation events. As stated, Salt Creek can produce smaller scale floods without the influence of the Fall River's backup floodwater, and flood patterns are largely dependent on the storm system's intensity, duration, and location.

Infiltration and stream blockage data were not implemented in the models reported in this study. Because ANUGA has not been validated to model a large watershed, like the Fall River, HEC-RAS may be a more appropriate modeling tool to simulate the effect that the Fall River has on Salt Creek. Additionally, HEC-RAS may offer more accurate flood results with the implementation of an infiltration operator and stream blockages simulations.

The results of this study will be made available to the City of Fredonia and surrounding rural residents to assist with flood risk abatement and to provide, in general, a better understanding of how and why floods occur within Salt Creek

# References


Adiat, K., Nawawi, M., & Abdullah, K. (2012). Integration of Geographic Information System and 2D Imaging to Investigate the Effects of Subsurface Conditions on Flood Occurrence. *Modern Applied Science, 6*(3), 11-21.

Alaui, A., Rogger, M., Peth, S., & Gunter, B. (2018). Does soil compaction increase floods? A review. *Journal of Hydrology, 557*, 631-642.

AMEC Foster Wheeler. (2017). *Hydrology Report: Wilson County, Kansas.* Kansas Department of Agriculture, Department of Water Resources.

Bailey, D. (2016, October). Wilson County Working Group Workshop. Fredonia, Kansas.

Birrell, K. (1966). Determination of clay contents in soils containing allophane. *New Zealand Journal of Agricultural Research*, 544-564.

Boeker, E., & van Grondelle, R. (1995). *Environmental Physics.* Chichester, England: John Wiley & Sons.

Bronstert, A., Niehoff, D., & Burger, G. (2002). Effects of climate and land-use change on storm runoffgeneration: present knowledge and modelling capabilities. *Hydrological Processes, 16*, 509-529.

Chegeniazadeh, A., & Nikraz, H. (2011). Permeability Test on Reinforced Clayey Sand. *World Academy of Science, Engineering and Technology*(78).

Chow, V. (1959). *Open Channel Hydraulics.* New York: McGraw-Hill.

Cornell University. (n.d.). *Northeast Region Certified Crop Adviser (NRCCA) Study Resources*. Retrieved from Cornell University: https://nrcca.cals.cornell.edu/

DeAngelis, A., Dominguez, F., Fan, Y., Robock, A., Kustu, M., & Robinson, D. (2010). Evidence of enhanced precipitation due to irrigation over the Great Plains of the United States. *Journal of Geophysical Research, 115*.

DeLaune, P. (2012). Impact of tillage on runoff in long term no-till wheat systems. *Soil and Tillage Research, 124*, 32-35.

Dunne, T., & Leopold, L. (1978). *Water in Environmental Planning.* New York: W.H. Freeman.

Elhakim, A. (2016). Estimation of soil permeability. *Alexandria Engineering Journal*.

EPA. (2016). *What Climate Change Means for Kansas.* Environmental Protection Agency.

FEMA. (2004). *Guidelines and Specifications for Flood Hazard Mapping Partners: D.4.3 Flood Frequency Analysis Methods.*

FEMA. (n.d.). *RiskMAP*. Retrieved April 2019, from https://www.fema.gov/media-library-data/1508774577071-a533ca97df7edae550cbc608750ca693/BLE_FACTSHEET.pdf

Fryirs, K., & Brierley, G. (2013). *Geomorphic Analysis of River Systems: An Approach to Reading the Landscape.* Blackwell Publishing.

Guo, Z., Huang, E., Liu, X., & Cao, S. (2007). Experimental Study on the Parameters That Cause River-Blocking by Debris Flow. *Computational Mechanics*, 251.

Gupta, A. (2008). *Relationship between the Mean Particle Size, the Size Factor, Optimum Moisture Content, and Permeability of Sandy Soils.* Department of Civil & Environmental Engineering, Delhi College of Engineering. Delhi: nternational Association for Computer Methods and Advances in Geomechanics (IACMAG).

Hey, D., & Philippi, N. (1995). Flood Reduction through Wetland Restoration: The Upper Mississippi River Basin as a Case History. *Restoration Ecology*, *3*(1), 4-17.

Hornberger, G., Raffensperger, J., Wiberg, P., & Eshleman, K. (1998). *Elements of Physical Hydrology.* Balitmore, Maryland: The John Hopkins UNiversity Press.

Kansas DASC. (2018). *Kansas Data and Support Center*. Retrieved from https://www.kansasgis.org

Kansas Geological Survey. (1999). *Osage Cuestas: Rocks and Minerals.*

Kansas Geological Survey. (2017). "Geologic Map" of Kansas Counties. Kansas Data Access and Support Center.

Kansas Geological Survey. (2018). *Water Well Completion Records (WWC5) Database*. Retrieved July 2018, from http://www.kgs.ku.edu/Magellan/WaterWell/index.html

Kumar, S., & Malik, R. (1990). Verification of quick capillary rise approach for determining pore geometrical characteristics in soils of varying texture. *Soil Science*, *150*(6), 883-888.

Milly, P., Wetherald, R., Duane, K., & Delworth, T. (2002). Increasing risk of great floods in a changing climate. *Nature*(415), 514-517.

Montgomery, D., Massong, T., & Hawley, S. (2003). Influence of debris flows and log jams on the location of pools and alluvial channel reaches, Oregon Coast Range. *GSA Bulletin*, *115*, 78-88.

Mungkasi, S., & Roberts, S. (2013). Validation of ANUGA hydraulic model using exact solutions to shallow water wave problems. *Journal of Physics*.

Nagy, L., Tabácks, A., Huszák, T., Mahler, A., & Varga, G. (2013). Comparison of permeability testing methods. *18th International Conference on Soil Mechanics and Geotechnical Engineering*, (pp. 399-402). Paris.

NASA. (n.d.). *Precipitation Measurment Missions*. Retrieved December 27, 2017, from National Aeronautics and Space Administration: https://pmm.nasa.gov/resources/faq/how-does-climate-change-affect-precipitation

National Climate Assessment. (2014). *Heavy Downpours Increasing*. Retrieved July 2018, from National Climate Assessment: https://nca2014.globalchange.gov/report/our-changing-climate/heavy-downpours-increasing#tab2-images

National Weather Service. (2018, November 3). *Advanced Hydrologic Prediction Service*. Retrieved from https://water.weather.gov/ahps2/hydrograph.php?wfo=ict&gage=frnk1

Natural Resource Covservation Service. (2009). *National Engineering Handbook: Chapter 7 - Hydrologic Soil Groups.* United States Department of Agriculture.

Nelson, P., Baldock, J., Clarke, P., Oades, J., & Churchman, G. (1999). Dispersed clay and organic matter in soil: their nature and associations. *Australian Journal of Soil Research, 37*(2), 289-316.

NOAA. (2017a). Retrieved January 2017, from Climate Data Online: https://www.ncdc.noaa.gov/cdo-web/

NOAA. (2017b). *Global Summary of the Year Station Details*. Retrieved November 2, 2017, from NOAA: https://www.ncdc.noaa.gov/cdo-web/datasets/GSOY/stations/GHCND:USC00142894/detail

NOAA-NWS. (n.d.). *Flood Damages Suffered in the UNited States During Water Year 2007.*

Ogawa, H., & Male, J. (1986). Simulating the flood mitigation roles of wetlands. *Journal of Water Resources Planning and Management, 112*, 114-128.

Pivot, J., Josien, E., & Martin, P. (2002). Farms adaptation to changes in flood risk: a management approach. *Hydrology*(267), 21-25.

Rahmani, V., Kastens, J., deNoyelles, F., Jakubauskas, M., Martinko, E., Huggins, D., . . . Blackwood, A. (2018). Examining Storage Capacity Loss and Sedimentation Rate of Large Reservoirs in the Central U.S. Great Plains. *Water, 10*(190).

Rawls, W., Brakensiek, D., & Saxton, K. (1982). Estimation of Soil Water Properties. *Transactions of the ASAE, 25*.

Roberts, S., Nielsen, O., Gray, D., Sexton, J., & Davies, D. (2015). *ANUGA User Manuel.* Geoscience Australia and Australian National University.

Sajikumar, N., & Remya, R. (2014). Impact of land cover and land use change on runoff characteristics. *Journal of Environmental Management*(161), 460-468.

Soil Survey Staff. (2017, November 4). *Web Soil Survey*. Retrieved from Natural Resources Conservation Service, United States Department of Agriculture: https://websoilsurvey.sc.egov.usda.gov/

Solinst Canada Ltd. (2017). Solinst User Guide.

South National Technical Center. (1991). *Measurement and Estimation of Permeability of Soils for Animal Waste Storage Facility Des'ign* . Retrieved from https://www.nrcs.usda.gov/Internet/FSE_DOCUMENTS/nrcs141p2_024050.pdf

Sullivan, K., Lisle, T., Dolloff, C., Grant, G., & Reid, L. (1986). Stream channels: The link between forests and fishes. In *Streamside Management: Forestry and Fishery Interactions* (pp. 39-97). Seattle: University of Washington.

Swanson, D. (1989). *Soil Survey of Wilson County, Kansas.* USDA.

Tarboton, D. (2003). *Rainfall-Runoff Processes.* Utah State University, Deptartment of Engineering.

U.S. Geological Survey. (2017). *USGS NED 1/3 arc-second n38w096 1 x 1 degree ArcGrid.* Retrieved March 7, 2017, from USGS: https://nationalmap.gov/

U.S. Geological Survey. (2018, October 23). *National Water Information System*. Retrieved from https://waterdata.usgs.gov/nwis/uv?site_no=07169500

United States Department of Agriculture. (2018, March 18). *Soil Texture Calculator*. Retrieved from https://www.nrcs.usda.gov/wps/portal/nrcs/detail/soils/survey/?cid=nrcs142p2_054167

United States Geological Survey. (2017). *The National Map.* Retrieved from United States Geological Survey: https://nationalmap.gov/elevation.html

USDA. (2012). *2012 Census of Agriculture Highlights.* USDA.

USDA. (n.d.). *Saturated Hydraulic Conductivity in Relation to Soil Texture*. Retrieved January 2018, from https://www.nrcs.usda.gov/wps/portal/nrcs/detail/soils/survey/office/ssr10/tr/?cid=nrcs144p2_074846

USDA-NASS. (2019, April 16). *2018 State Agriculture Overview*. Retrieved from https://www.nass.usda.gov/Quick_Stats/Ag_Overview/stateOverview.php?state=KANSAS

USDA-NRCS. (2017). *Soil Survey Manual.* Retrieved April 2019, from Natural Resource Conservation Service: https://www.nrcs.usda.gov/wps/portal/nrcs/detail/soils/ref/?cid=nrcs142p2_054253

Van Drie, R., Simon, M., & Schymitzek, I. (2008). 2D Hydraulic Modelling over a Wide Range of Applications with ANUGA. *Engineers Australia: 9th National Conference on Hydraulics in Water Engineering.* Darwin, Australia.

Volkmer, A. (2014). *Infiltration and Runoff Parameters for Tilled and No-till Row Crops.* University of Nebraska-Lincoln.

Walker, E. (2013). *Salt Creek Project.* Unpublished Report.

Whiting, D., Wilson, C., & Card, A. (2003). *Estimating Soil Texture: Sandy, Loamy, or Clayey?* Colorado State University, Cooperative Extension.

*World population projected to reach 9.7 billion by 2050*. (2015, July 29). Retrieved January 9, 2017, from United Nations: Department of Economic and Social Affairs: http://www.un.org/en/development/desa/news/population/2015-report.html

Wright, J. (2007). *Floodplain Management: Principles and Current Practices.* Retrieved from FEMA Emergency Management Institute: https://training.fema.gov/hiedu/aemrc/courses/coursetreat/fm.aspx

Yusuf, S., Guluda, D., & Jayanegara, T. (2017). Surface runoff estimation from various land use in Mapili Watershed using SCS Curve Number and Geographic Information System. *IOP Conference Series: Earth and Environmental Science. 54.* IOP Publishing.

Zotarelli, L., Dukes, M. D., & Barreto, T. P. (n.d.). *Interpretation of Soil Moisture Content to Determine Soil Field Capacity and Avoid Over Irrigation in Sandy Soils Using Soil Moisture Measurements.* Retrieved from University of Florida: http://hos.ufl.edu/

# Appendix A – Soil Analyses

| Name | Latitude | Longitude | Depth Min (cm) | Depth Max (cm) | Location Details |
|---|---|---|---|---|---|
| 1 | 37.572350 | -95.862106 | 5.1 | 132.1 | SW of HOBO-2 |
| 2 | 37.573641 | -95.849883 | 5.1 | 45.7 | Dry streambed |
| 3 | 37.533238 | -95.838701 | 5.1 | 152.4 | West Park, E of Salt Creek |
| 4 | 37.533833 | -95.838760 | 96.5 | 101.6 | In stream |
| 5 | 37.588583 | -95.861424 | 10.2 | 132.1 | 1500 Rd, in dry stream |
| 6 | 37.324092 | -95.475230 | 10.2 | 132.1 | In field |
| 7 | 37.530399 | -95.839233 | 58.4 | 83.8 | Dry streambed |
| 8 | 37.562073 | -95.832397 | 5.1 | 96.5 | Myers |
| 9 | 37.544319 | -95.839203 | 12.7 | 91.4 | Dry streambed |
| 10 | 37.533173 | -95.816109 | 7.6 | 132.1 | Urban yard |

**Table A.1:** Location of soil samples.

| Site Sample Depths (1-5) (cm) | | | | | | | | | |
|---|---|---|---|---|---|---|---|---|---|
| Site 1 | | Site 2 | | Site 3 | | Site 4 | | Site 5 | |
| Top | Bottom | Top | Bottom | Top | Bottom | Top | Bottom | Top | Bottom |
| 5 | 18 | 5 | 25 | 5 | 15 | 97 | 102 | 10 | 28 |
| 18 | 34 | 25 | 41 | 15 | 23 | | | 28 | 43 |
| 34 | 53 | 41 | 46 | 23 | 30 | | | 43 | 64 |
| 53 | 61 | | | 30 | 41 | | | 64 | 74 |
| 61 | 79 | | | 41 | 53 | | | 74 | 91 |
| 79 | 94 | | | 53 | 64 | | | 91 | 102 |
| 94 | 112 | | | 64 | 72 | | | 102 | 114 |
| 112 | 132 | | | 72 | 79 | | | 114 | 122 |
| | | | | 79 | 91 | | | 122 | 132 |
| | | | | 91 | 99 | | | | |
| | | | | 99 | 109 | | | | |
| | | | | 109 | 117 | | | | |
| | | | | 117 | 132 | | | | |
| | | | | 132 | 135 | | | | |
| | | | | 135 | 142 | | | | |
| | | | | 142 | 147 | | | | |
| | | | | 147 | 152 | | | | |

**Table A.2a:** Soil sample depths in centimeters for sites 1-5. Green boxes indicate depths chosen for analysis.

| Site Sample Depths (6-10) (cm) | | | | | | | | | |
|---|---|---|---|---|---|---|---|---|---|
| Site 6 | | Site 7 | | Site 8 | | Site 9 | | Site 10 | |
| Top | Bottom | Top | Bottom | Top | Bottom | Top | Bottom | Top | Bottom |
| 10 | 25 | 58 | 74 | 5 | 18 | 13 | 20 | 8 | 23 |
| 25 | 41 | 74 | 81 | 18 | 30 | 20 | 25 | 23 | 38 |
| 41 | 53 | 81 | 84 | 30 | 41 | 25 | 33 | 38 | 43 |
| 53 | 64 | | | 41 | 51 | 33 | 41 | 43 | 56 |
| 64 | 76 | | | 51 | 61 | 41 | 48 | 56 | 71 |
| 76 | 86 | | | 61 | 74 | 48 | 56 | 71 | 81 |
| 86 | 99 | | | 74 | 84 | 56 | 69 | 81 | 97 |
| 99 | 109 | | | 84 | 97 | 69 | 79 | 97 | 107 |
| 109 | 127 | | | | | 79 | 86 | 107 | 114 |
| 127 | 132 | | | | | 86 | 91 | 114 | 122 |
| | | | | | | | | 122 | 132 |

**Table A.2b:** Soil sample depths in centimeters for sites 6-10. Green boxes indicate depths chosen for analysis.

| Site ID | Min Depth | Max Depth | Trial # | Dx (10) | Dx (50) | Dx (90) |
|---|---|---|---|---|---|---|
| | cm | cm | | µm | µm | µm |
| Site 1 | 5 | 18 | 1 | 3.98 | 25 | 115 |
| | | | 2 | 3.95 | 24.6 | 113 |
| | | | 3 | 3.92 | 24.4 | 120 |
| | | | Average | 3.95 | 24.7 | 116 |
| | 53 | 61 | 1 | 0.866 | 4.74 | 26 |
| | | | 2 | 0.87 | 4.8 | 26.3 |
| | | | 3 | 0.871 | 4.86 | 26.3 |
| | | | Average | 0.869 | 4.8 | 26.2 |
| | 122 | 132 | 1 | 1.56 | 5.85 | 19.7 |
| | | | 2 | 1.54 | 5.84 | 19.7 |
| | | | 3 | 1.53 | 5.83 | 19.5 |
| | | | Average | 1.54 | 5.84 | 19.6 |

**Table A.3a** Particle size analysis for Site 1.

| Site ID | Min Depth | Max Depth | Trial # | Dx (10) | Dx (50) | Dx (90) |
|---|---|---|---|---|---|---|
| | cm | cm | | µm | µm | µm |
| Site 2 | 41 | 46 | 1 | 0.838 | 3.83 | 17.7 |
| | | | 2 | 0.839 | 3.86 | 17.8 |
| | | | 3 | 0.841 | 3.87 | 17.9 |
| | | | Average | 0.839 | 3.86 | 17.8 |

**Table A.3b** Particle size analysis for Site 2.

| Site ID | Min Depth | Max Depth | Trial # | Dx (10) | Dx (50) | Dx (90) |
|---|---|---|---|---|---|---|
| | cm | cm | | µm | µm | µm |
| Site 3 | 5 | 15 | 1 | 4.27 | 27.5 | 237 |
| | | | 2 | 3.96 | 23.7 | 162 |
| | | | 3 | 3.93 | 23.4 | 162 |
| | | | Average | 4.05 | 24.9 | 187 |
| | 72 | 79 | 1 | 7.11 | 37.3 | 111 |
| | | | 2 | 6.82 | 36.3 | 107 |
| | | | 3 | 6.55 | 35.4 | 103 |
| | | | Average | 6.82 | 36.3 | 107 |
| | 142 | 147 | 1 | 8.65 | 36 | 106 |
| | | | 2 | 8.27 | 33.8 | 93.7 |
| | | | 3 | 8.22 | 33.1 | 90.1 |
| | | | Average | 8.38 | 34.2 | 96.6 |

**Table A.3c** Particle size analysis for Site 3.

| Site ID | Min Depth | Max Depth | Trial # | Dx (10) | Dx (50) | Dx (90) |
|---|---|---|---|---|---|---|
| | cm | cm | | µm | µm | µm |
| Site 4 | 97 | 102 | 1 | 1.27 | 8.85 | 52 |
| | | | 2 | 1.23 | 8.3 | 40.6 |
| | | | 3 | 1.23 | 8.3 | 39.2 |
| | | | Average | 1.24 | 8.47 | 43.3 |

**Table A.3d** Particle size analysis for Site 4.

| Site ID | Min Depth | Max Depth | Trial # | Dx (10) | Dx (50) | Dx (90) |
|---|---|---|---|---|---|---|
| | cm | cm | | µm | µm | µm |
| Site 5 | 10 | 28 | 1 | 1.56 | 10.3 | 39.5 |
| | | | 2 | 1.59 | 10.7 | 40.8 |
| | | | 3 | 1.57 | 10.5 | 37.5 |
| | | | Average | 1.57 | 10.5 | 39.2 |
| | 43 | 64 | 1 | 1.96 | 15.9 | 65.1 |
| | | | 2 | 1.96 | 15.8 | 60.1 |
| | | | 3 | 1.97 | 15.9 | 60.4 |
| | | | Average | 1.96 | 15.9 | 61.9 |
| | 122 | 132 | 1 | 2.08 | 12.4 | 45.3 |
| | | | 2 | 2.01 | 11.6 | 43 |
| | | | 3 | 1.97 | 11.1 | 41.4 |
| | | | Average | 2.02 | 11.7 | 43.3 |

**Table A.3e** Particle size analysis for Site 5.

| Site ID | Min Depth | Max Depth | Trial # | Dx (10) | Dx (50) | Dx (90) |
|---|---|---|---|---|---|---|
| | cm | cm | | µm | µm | µm |
| Site 6 | 10 | 25 | 1 | 1.05 | 5.95 | 31.4 |
| | | | 2 | 1.03 | 5.75 | 26.6 |
| | | | 3 | 1.03 | 5.74 | 26.1 |
| | | | Average | 1.04 | 5.81 | 27.7 |
| | 53 | 64 | 1 | 1.07 | 6.74 | 32.2 |
| | | | 2 | 1.06 | 6.61 | 30.6 |
| | | | 3 | 1.05 | 6.55 | 29.5 |
| | | | Average | 1.06 | 6.63 | 30.7 |
| | 127 | 132 | 1 | 0.848 | 3.67 | 14.3 |
| | | | 2 | 0.851 | 3.7 | 14.6 |
| | | | 3 | 0.851 | 3.72 | 14.7 |
| | | | Average | 0.85 | 3.7 | 14.6 |

**Table A.3f** Particle size analysis for Site 6.

| Site ID | Min Depth | Max Depth | Trial # | Dx (10) | Dx (50) | Dx (90) |
|---|---|---|---|---|---|---|
| | cm | cm | | µm | µm | µm |
| Site 7 | 74 | 81 | 1 | 5.43 | 47.9 | 157 |
| | | | 2 | 5.16 | 44.5 | 148 |
| | | | 3 | 4.8 | 40 | 129 |
| | | | Average | 5.12 | 44 | 144 |

**Table A.3g** Particle size analysis for Site 7.

| Site ID | Min Depth | Max Depth | Trial # | Dx (10) | Dx (50) | Dx (90) |
|---|---|---|---|---|---|---|
| | cm | cm | | µm | µm | µm |
| Site 8 | 18 | 30 | 1 | 2.45 | 16.5 | 109 |
| | | | 2 | 2.37 | 15.5 | 81.1 |
| | | | 3 | 2.65 | 19.9 | 1110 |
| | | | Average | 2.48 | 17.1 | 186 |
| | 74 | 84 | 1 | 2.34 | 11.2 | 71.3 |
| | | | 2 | 2.25 | 10.3 | 59.4 |
| | | | 3 | 2.2 | 9.68 | 51.9 |
| | | | Average | 2.26 | 10.4 | 61 |
| | 84 | 97 | 1 | 0.991 | 7.97 | 42.4 |
| | | | 2 | 0.992 | 8.08 | 39.9 |
| | | | 3 | 0.993 | 8.17 | 39.2 |
| | | | Average | 0.992 | 8.07 | 40.5 |

**Table A.3h** Particle size analysis for Site 8

| Site ID | Min Depth | Max Depth | Trial # | Dx (10) | Dx (50) | Dx (90) |
|---|---|---|---|---|---|---|
| | cm | cm | | µm | µm | µm |
| Site 9 | 20 | 25 | 1 | 2.16 | 9.14 | 38 |
| | | | 2 | 2.13 | 8.84 | 35.1 |
| | | | 3 | 2.09 | 8.57 | 32.6 |
| | | | Average | 2.13 | 8.84 | 35.2 |
| | 69 | 79 | 1 | 3.32 | 30.2 | 147 |
| | | | 2 | 3.32 | 30.3 | 147 |
| | | | 3 | 3.07 | 26 | 115 |
| | | | Average | 3.23 | 28.8 | 135 |
| | 86 | 91 | 1 | 2.27 | 10.8 | 74.3 |
| | | | 2 | 2.29 | 11.2 | 82.9 |
| | | | 3 | 2.25 | 10.7 | 65 |
| | | | Average | 2.27 | 10.9 | 73.7 |

**Table A.3i** Particle size analysis for Site 9.

| Site ID | Min Depth | Max Depth | Trial # | Dx (10) | Dx (50) | Dx (90) |
|---|---|---|---|---|---|---|
| | cm | cm | | µm | µm | µm |
| Site 10 | 23 | 38 | 1 | 2.79 | 15.4 | 50.9 |
| | | | 2 | 2.75 | 15.3 | 50.3 |
| | | | 3 | 2.76 | 15.4 | 51.1 |
| | | | Average | 2.77 | 15.4 | 50.8 |
| | 56 | 71 | 1 | 2.81 | 23.1 | 570 |
| | | | 2 | 2.27 | 13.4 | 70.3 |
| | | | 3 | 2.35 | 14.6 | 108 |
| | | | Average | 2.45 | 16.2 | 204 |
| | 122 | 132 | 1 | 1.87 | 11.9 | 48.8 |
| | | | 2 | 1.88 | 12.2 | 50.3 |
| | | | 3 | 1.82 | 11.5 | 43.6 |
| | | | Average | 1.85 | 11.8 | 47.4 |

**Table A.3j** Particle size analysis for Site 10.

| | Site 1: 5-18cm | Site 1: 53-61cm | Site 1: 112-132cm |
|---|---|---|---|
| Grain Size | Percent of Sample | Percent of Sample | Percent of Sample |
| coarse sand | 0.47% | 0.00% | 0.00% |
| medium sand | 2.15% | 0.00% | 0.00% |
| fine sand | 7.76% | 0.38% | 0.00% |
| very fine sand | 14.17% | 2.10% | 0.83% |
| silt | 70.69% | 71.11% | 83.73% |
| clay | 4.75% | 26.39% | 15.44% |
| **Classification** | **Silt Loam** | **Silt Loam** | **Silt Loam** |

**Table A.4a:** Soil particle size distribution by percent for Site 1.

| | **Site 2: 41-46cm** |
|---|---|
| Grain Size | Percent of Sample |
| coarse sand | 0.0% |
| medium sand | 0.0% |
| fine sand | 0.1% |
| very fine sand | 0.66% |
| silt | 70.22% |
| clay | 29.02% |
| **Classification** | **Silt Clay Loam** |

**Table A.4b:** Soil particle size distribution by percent for Site 2.

| | **Site 3: 5-15cm** | **Site 3: 72-79cm** | **Site 3: 142-147** |
|---|---|---|---|
| Grain Size | Percent of Sample | Percent of Sample | Percent of Sample |
| coarse sand | 0.23% | 0.00% | 0.00% |
| medium sand | 5.39% | 0.00% | 0.06% |
| fine sand | 10.57% | 8.99% | 7.14% |
| very fine sand | 13.93% | 25.51% | 22.87% |
| silt | 65.76% | 62.52% | 67.25% |
| clay | 4.13% | 2.98% | 2.64% |
| **Classification** | **Silt Loam** | **Very Fine Sandy Loam** | **Silt Loam** |

**Table A.4c:** Soil particle size distribution by percent for Site 3.

| | **Site 4: 97-102** |
|---|---|
| Grain Size | Percent of Sample |
| coarse sand | 0.40% |
| medium sand | 0.57% |
| fine sand | 0.42% |
| very fine sand | 5.71% |
| silt | 75.99% |
| clay | 16.95% |
| **Classification** | **Silt Clay Loam** |

**Table A.4d:** Soil particle size distribution by percent for Site 4.

| | **Site 5: 10-28cm** | **Site 5: 43-64cm** | **Site 5: 122-132** |
|---|---|---|---|
| Grain Size | Percent of Sample | Percent of Sample | Percent of Sample |
| coarse sand | 0.00% | 0.00% | 0.00% |
| medium sand | 0.34% | 0.72% | 0.00% |
| fine sand | 1.83% | 2.21% | 0.13% |
| very fine sand | 3.69% | 11.04% | 6.23% |
| silt | 80.51% | 75.12% | 82.91% |
| clay | 13.62% | 10.93% | 10.73% |
| **Classification** | **Silt Loam** | **Silt Loam** | **Silt Loam** |

**Table A.4e:** Soil particle size distribution by percent for Site 5.

| | **Site 6: 10-25cm** | **Site 6: 53-64cm** | **Site 6: 127-132** |
|---|---|---|---|
| Grain Size | Percent of Sample | Percent of Sample | Percent of Sample |
| coarse sand | 0.20% | 0.06% | 0.00% |
| medium sand | 0.36% | 0.26% | 0.00% |
| fine sand | 0.39% | 0.68% | 0.00% |
| very fine sand | 1.68% | 2.40% | 0.09% |
| silt | 75.44% | 75.74% | 70.11% |
| clay | 21.90% | 20.84% | 29.77% |
| **Classification** | **Silt Loam** | **Silt Loam** | **Silty Clay Loam** |

**Table A.4f:** Soil particle size distribution by percent for Site 6.

| | **Site 7: 74-81cm** |
|---|---|
| Grain Size | Percent of Sample |
| coarse sand | 0.27% |
| medium sand | 2.48% |
| fine sand | 13.95% |
| very fine sand | 32.07% |
| silt | 48.36% |
| clay | 2.90% |
| **Classification** | **Very Fine Sandy Loam** |

**Table A.4g:** Soil particle size distribution by percent for Site 7.

| | **Site 8: 18-30cm** | **Site 8: 74-84cm** | **Site 8: 84-97cm** |
|---|---|---|---|
| Grain Size | Percent of Sample | Percent of Sample | Percent of Sample |
| coarse sand | 4.91% | 0.00% | 0.00% |
| medium sand | 3.13% | 0.00% | 0.00% |
| fine sand | 4.40% | 3.22% | 0.33% |
| very fine sand | 8.27% | 9.12% | 5.32% |
| silt | 71.06% | 78.61% | 73.08% |
| clay | 8.20% | 9.05% | 21.24% |
| **Classification** | **Silt Loam** | **Silt Loam** | **Silt Loam** |

**Table A.4h:** Soil particle size distribution by percent for Site 8.

| | **Site 9: 20-25cm** | **Site 9: 69-79cm** | **Site 9: 86-91cm** |
|---|---|---|---|
| Grain Size | Percent of Sample | Percent of Sample | Percent of Sample |
| coarse sand | 0.00% | 0.00% | 0.08% |
| medium sand | 0.00% | 1.72% | 1.60% |
| fine sand | 0.21% | 11.78% | 4.57% |
| very fine sand | 4.44% | 19.16% | 8.06% |
| silt | 85.32% | 61.71% | 76.60% |
| clay | 10.02% | 5.64% | 9.05% |
| **Classification** | **Silt Loam** | **Coarse Sand** | **Silt Loam** |

**Table A.4i:** Soil particle size distribution by percent for Site 9.

| | **Site 10: 23-38cm** | **Site 10: 56-71cm** | **Site 10: 122-132cm** |
|---|---|---|---|
| Grain Size | Percent of Sample | Percent of Sample | Percent of Sample |
| coarse sand | 0.00% | 4.70% | 0.00% |
| medium sand | 0.48% | 3.79% | 0.41% |
| fine sand | 2.63% | 5.65% | 1.79% |
| very fine sand | 6.51% | 8.26% | 6.22% |
| silt | 83.07% | 69.48% | 79.60% |
| clay | 7.28% | 8.16% | 11.97% |
| **Classification** | **Silt** | **Silt Loam** | **Silt Loam** |

**Table A.4j:** Soil particle size distribution by percent for Site 10.

| Site | Depth, cm | Ks | Hf | Wet Soil Ponding Time (min) | | | Dry Soil Ponding Time (min) | | |
|---|---|---|---|---|---|---|---|---|---|
| *site ID* | *depth of sample* | *µm/s* | *cm* | *1.12cm/hr* | *2.54cm/hr* | *3.50cm/hr* | *1.12cm/hr* | *2.54cm/hr* | *3.50cm/hr* |
| 9 | 69 to 79 | 0.83 | 21.85 | 42.6 | 6.9 | 3.06 | 127.8 | 20.4 | 9 |
| 1 | 5 to 18 | 0.63 | 21.85 | 29.7 | 5.04 | 2.28 | 89.4 | 15 | 6.6 |
| 1 | 112 to 132 | 0.35 | 21.85 | 14.34 | 2.7 | 1.2 | 44.4 | 7.8 | 3.6 |
| 3 | 72 to 79 | 0.34 | 21.85 | 14.82 | 2.7 | 1.2 | 43.2 | 7.8 | 3.6 |
| 5 | 43 to 64 | 0.22 | 27.30 | 11.1 | 2.1 | 0.96 | 33.6 | 6 | 3 |
| 5 | 122 to 132 | 0.17 | 23.90 | 7.38 | 1.38 | 0.66 | 22.2 | 4.2 | 1.92 |
| 6 | 53 to 64 | 0.17 | 23.90 | 7.38 | 1.38 | 0.66 | 22.2 | 4.2 | 1.92 |
| 3 | 142 to 147 | 0.16 | 23.90 | 6.96 | 1.32 | 0.6 | 20.82 | 3.9 | 1.8 |
| 10 | 23 to 38 | 0.15 | 29.22 | 7.92 | 1.5 | 0.72 | 23.76 | 4.5 | 2.1 |
| 8 | 74 to 84 | 0.11 | 29.22 | 5.76 | 1.08 | 0.48 | 17.22 | 3.3 | 1.5 |
| 9 | 86 to 91 | 0.10 | 29.22 | 5.22 | 1.02 | 0.48 | 15.6 | 3 | 1.38 |

**Table A.5:** Results of the ponding time calculations described in Section 2.3.3.1